REPORT DOCUMENTATION PAGE

AFRL-SR-BL-TR-01-

0135

1. AGENCY USE ONLY (Leave blank)	2. REPORT DATE 10/15/00	3. REPORT TYPE AND DA FINAL 01 MAY 1996 -

4. TITLE AND SUBTITLE
Molecular Control Over the Interfacial Properties of High-T_c Superconductors

5. FUNDING NUMBERS
F49620-96-1-0155

6. AUTHOR(S)
Dr. David Kanis

7. PERFORMING ORGANIZATION NAME(S) AND ADDRESS(ES)

Chicago State University
Office of Sponsored Programs
9501 S. King Drive
Chicago, IL 60628

8. PERFORMING ORGANIZATION REPORT NUMBER
5-53657
5-53734
5-53784

9. SPONSORING / MONITORING AGENCY NAME(S) AND ADDRESS(ES)

Capt. Hugh DeLong
AFOSR/NL
110 Duncan Avenue Room B115
Bolling AFB DC 20332-8080

10. SPONSORING / MONITORING AGENCY REPORT NUMBER

11. SUPPLEMENTARY NOTES

12a. DISTRIBUTION / AVAILABILITY STATEMENT
Approved for Public Release: Distribution Unlimited

12b. DISTRIBUTION CODE

13. ABSTRACT ***(Maximum 200 Words)***

The surface coordination chemistry of the cuprate superconductor $YBa_2Cu_3O_{7-\gamma}$ was extensively surveyed for the purpose of understanding the factors that govern the formation of robust, highly-ordered monolayers on these superconductor surfaces. Of the many functionalities investigated, long-chain primary amines formed the densest packed monolayer structure on both ceramic pellets and thin film substrates of $YBa_2Cu_3O_{7-\gamma}$. Evidence for copper-amine interactions was obtained through SERS, and a computational model to accurately determine the local structure of the monolayer material was developed and implemented. Results of the computational study agree with experimentally determined properties of the materials. The computational studies also suggest that harmful water molecules are not able to penetrate the monolayer structure to damage the superconductor. This has been confirmed experimentally. Experimental evidence for two plausible mechanisms of monolayer formation was obtained in these studies. In addition, all surface modifications examined in this work did not damage the inherent superconducting properties of the bulk material.

14. SUBJECT TERMS			15. NUMBER OF PAGES 56
			16. PRICE CODE
17. SECURITY CLASSIFICATION OF REPORT Unclas	18. SECURITY CLASSIFICATION OF THIS PAGE Unclas	19. SECURITY CLASSIFICATION OF ABSTRACT Unclas	20. LIMITATION OF ABSTRACT

Air Force Office of Scientific Research

Final Report – for Grant F49620-96-1-0155

Molecular Control over the Interfacial Properties of High-T_c Superconductors

Principal Investigator

David R. Kanis

Department of Chemistry and Physics
Chicago State University
9501 South King Drive
Chicago, IL 60628

Co-Principal Investigators

Chad A. Mirkin

Department of Chemistry
Northwestern University
Evanston, IL 60208-3113

John T. McDevitt

Department of Chemistry
University of Texas-Austin
Austin, Texas 78712-1167

October 15, 2000

I. Objectives:

The principle aim of this research effort is to understand the factors that govern the formation of highly-ordered monolayers on high temperature superconductor surfaces and use this fundamental information to chemically tailor high-T_c surfaces and their interfacial properties. Another aim of this research is to prepare a number of these self-assembled monolayer materials to determine the optimal conditions for preparing such materials. These objectives are unchanged from our original proposal.

II. Research Accomplishments and New Findings:

The research accomplishments associated with this grant can be classified into four general areas: 1) the preparation of materials, 2) the surface coordination structure of the self-assembled monolayer atop a superconductor surface, 3) the potential applications of the prepared materials, and 4) the mechanisms for the growth of the self-assembled monolayers. Summaries of the accomplishments in each of these areas will be presented herein, along with references to the representative attached publications that provide details of the research findings.

Preparation of Materials

The surface coordination chemistry of the cuprate superconductor $YBa_2Cu_3O_{7-\gamma}$ was extensively surveyed using cyclic voltammetry in conjunction with redox-active ferrocenyl containing adsorbate molecules. A total of fifteen different adsorbates were examined in these experiments including a primary, a secondary, a tertiary, and an aryl amine, a thiol, a disulfide, a selenol, an alcohol, an amide, a phosphine, an azide, a nitrile, a pyridine, a bromide and a chloride. The details of these experiments are described in Papers 1 and 2. Of these functional groups, the primary amine was found to have the greatest surface coverage on both the ceramic pellet substrates and thin film substrates of $YBa_2Cu_3O_{7-\gamma}$. Moreover, eight of the functional groups displayed no appreciable surface coverage. Resistivity versus temperature plots for a $YBa_2Cu_3O_{7-\gamma}$ thin film coated with a primary amine displays a T_c identical to that of the untreated material. These findings are very important since they suggest that primary amines have the largest surface coverage atop $YBa_2Cu_3O_{7-\gamma}$ and that there is no damage to the bulk superconducting properties as a result of the surface modifications. Also the surface coverage of a ferrocenyl containing primary amine atop $Bi_2Sr_2CaCu_3O_8$ (another cuprate superconductor) was examined and showed similar results to $YBa_2Cu_3O_{7-\gamma}$. This suggests that some sort of copper-amine coordination chemistry is driving the affinity of amines for the surface.

The publication labeled as Paper 1 is also important because it delineates the experimental procedures used to prepare the stable and robust self-assembled monolayers of these materials. These procedures were used throughout the grant period to produce materials.

Structural Characterization of Monolayers atop the Superconductor Surface

One of the more important aspects of this research examined the structure of the self-assembled monolayers atop $YBa_2Cu_3O_{7-\gamma}$. Because of the poor optical properties of $YBa_2Cu_3O_{7-\gamma}$ it is difficult to do conventional IR and Raman Spectroscopy using on the monolayer structures formed atop the superconductor surface. However, using Surface-Enhanced Raman Spectroscopy with the SAM surface modified with gold colloids, direct evidence for a copper-nitrogen interaction was reported for a 4-aminopyridine monolayer on $YBa_2Cu_3O_{7-\gamma}$. The details of this finding are found in Paper 3.

This headgroup-surface interaction makes a lot of sense from an inorganic chemistry perspective and permitted us to examine the adsorbate structure in more detail. Paper 4 discusses the details of a theoretical and infra-red spectroscopy study of the monolayers. A reliable computational method of predicting local structure and tilt angle for a given adsorbate onto $YBa_2Cu_3O_{7-\gamma}$ was developed, implemented, and reported in this contribution. The molecular mechanics-based algorithm was used to examine various alkylamine adsorbates and later was employed to study thiols and fluorinated alkylamine adsorbates. It was assumed that the primary interaction driving the spontaneous self-assembly process for the amines was the copper-nitrogen affinity. While we did have some evidence from computational studies that this was indeed the case, the SERS experiment (described above) was crucial to confirming our suspicions. Using the copper-nitrogen interactions as anchors, we examined various surface substitution patterns. The study concluded that the electronic footprint of primary amines were too large to cover every copper atom, but were small enough to sit upon every other copper center. The tails could then interact to produce a tightly packed monolayer. Two plausible geometries for these tails were uncovered using the computational approach. The tilt angle from these predicted geometries was found to be nearly identical to that measured on the primary amine/YBCO material with Grazing Reflectance Infrared Fourier Transform Spectroscopy (GRIFTS). This study also concluded that the footprints for secondary and tertiary amines are simply too large to result in any type of tight-packing of SAMS. In summary, the amines occupy every second copper center in an alternating fashion, then the tails interact to form nearly a crystalline structure that can exclude unwanted substances such as water or oxygen. Further molecular dynamics studies confirmed that water cannot penetrate the computationally-determined monolayer structure for primary amines.

Potential Uses for the materials.

Thin films of $(BEDT\text{-}TTF)_2I_3$ have been deposited onto a variety of substrates including glass, Si, MgO, Al_2O_3 and $LaAlO_3$ as well as $YBa_2Cu_3O_{7-\gamma}$. Details of these experiments are provided in Paper 5. Measurements by x-ray powder diffraction, atomic force microscopy and scanning electron microscopy reveal that when the organic material is deposited directly onto the cuprate superconductor films, poorly-crystalline and predominantly-disordered organic films are obtained. This behavior is in direct contrast to results acquired when $(BEDT\text{-}TTF)_2I_3$ films are deposited onto other substrates where highly-crystalline, *c*-axis oriented films of both nonsuperconducting-α and superconducting-β phases of $(BEDT\text{-}TTF)_2I_3$ are easily obtained. The self-assembly of an alkylamine monolayer onto the cuprate superconductor surface before $(BEDT\text{-}TTF)_2I_3$ thin film deposition fosters growth of ordered and crystalline organic films. The present work represents an important step in the direction of developing novel organic superconductor - insulator - cuprate superconductor structures.

The superconductor/insulator/superconductor tunnel junction can be used a fabricate a number of useful devices such as SQUIDS, ultrafast digital logic circuits, or submillimeter wave detectors. It is often difficult to control the thickness of the insulator layer in the conventional materials of this type. The monolayer organization process examined in this research providea easy control over the chemical composition, uniformity, and thickness of the organic layer. A $YBa_2Cu_3O_{7-\gamma}$/self-assembled monolayer/Cu tunnel junction was fabricated and examined. As detailed in Paper 6, the results are promising, but require further study.

Mechanism for the Formation of the Self-Assembled Monolayers

We believe we understand the structure of the self-assembled monolayer, where it is attached to the surface, and how to characterize the resulting material, but how does it form? The discussion concerning the mechanism for the self-assembly of thiols on gold has been ongoing for nearly 20 years with very little agreement in the scientific community. Much effort was allocated to determine the organization mechanism in our materials, and like the gold/thiol system, there is much controversy surrounding the formation of these SAMS. Our research has determined two plausible pathways for self-assembly of the primary amines on the YBCO surface. Surprisingly, there appears to be good experimental evidence for both pathways. While both of the co-PI's on this grant have strong opinions concerning which mechanism most closely resembles the actual process, I think it is safe to say that neither has been shown to be the definitive answer.

Mechanism 1: In this mechanism (Paper 7) alkylamine reagents etch away the passivation layer of the HTSC until fresh $YBa_2Cu_3O_7$ is uncovered. At that point, the amines adsorb and organize on the surface. The monolayers go on to form a pristine monolayer atop the superconducing material. XPS data supports the etching away of the passivation layer. Additional evidence for this mechanism is provided by atomic absorption spectroscopy, GC-MS, GRIFTS data, and four-point conductivity data.

Mechanism 2: In this mechanism (Papers 8 and 9) alkylamine reagents become oxidized to alkylimines upon their exposure to HTSC's and the superconductor is reduced. The resulting oxygen-deficient region now supports the formation of the self-assembled monolayers. Specifically, the amines attack the resulting Cu^{2+} atoms via an associative mechanism. Evidence for this mechanism comes from XPS, SERS, and secondary ion mass spectrometry.

III. Primary Personnel Associated with the Project:

Personnel at all three universities are actively involved in this project. The project involved 3 faculty, 2 postdoctoral fellows, seven graduate students, and six undergraduates.

Project Participant	*Status*	*Institution*
David R. Kanis	Faculty	CSU
Chad A. Mirkin	Faculty	NWU
John T. McDevitt	Faculty	UTA
Richard Piner	Postdoctoral Fellow	NWU/CSU
Jianai Zhao	Postdoctoral Fellow	UTA
Feng Xu	Graduate Student	NWU
Jin Zhu	Graduate Student	NWU
Jason Richie	Graduate Student	UTA
Marvin Clevenger	Graduate Student	UTA
Kate Lo	Graduate Student	UTA
Andra Wells	Graduate Student	UTA
Cyndi Wells	Graduate Student	UTA
Luckner Jean	Undergraduate Student	CSU/UTA
Carl Ankrum	Undergraduate Student	CSU/UTA
Brian Clay	Undergraduate Student	CSU/NWU
Michael Cannon	Undergraduate Student	CSU/NWU
Susan Schofer	Undergraduate Student	NWU

Current status of minority undergraduate students that spent summers in the McDevitt/Mirkin laboratories as part of this project:

Luckner Jean Matriculated to the Illinois Institute of Technology and received an engineering degree in chemical engineering. He will be attending graduate school in the fall of 2001.

Carl Ankrum Matriculated to the Illinois Institute of Technology and will be receiving a degree in Acoustical Engineering in the spring of 2002.

Brian Clay Graduated from Chicago State University with a B.S. in Chemistry. Graduated with Honors. Has worked at the EPA for two years and is currently applying to both medical schools and graduate schools.

Michael Cannon Received a B.S. in Chemistry from Chicago State University and was certified to teach high school chemistry. He is currently a high school chemistry teacher on the west side of Chicago in a very poor neighborhood.

IV. Published Papers from this Grant:

1. Xu. F.; Zhu, J.; Mirkin, C.A. "A Monolayer Growth and Exchange Kinetics for Alkylamines on the High Temperature Superconductor $YBa_2Cu_3O_{7-\delta}$, *Langmuir*, **2000**, *16*, 2169-2176.

2. "Surface Cleaning and Adsorbate Layer Formation: The Dual Role of Alkylamines in the Formation of Self-Assembled Monolayers on Cuprate Superconductors", *J. Am. Chem. Soc.*, **1999**, *121*, 7447-7448.

3. Walter, D.G.; Campbell, D.J.; Mirkin, C.A. "Photon-Gated Electron Transfer in Two-Component Self-Assembled Monolayers," *J. Phys. Chem. B* **1999**, *103*, 402-405.

4. Xu.F.; Chen, K.; Mirkin, C.A.; Ritchie, J.E.; McDevitt, J.T.; Cannon, M.O.; Kanis, D.R. "The Surface Coordination Chemistry of $YBa_2Cu_3O_{7-\delta}$," *Langmuir*, **1998**, *14*, 6505-6511.

5. Zhu, J.; Mirkin, C.A.; Braun, R.M.; Winograd, N. "Direct Oxidation of Alkylamines by $YBa_2Cu_3O_{7-\delta}$: A Key Step in the Formation of Self-Assembled Monolayers on Cuprate Superconductors," *J. Am. Chem. Soc.*, **1998**, *120*, 5126-5127.

6. Ritchie, J.E.; Wells, C.A.; Zhou, J.; Zhao, J.; McDevitt, J.T.; Ankrum, C.R.; Luckner J., Kanis, D.R. "Infrared and Computational Studies of Spontaneously Adsorbed Amine Reagents on $YBa_2Cu_3O_7$: Structural Characterization of Monolayers atop Anisotropic Superconductor Surfaces," *J. Am. Chem. Soc.*, **1998**, *120*, 2733-2745.

7. Mirkin, C.A.; Xu, F.; Zhu, J. "Controlling the Surface Properties of High Temperature Superconductors," *Adv. Mater.*, **1997**, *9*, 167-173.

8. McDevitt, J.T.; Ritchie, J.E.; Clevenger, M.B.; Lo, R.; Zhou, J.; Xu, F.; Mirkin, C.A. "Molecular Engineering of Organic Conductor / High-T_c Superconductor Assemblies," *Syn. Met.*, **1997**, *84*, 407-408.

9. Zhu, J.; Xu, F.; Schofer, S. J.; Mirkin, C. A. "The First Raman Spectrum of an Organic Monolayer on a High Temperature Superconductor: Direct Spectroscopic Evidence for a Chemical Interaction between an Amine and $YBa_2Cu_3O_{7-\delta}$," *J. Am. Chem. Soc.*, **1997**, *119*, 235-236.

10. McDevitt, J.T.; Lo, R.-K.; Ritchie, J.E.; Zhao, J.; Mirkin, C.A.; Xu, F.; and Chen K. "Molecular Level Control of the Surface Properties of High-T_c Superconductor Materials", Proceedings of the 10th Anniversary HTS Workshop on Physics, Materials and Applications, Edited by B. Batlogg, C.W. Chu, W.K.

Chu, D.U. Gubser, K.A. Muller, World Scientific, Singapore, *TCSUH Symposium Series*, Houston, TX, March **1996**, pp 181-182.

11. McDevitt, J.T.; Ritchie, J.E.; Jones, C.T.; Wells A.D.; and Mirkin, C.A. "Preparation and Study of Conductive Polymer / High-T_c Superconductor Assemblies," *Mat. Res. Soc. Symp. Proc.* Vol. 451 Boston, MA, September **1996**, pp 307-314.

12. Xu, F.; Chen, K.; Zhu, J.; Campbell, D.J.; Mirkin, C.A.; Lo, R.-K.; Zhao, J.; McDevitt, J.T. "Probing the Surface Coordination Chemistry of $YBa_2Cu_3O_{7-\delta}$," *Proc. Electrochem. Soc.*, **1996**, *3*.

13. J. T. McDevitt, J.P. Zhou C. E. Jones, R.-K. Lo, J. E. Ritchie, J. Zhao, C. A. Mirkin, F. Xu, K. Chen and J. Talvacchio, "Molecular and Crystal Engineering of High-T_c Superconductor Thin Film Structures and Devices," *ISTEC Conference Proceedings*, Iwate, Japan, June, **1996**.

14. Clevenger, M.B.; Zhao, J.; and McDevitt, J.T. "Use of a Self-Assembled Monolayer for the Preparation of Crystalline Organic Superconductor / High-T_c Superconductor Structures", *Chem. Mater.*, **1996,** *8*, 2693-2696.

15. McDevitt, J.T.; Lo, R.-K. Zhou, J.P.; Haupt, S.G.; Zhao, J.; Jurbergs, D.C.; Chen, K. and Mirkin, C.A. "Molecular Level Control Over the Interfacial Properties of High-T_c Superconductors", *Chem. Mater.*, **1996,** *8*, 811-813.

16. Lo, R.-K.; Zhou, J.; Zhao, J.; McDevitt, J.T.; Xu, F.; and Mirkin, C.A. "Polypyrrole Growth on $YBa_2Cu_3O_7$ Modified with Self-Assembled Monolayer of a N-(3-aminopropyl) Pyrrole: Hardwiring the Electronic Hot Spots on a Superconductor." *J. Am. Chem. Soc.*, **1996**, *118*, 11295-11296.

V. Honors/Awards Received During Grant Period

Kanis	Chicago State University Faculty Excellence Award (3 years)
Kanis	Project Kaleidoscope Faculty for the 21st Century Class of 1997
Kanis	Promoted to Associate Professor of Chemistry
McDevitt	Promoted to Professor of Chemistry
Mirkin	Promoted to Professor of Chemistry
Mirkin	Promoted to Charles E. and Emma H. Morrison Professor of Chemistry
Mirkin	B.F. Goodrich Collegiate Inventors Award (Given for the most outstanding collegiate invention in all of science, engineering, and medicine).
Mirkin	Materials Research Society Outstanding Young Investigator
Mirkin	ACS in Pure Chemistry
Mirkin	PLU Fresenius Award
Mirkin	Camille-Dreyfus Teacher-Scholar Award
Mirkin	E. Bright Wilson Prize

Surface Coordination Chemistry of $YBa_2Cu_3O_{7-\delta}$

Feng Xu, Kaimin Chen,† Richard D. Piner, and Chad A. Mirkin*

Department of Chemistry, Northwestern University, 2145 Sheridan Road, Evanston, Illinois 60208

Jason E. Ritchie‡ and John T. McDevitt*

Department of Chemistry and Biochemistry, University of Texas at Austin, Austin, Texas 78712

Michael O. Cannon and David Kanis*

Department of Chemistry, Chicago State University, Chicago, Illinois

Received February 5, 1998. In Final Form: August 13, 1998

The surface coordination chemistry of the cuprate superconductor, $YBa_2Cu_3O_{7-\delta}$ has been extensively surveyed using cyclic voltammetry in conjunction with a series of redox-active ferrocenyl containing adsorbate molecules. Evidence supporting the adsorption of molecules with primary alkylamine, secondary alkylamine, tertiary alkylamine, arylamine, thiol, disulfide, and selenol functionalities is reported. Cyclic voltammetry, atomic force microscopy, scanning electron microscopy, X-ray powder diffraction and resistivity vs temperature measurements were utilized to evaluate the influence of the modification conditions on the bulk and surface properties of the high-T_c superconductor. The spontaneous adsorption of redox-active alkylamines, arylamines, and thiols onto the surfaces of cuprate materials has been shown to produce stable and robust monolayer films with no apparent damage to the bulk properties of the underlying superconductors. Of the molecules studied thus far, primary alkylamines have been determined to be the optimum adsorbates based upon surface coverage values and monolayer durability. Tertiary alkylamines form monolayers on $YBa_2Cu_3O_{7-\delta}$ with an electrochemical persistence comparable to primary alkylamine monolayers, suggesting that hydrogen binding with the surface is not necessary for adsorption. We propose that amines act as Lewis bases and bind to Lewis acidic Cu surface site(s) in $YBa_2Cu_3O_{7-\delta}$ to form stable coordination bond(s).

Introduction

Surface modification chemistry, often referred to in the literature as molecular "self-assembly", has been developed and used extensively for three of the four important classes of electronic materials: metals, semiconductors, and insulators.[1,2] To date, monolayer films have been investigated for a wide range of adsorbate types and substrates: some of these include thiols, disulfides, sulfides, amines, and phosphines on Au,[1] carboxylic acids on metal oxides,[1a,c] trichloro- and trialkoxysilanes on oxide surfaces,[1a,c] thiols on GaAs,[2a] CdSe,[2b] CdS,[2b] InP,[2c] Cu,[3] and Ag,[1c] and thiols,[4a] olefins,[4b] isonitriles,[4c] and pyridine[4d] on Pt. This chemistry, which involves the chemical attachment of adsorbate molecules to a surface of interest and occasionally ordering of those adsorbate molecules into distinct and characterizable surface structures,[1,5] has been applied to a variety of fundamentally and technologically important areas. For example, chemical sensors,[6] novel photoresists,[7] materials with enhanced nonlinear optical properties,[8] contact microprinting methods,[9] and

* To whom correspondence should be addressed. E-mail: camirkin@chem.nwu.edu, mcdevitt@huckel.cm.utexas.edu.

† Now with Medtronics Inc. MN.

‡ Now with Kenan Laboratories of Chemistry, University of North Carolina, Chapel Hill, NC 27599.

(1) For reviews on monolayer films, see: (a) Ulman, A. *Chem. Rev.* **1996**, *96*, 1533. (b) Dubois, L. H.; Nuzzo, R. G. *Annu. Rev. Phys. Chem.* **1992**, *43*, 437. (c) Ulman, A. *An Introduction to Ultrathin Organic Films: From Langmuir–Blodgett to Self-assembly*; Academic: Boston, MA, 1991. (d) Bain, C. D.; Whitesides, G. M. *Angew. Chem., Int. Ed. Engl.* **1989**, *28*, 506.

(2) (a) Sheen, C. W.; Shi, J.-X.; Martensson, J.; Parikh, A. N.; Allara, D. L. *J. Am. Chem. Soc.* **1992**, *114*, 1514. (b) Natan, M. J.; Thackeray, J. W.; Wrighton, M. S. *J. Phys. Chem.* **1986**, *90*, 4089. (c) Gu, Y.; Lin, B.; Smentkowski, V. S.; Waldeck, D. H. *Langmuir* **1995**, *11*, 1849.

(3) (a) Laibinis, P. E.; Whitesides, G. M. *J. Am. Chem. Soc.* **1992**, *114*, 1990. (b) Laibinis, P. E.; Whitesides, G. M.; Allara, D. L.; Tao, Y.-T.; Parikh, A. N.; Nuzzo, R. G. *J. Am. Chem. Soc.* **1991**, *113*, 7152.

(4) (a) Lee, T. R.; Laibinis, P. E.; Folkers, J. P.; Whitesides, G. M. *Pure Appl. Chem.* **1991**, *63*, 821. (b) Lane, R. F.; Hubbard, A. T. *J. Phys. Chem.* **1973**, *77*, 1401. (c) Hickman, J. J.; Zou, C.; Ofer, D.; Harvey, P. D.; Wrighton, M. S.; Laibinis, P. E.; Bain, C. D.; Whitesides, G. M. *J. Am. Chem. Soc.* **1989**, *111*, 7271. (d) Stern, D. A.; Laguren-Davidson, L.; Frank, D. G.; Gui, J. Y.; Lin, C. H.; Lu, F.; Salaita, G. N.; Walton, N.; Zapien, D. C.; Hubbard, A. T. *J. Am. Chem. Soc.* **1989**, *111*, 877.

(5) (a) Caldwell, W. B.; Campbell, D. J.; Chen, K.; Herr, B. R.; Mirkin, C. A.; Malik, A.; Durbin, M. K.; Huang, K. G.; Dutta, P. *J. Am. Chem. Soc.* **1995**, *117*, 6071 and references therein. (b) Shi, X.; Caldwell, W. B.; Chen, K.; Mirkin, C. A. *J. Am. Chem. Soc.* **1994**, *116*, 11598. (c) Dhirani, A.-A.; Zehner, R. W.; Hsung, R. P.; Guyot-Sionnest, P.; Sita, L. R. *J. Am. Chem. Soc.* **1996**, *118*, 3319. (d) Liu, G.; Fenter, P.; Chidsey, C. E. D.; Ogletree, D. F.; Eisenberger, P.; Salmeron, M. *J. Chem. Phys.* **1994**, *101*, 4301. (e) Alves, C. A.; Porter, M. D. *Langmuir* **1993**, *9*, 3507. (f) Alves, C. A.; Smith, E. L.; Porter, M. D. *J. Am. Chem. Soc.* **1992**, *114*, 1222.

(6) (a) Mirkin, C. A.; Ratner, M. A. *Annu. Rev. Phys. Chem.* **1992**, *43*, 719. (b) Mirkin, C. A.; Valentine, J. R.; Ofer, D.; Hickman, J. J.; Wrighton, M. S. In *Biosensors and Chemical Sensors: Optimizing Performance through Polymeric Materials*; Edelman, P. G., Wang, J., Eds; ACS Symposium Series 487; American Chemical Society: Washington, DC, 1992; Chapter 17. (c) Hickman, J. J.; Ofer, D.; Laibinis, P. E.; Whitesides, G. M.; Wrighton, M. S. *Science* **1991**, *252*, 688. (d) Wells, M.; Crooks, R. M. *J. Am. Chem. Soc.* **1996**, *118*, 3988. (e) Elghanian, R.; Storhoff, J. J.; Mucic, R. C.; Letsinger, R. L.; Mirkin, C. A. *Science* **1997**, *277*, 1078. (f) Storhoff, J. J.; Elghanian, R.; Mucic, R. C.; Mirkin, C. A.; Letsinger, R. L. *J. Am. Chem. Soc.* **1998**, *120*, 1959.

(7) (a) Wollman, E. W.; Kang, D.; Frisbie, C. D.; Lorkovic, I. M.; Wrighton, M. S. *J. Am. Chem. Soc.* **1994**, *116*, 4395. (b) Wollman, E. W.; Frisbie, C. D.; Wrighton, M. S. *Langmuir* **1993**, *9*, 1517. (c) Tarlov, M. J.; Burgess, Jr., D. R. F.; Gillen, G. *J. Am. Chem. Soc.* **1993**, *115*, 5305.

10.1021/la980143n CCC: $15.00
Published on Web 10/02/1998

Scheme 1

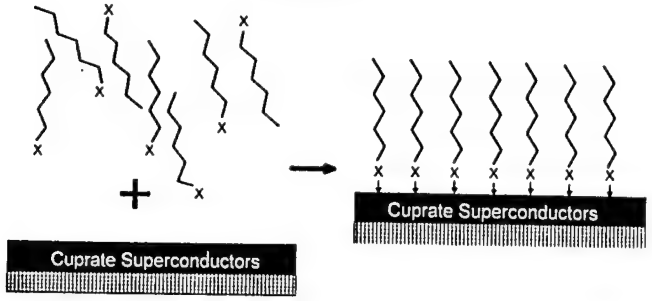

optically sensitive interfaces for proof-of-concept molecule-based actinometers[10] all have been developed via monolayer self-assembly methodology. In addition, self-assembled monolayers have been used to address important issues involving surface wetting,[1] interfacial electron transfer,[11] molecular conductivity,[12] and adhesion.[13]

Recently, we reported the first direct method for chemically modifying the surfaces of cuprate high-temperature superconductors (HTSCs) with monolayers of organic molecules with surface binding functional groups, Scheme 1 (X stands for surface binding functional groups).[14] This preliminary survey showed that alkylamines and a few other adsorbates such as arylamines and alkanethiols form films of varying degrees of stability and adsorbate coverage. Since then, it has been shown that judiciously designed organic monolayers for HTSC materials can be used for corrosion inhibition,[15] polymer adhesion[15] and nucleation,[16] preparation of organic superconductor/insulator/high-T_c superconductor trilayer structures,[17] and the fabrication of metal/insulator/superconductor tunnel junctions.[18] In this article we report a more extensive study of the types of functional groups that adsorb onto the surfaces of cuprate superconductors and the conditions necessary for forming electrochemically persistent monolayers. We also address possible binding interactions, in a preliminary manner, between the amino functional groups and the superconductor $YBa_2Cu_3O_{7-\delta}$.

Experimental Section

General Methods. Ferrocenecarboxylic acid, oxalyl chloride, methylamine hydrochloride, dimethylamine hydrochloride, triethylamine, propylamine, 1,4-diaminobutane, sodium azide, potassium cyanide, yttrium(III) oxide, copper(II) oxide, and barium carbonate were purchased from Aldrich Chemical Co., Inc., and used without further purification. Tetrabutylammonium hexafluorophosphate (n-Bu_4NPF_6) was recrystallized three times from ethanol and stored in a nitrogen atmosphere glovebox prior to use. Acetonitrile (CH_3CN), dichloromethane (CH_2Cl_2), and pentane were dried by refluxing over calcium hydride, while tetrahydrofuran (THF) and diethyl ether (Et_2O) were dried and distilled over sodium–benzophenone. Methanol and N,N'-dimethylformamide (DMF) were purchased from Fisher Scientific Inc. and used as received. NMR spectra were recorded on a Varian Gemini-300 FT NMR spectrometer, and electron impact (EI) mass spectra were obtained using a Fisions VG 70-250 SE mass spectrometer. Infrared absorption spectra were recorded on a Nicolet 520 Fourier transform infrared spectrometer with a MCT (HgCdTe) detector that was cooled with liquid nitrogen. Compounds p-ferrocenylaniline, **4**,[14] 11-mercaptoundecanoylferrocene, **5**,[19] bis[10-(ferrocenylcarbonyl)decyl] disulfide, **6**,[19] 6-ferrocenylhexaneselenol, **7**, ferrocenylmethanol, **8**,[14] 2-(ferrocenylcarboxamido)ethyl ferrocenylcarboxamide, **9**,[14] and 2-(diphenylphosphino)ethoxyferrocene, **10**, were prepared via literature methods. 6-(Ferrocenylcarbonyl)pentyl bromide, **14**, 4-(ferrocenylcarbonyl)propyl chloride, **15**, and 6-ferrocenylhexyl bromide were synthesized via routes similar to literature methods,[20,21] and ^1H NMR and mass spectra of these compounds match those reported in the literature. Details regarding the synthesis and characterization of compounds **1**–**3** and **11**–**13** are reported in the Supporting Information.

Preparation of $YBa_2Cu_3O_{7-\delta}$ Ceramic Samples. Y_2O_3 (99.9%), CuO (99.99+%), and $BaCO_3$ (99.99%) powder were mechanically blended in an agate ball mill. The powder was then pressed into 13 mm diameter pellets (applied pressure ~4000 psi, ~1 mm thick). The pellets were sintered at 900 °C for 1 day, ground with a mortar and a pestle, and resintered at 900 °C for another 24 h. This process was repeated two times. The subsequent material was then annealed at 450 °C overnight under an oxygen flow (pressure = 1 atm), followed by slow cooling under oxygen flow to room temperature. All samples displayed oxygen stoichiometries of 6.92–6.96, which were determined by iodometric titration,[22] and a superconducting transition temperature of ~92 K. XRD studies showed that the pellets prepared under these conditions were single-phase, orthorhombic $YBa_2Cu_3O_{7-\delta}$. Pellets were then fabricated into epoxy-encapsulated electrodes via literature methods.[23]

Preparation of $Bi_2Sr_2CaCu_2O_8$ Ceramic Samples. Superconductor $Bi_2Sr_2CaCu_2O_x$ powder (99.999%) was purchased from Strem Chemicals Inc. It was then pressed into pellets and calcined at 800 °C in air. The resulting pellet was characterized by powder XRD and magnetism measurements. The XRD patterns for such samples matched that of single phase $Bi_2Sr_2CaCu_2O_8$ and displayed a superconducting transition temperatures of 82 K.[24]

Preparation of $YBa_2Cu_3O_{7-\delta}$ Thin Films. High-T_c thin films were prepared using the method of pulsed laser ablation (PLD). Likewise, a stoichiometric target of $YBa_2Cu_3O_{7-\delta}$ was mounted in a deposition chamber which was evacuated to a base pressure of 1×10^{-7} Torr. A KrF excimer laser beam (248 nm, pulse width 30 ns) was focused onto the target at an angle of 45° to produce an energy density at the target surface of ~2 J·cm^2.

(8) Marks, T. J.; Ratner,M. A. *Angew. Chem., Int. Ed. Engl.* **1995**, *34*, 155.
(9) (a) Kumar, A.; Abbott, N. L.; Kim, E.; Biebuyck, H. A.; Whitesides, G. M. *Acc. Chem. Res.* **1995**, *28*, 219. (b) Xia, Y.; Whitesides, G. M. *J. Am. Chem. Soc.* **1995**, *117*, 3274. (c) Kumar, A.; Whitesides, G. M. *Appl. Phys. Lett.* **1993**, *63*, 2002.
(10) (a) Kawanishi, Y.; Tamaki, T.; Sakuragi, M.; Seki, T.; Suzuki, Y.; Ichimura, K. *Langmuir* **1992**, *8*, 2601. (b) Ichimura, K.; Suzuki, Y.; Seki, T.; Hosoki, A.; Aoki, K. *Langmuir* **1988**, *4*, 1214.
(11) (a) Finklea, H. O. In *Electroanalytical Chemistry*; Bard, A. J., Ed.; Marcel Dekker: New York, 1995; Vol. 19, Chapter II, p 109. (b) Herr, B. R.; Mirkin, C. A. *J. Am. Chem. Soc.* **1994**, *116*, 1157. (c) Campbell, D. J.; Herr, B. R.; Hulteen, J. C.; Van Duyne, R. P.; Mirkin, C. A. *J. Am. Chem. Soc.* **1996**, *118*, 10211. (d) Weber, K.; Hockett, L. A.; Creager, S. E. *J. Phys. Chem. B* **1997**, *101*, 8286.
(12) (a) Bumm, L. A.; Arnold, J. J.; Cygan, M. T.; Dunbar, T. D.; Burgin, T. P.; Jones, L., II; Allara, D. L.; Tour, J. M.; Weiss, P. S. *Science* **1996**, *271*, 1705. (b) Samanta, M. P.; Tian, W.; Datta, S.; Henderson, J. I.; Kubiak, C. P. *Phys. Rev. B* **1996**, *53*, 7626.
(13) Rozsnyai, L. F.; Wrighton, M. S. *Chem. Mater.* **1996**, *8*, 309.
(14) Chen, K.; Mirkin, C. A.; Lo, R.; Zhao, J.; McDevitt, J. T. *J. Am. Chem. Soc.* **1995**, *117*, 6374.
(15) McDevitt, J. T.; Mirkin, C. A.; Lo, R.; Chen, K.; Zhou, J.; Xu, F.; Haupt, S. G.; Zhao, J.; Jurbergs, D. C. *Chem. Mater.* **1996**, *8*, 811.
(16) Lo, R.-K.; Ritchie, J. E.; Zhou, J.-P.; Zhao, J.; McDevitt, J. T.; Xu, F.; Mirkin, C. A. *J. Am. Chem. Soc.* **1996**, *118*, 11295.
(17) Clevenger, M. B.; Zhao, J.; McDevitt, J. T. *Chem. Mater.* **1996**, *8*, 2693.
(18) (a) Covington, M.; Xu, F.; Mirkin, C. A.; Feldmann, W. L.; Greene, L. H. *Czech. J. Phys.* **1996**, *46*, 1341. (b) Covington, M.; Aprili, M.; Paraoanu, E.; Greene, L. H.; Xu, F.; Zhu, J.; Mirkin, C. A. *Phy. Rev. Lett.* **1997**, *79*, 277.
(19) Hickman, J. J.; Ofer, D.; Zou, C.; Wrighton, M. S.; Laibinis, P. E.; Whitesides, G. M. *J. Am. Chem. Soc.* **1991**, *113*, 1128.
(20) Fort, Y.; Caubere, P. Gautier, J. C.; Mondet, J. C. *J. Organomet. Chem.* **1993**, *452*, 111.
(21) Creager S. E.; Rowe, G. K. *J. Electroanal. Chem.* **1994**, *370*, 203.
(22) Otzschi, K. Ph.D. Thesis, University of Tokyo, 1995.
(23) (a) Riley, D. R.; McDevitt, J. T. *J. Electroanal. Chem.* **1990**, *295*, 373. (b) McDevitt, J. T.; Longmire, M.; Gollmar, R.; Jernigan, J. C.; Dalton, E. F.; McCarley, R.; Murray, R. W.; Little, W. A.; Yee, G. T.; Holcomb, M. J.; Hutchinson, J. E.; Collman, J. P. *J. Electroanal. Chem.* **1988**, *243*, 465.
(24) Jin, S.-G.; Zhu, Z.-Z.; Liu, L.-M.; Huang, Y.-L. *Solid State Comm.* **1990**, *74*, 1087.

Table 1. Surface Coverages for Redox-Active Adsorbates

"Ligands" (Fc: ferrocenyl)		surface coverage[a] ($\times 10^{-9}$ mol/cm^2)	
formula	no.	ceramic	thin film
$FcC(O)NH(CH_2)_4NH_2$ (alkyl amine)	1	4	2
$Fc(CH_2)_6NHCH_3$ (secondary amine)	2	0.7	0.2
$Fc(CH_2)_6N(CH_3)_2$ (tertiary amine)	3	0.5	0.05
p-Fc-$C_6H_4NH_2$ (aryl amine)	4	0.4	0.02
$FcC(O)(CH_2)_{10}SH$ (thiol)	5	2	0.9
$(FcC(O)(CH_2)_{10}S)_2$ (disulfide)	6	0.5	0.03
$Fc(CH_2)_6SeH$ (selenol)	7	0.7	0.1
$FcCH_2OH$ (alcohol)	8	NS[b]	NS
$(FcC(O)NHCH_2)_2$ (amide)	9	NS	NS
$FcO(CH_2)_2PPh_2$ (phosphine)	10	NS	NS
$FcC(O)(CH_2)_5N_3$ (azide)	11	NS	NS
$Fc(CH_2)_6CN$ (nitrile)	12	NS	NS
$FcC(O)NHCH_2C_5H_4N$ (pyridine)	13	NS	NS
$FcC(O)(CH_2)_5Br$ (bromide)	14	NS	NS
$FcC(O)(CH_2)_3Cl$ (chloride)	15	NS	NS

[a] All data reported in this table were calculated from cyclic voltammetry performed in 0.1 M n-Bu_4NPF_6/CH_3CN. All electrodes were modified in ~1 mM CH_3CN solutions of the adsorbates. [b] No significant surface coverage was measured.

The substrates (MgO 100) were mounted at a distance of 5 cm from the target surface. Optimal results were obtained for films deposited at a substrate heater temperature of 770 °C with a deposition rate of ~1 Å per pulse and oxygen partial pressure of ~100 mTorr. After deposition, the samples were cooled to 450 °C and were kept at this temperature for approximately 20 min in the presence of 1 Torr of oxygen. The films were then cooled to room temperature in the same oxygen atmosphere. All film samples prepared by these methods were shown to exhibit single-phase behavior by XRD with c-axis orientation perpendicular to the substrate surface.

Atomic Force Microscopy Measurements. All data presented in this paper were obtained with a Park Scientific Model CP AFM with a combined AFM/LFM head. Cantilevers (model no. MLCT-AUNM) with the following specifications were obtained from Park Scientific: gold coated microlever, silicon nitride tip, cantilever A, and spring constant = 0.05N/m. The AFM is mounted in a Park vibration isolation chamber, which has been modified with a dry nitrogen purge line.

Scanning Electron Microscopy. Surface morphologies of each batch of $YBa_2Cu_3O_{7-\delta}$ ceramic pellets were examined by a Hitachi S570 scanning electron microscope. Accelerating voltage was 15 or 20 keV. Working distance was in the range of 25–30 mm, and samples were connected to a metal sample holder with a conducting graphite tape.

Modification of HTSC Electrodes with Adsorbates 1–15. All modification and electrochemical measurements were performed in a Vacuum Atmospheres glovebox under dry nitrogen environment. Epoxy-encapsulated ceramic electrodes that were prepared by literature methods[23] were cut with a razor blade and sanded with 300 grit sand paper until a small portion of the ceramic was exposed. The electrodes were then sonicated in dry CH_3CN to remove ceramic debris. After sonication, the ceramic electrodes were immediately transferred into the glovebox. In the case of thin film substrates, they were stored in a plastic container with drierite (97% $CaSO_4$, 3% $CoCl_2$) prior to use. Both thin film and ceramic substrates were soaked in 1 mM CH_3CN solution of adsorbates **1**–**15** for 2 days. The electrodes were then removed from the soaking solution and rinsed with copious amounts of CH_2Cl_2 and CH_3CN prior to making any physical measurements.

Electrochemical Measurements. Cyclic voltammetry was performed on a Pine AFRDE4 or Pine AFRDE5 bipotentiostat with a Kipp en Zonen BD90 X-Y or Linseis LY 1400 recorder. A conventional three-electrode cell was used for all electrochemical experiments. Each cell consisted of a ceramic or thin film superconductor working electrode, a Pt gauze counter electrode, and a $Ag/AgNO_3(CH_3CN)$ reference electrode or a Ag wire quasi-reference electrode. All electrochemical measurements were performed in 0.1 M n-Bu_4NPF_6/CH_3CN solution unless otherwise noted. Note: when thin film electrodes were soaked in pentane solutions of **10**–**12** and subsequently rinsed with THF, they occasionally exhibited evidence for adsorption of these molecules by cyclic voltammetry in 0.1 M n-Bu_4NPF_6/THF. However, the electrochemical response was nonideal and reproducibility under these conditions was low.

Results and Discussion

Adsorption Behavior and Cyclic Voltammetry of Redox-Active "Ligands" 1–15 on Ceramic $YBa_2Cu_3O_{7-\delta}$. Polycrystalline HTSC substrates were modified by soaking them in 1 mM CH_3CN solutions of the appropriate redox-active adsorbate molecules at room temperature for 2 days; surface coverages were determined by cyclic voltammetry and the current associated with oxidation/reduction of the redox-active ferrocenyl groups. The ferrocenyl group was chosen as the electrochemical probe for three reasons: (1) ferrocene has stable electrochemical behavior in various solvent media; (2) its $E_{1/2}$ is compatible with the potential windows of stability associated with the cuprate superconductors;[23] (3) the organic chemistry of ferrocene is well-established, so it can be easily functionalized with potential surface binding functionalities.[25] Others also have taken advantage of the ferrocenyl moiety as a redox probe for studying monolayer related processes.[11,26]

A series of epoxy-encapsulated polycrystalline $YBa_2Cu_3O_{7-\delta}$ ceramic electrodes and c-axis-oriented $YBa_2Cu_3O_{7-\delta}$ thin film electrodes were soaked in 1 mM CH_3CN solutions of each redox-active ferrocenyl adsorbate molecule, Table 1. Functional groups explored include: a primary alkylamine **1**, a secondary alkylamine **2**, a tertiary alkylamine **3**, an arylamine **4**, a thiol **5**, a disulfide **6**, a selenol **7**, an alcohol **8**, an amide **9**, a phosphine **10**, an azide **11**, a nitrile **12**, a pyridine **13**, a bromide **14**, and a chloride **15**. After soaking for 2 days in solutions of the redox-active species, the electrodes were thoroughly rinsed with CH_3CN and CH_2Cl_2, solvents in which the molecular species are highly soluble. Cyclic voltammetry and the redox activity of the ferrocenyl groups were then used to determine the extent of surface modification for each adsorbate and the electrochemical stabilities of the resulting monolayers.

Only compounds **1**–**7** exhibit significant measurable surface coverages, Table 1. For example, the cyclic voltammetry of a polycrystalline $YBa_2Cu_3O_{7-\delta}$ ceramic electrode modified with **1** exhibited a wave associated with

(25) *Ferrocenes: Homogeneous catalysis, organic synthesis, materials science*; Togni, A., Hayashi, T., Eds.; VCH: New York, 1995.

(26) (a) Chidsey, C. E. D.; Carolyn, R. B.; Putvinski, T. M.; Mujsce, A. M. *J. Am. Chem. Soc.* **1990**, *112*, 4301. (b) Chidsey, C. E. D. *Science* **1991**, *251*, 919. (c) Gardner, T. J.; Frisbie, C. D.; Wrighton, M. S. *J. Am. Chem. Soc.* **1995**, *117*, 6927. (d) Collard, D. M.; Fox, M. A. *Langmuir* **1991**, *7*, 1192.

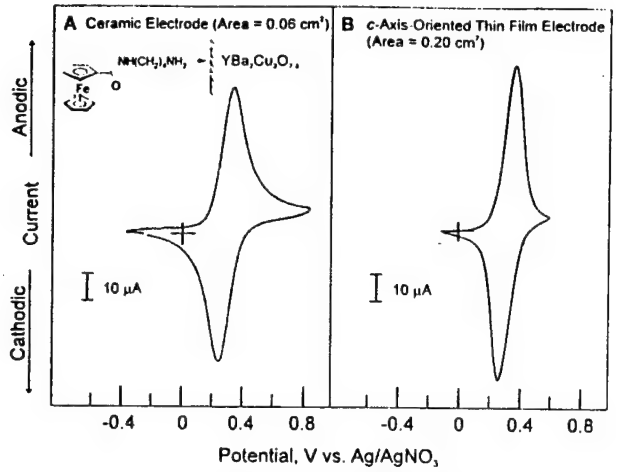

Figure 1. Cyclic voltammetry of a redox-active adsorbate **1** on (A) a *c*-axis-oriented thin film $YBa_2Cu_3O_{7-\delta}$/MgO(100) electrode; and (B) an epoxy-encapsulated polycrystalline $YBa_2Cu_3O_{7-\delta}$ ceramic electrode. Scan rates in both experiments were 200 mV/s. Electrochemistry was done in 0.1 M *n*-Bu_4NPF_6/CH_3CN solution.

ferrocenyl oxidation/reduction at $E_{1/2} = +0.30$ V vs Ag/$AgNO_3$ nonaqueous reference electrode, Figure 1A. This response, which is quite comparable to that observed for surface-confined monolayers of ferrocenyl alkanethiols adsorbed onto noble metal substrates,[27] was persistent over repeated cycling in the potential window between −0.35 and +0.85 V vs Ag/$AgNO_3$. The surface coverage for **1** on the $YBa_2Cu_3O_{7-\delta}$ ceramic electrode, Table 1, which was determined by integrating the current associated with ferrocenyl oxidation/reduction, was 4×10^{-9} mol/cm^2, and it is approximately 10 times that expected for a monolayer of **1** on an ideally flat substrate (0.45×10^{-9} mol/cm^2).[14] Note that adsorbate surface coverages for SAMs comprised of ferocenylalkanethiols on Au(111) typically exhibit surface coverages in the range of 0.3 to 0.7×10^{-9} mol/cm^2, depending upon surface roughness.[27] The large surface coverage values for the ceramic HTSC electrodes can be attributed, in part, to the extremely rough surface morphologies and high porosities that are characteristic of such electrodes.[28] SEM images of $YBa_2Cu_3O_{7-\delta}$ pellets show that the ceramic material is microporous and consists of micron-sized grains with distinct boundaries, Figure 2A. Adsorbate molecules also may diffuse through the micropores of the electrode and adsorb onto the internal surface of the electrodes, thus contributing to the high surface coverages.

Compounds **8**−**15** which have functionalities that potentially could serve as ligands for metal ions were repeatedly examined by electrochemistry. They displayed no significant measurable coverages under adsorption conditions comparable to those used for adsorbates **1**−**7**.

Adsorption Behavior of 1−15 on *c*-Axis-Oriented $YBa_2Cu_3O_{7-\delta}$ Thin Films. If one is to use surface modification chemistry for the preparation of superconducting devices, it is important to demonstrate the viability of such chemistry on oriented thin films of $YBa_2Cu_3O_{7-\delta}$ and determine the effect of chemical modification on the superconducting properties of such materials. Accordingly, compounds **1**−**7** were found to adsorb spontaneously onto laser ablated *c*-axis-oriented films of $YBa_2Cu_3O_{7-\delta}$ to form redox-active monolayers; surface coverage data is given in Table 1. For example, the cyclic voltammetry of a *c*-axis-oriented film of $YBa_2Cu_3O_{7-\delta}$ modified with **1** exhibits a wave indicative of a surface confined species, associated with ferrocenyl oxidation/reduction at +0.30 V vs Ag/$AgNO_3$ electrode (ΔE_p approaching 0 at low scan rates and $i_p \propto$ scan rate), Figure 1B. The surface coverage for **1** on the $YBa_2Cu_3O_{7-\delta}$ film (2×10^{-9} mol/cm^2) is lower than that measured for ceramic electrodes modified with **1**, but it is still larger than that expected for a perfectly flat surface. Indeed, AFM images of these superconductor films show that they are substantially rough on the hundred nanometer scale, Figure 3.

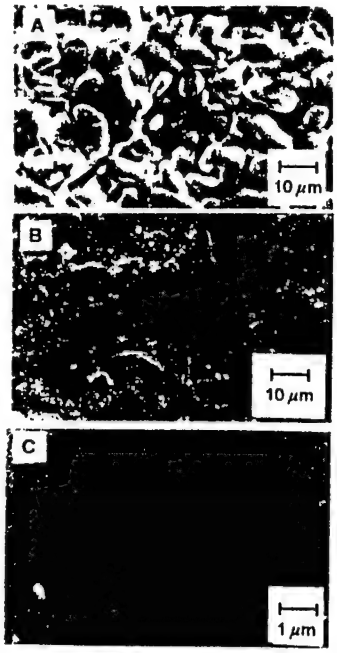

Figure 2. Series of scanning electron micrographs for a number of $YBa_2Cu_3O_{7-\delta}$ samples having different geometries. Shown in part A is an as prepared ceramic pellet, part B shows a similar sample that was treated with 300 grit sand paper, and part C shows a *c*-axis-oriented thin film of $YBa_2Cu_3O_{7-\delta}$ (1500 Å) that is supported on a single-crystal MgO (100) substrate.

Of the 15 compounds studied, primary alkylamine **1** always yielded the largest surface coverages and the most persistent electrochemical response. For monolayers of **1**, some loss of signal was typically observed during the first few scans, which may be attributed to the release of adsorbates physically trapped in the porous superconductor and/or the desorption of weakly bonded adsorbate molecules. However, subsequent scanning between −0.2 and +0.6 V vs Ag/$AgNO_3$ (up to 50 cycles at 200 mV/s) did not result in detectable loss in electroactivity. Primary alkylamine **1**, secondary alkylamine **2**, and tertiary alkylamine **3** display a decreasing trend in apparent surface coverage (Γ):

$$\Gamma(\text{primary amine}) > \Gamma(\text{secondary amine}) > \Gamma(\text{tertiary amine}) \quad (1)$$

which is presumably due to the respective increase in molecular footprints and also the inefficiency in packing that accompanies an increase in headgroup size. The variations in substrate surface roughness also could contribute to this apparent trend. Note, however, that the electrochemical stabilities of monolayer films of secondary amine **2** and tertiary amine **3** on $YBa_2Cu_3O_{7-\delta}$

(27) (a) Murray, R. W. In *Molecular Design of Electrode Surfaces*; Marray, R. W., Ed.; Wiley: New York, 1992. (b) Finklea, H. O. In *Electroanalytical Chemistry*; Bard, A. J., Ed.; Marcel Dekker: New York, 1995; Vol. 19, Chapter V, p 248.

(28) McDevitt, J. T.; Haupt, S. G.; Jones, C. E. In *Electroanalytical Chemistry*; Bard, A. J., Rubinstein, I., Eds.; Marcel Dekker: New York, 1996; Vol. 19, p 338.

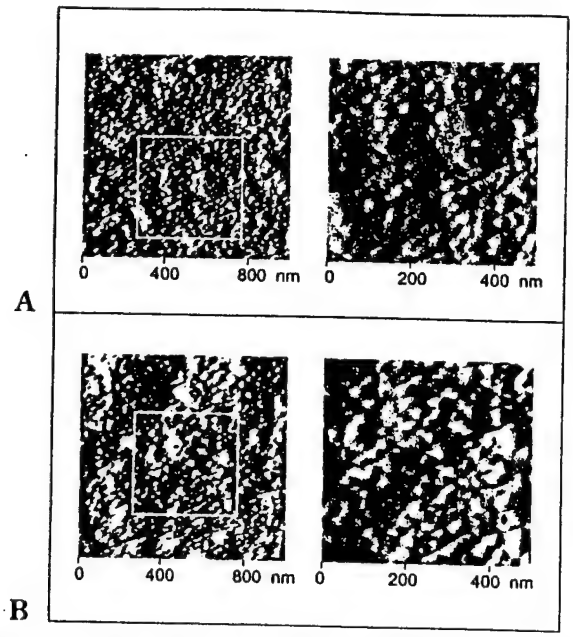

Figure 3. AFM images of a *c*-axis-oriented $YBa_2Cu_3O_{7-\delta}$ thin film electrode: (A) before modification; (B) after soaking in a dry 1 mM CH_3CN solution of **1** for 2 days. Images on the right side correspond to squares on the left side. Images were recorded in force mode.

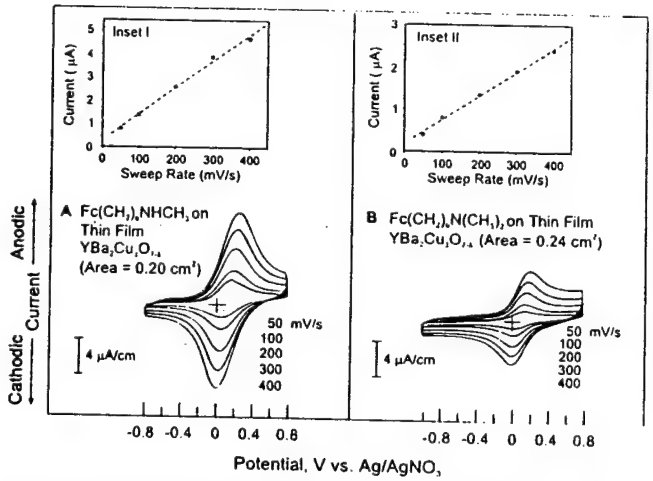

Figure 4. Cyclic voltammetry of surface-confined secondary amine **2** (A) and tertiary amine **3** (B) on *c*-axis-oriented thin film $YBa_2Cu_3O_{7-\delta}$/MgO(100) electrodes. Insets I and II show the expected linear relationships between sweep rate and peak current for surface confined redox-active species. Electrochemistry was done in 0.1 M *n*-Bu_4NPF_6/CH_3CN solution.

are comparable to that of primary amine **1** as evidenced by the persistence of their electrochemical responses, Figure 4A and 4B. Monolayers of compounds **1**–**3** each displayed greater than 90% of the original electroactivity after 50 cycles. In contrast, monolayer films of alkanethiol **5**, alkyl disulfide **6**, and alkaneselenol **7** on $YBa_2Cu_3O_{7-\delta}$ thin films (and ceramic) electrodes exhibited a slow, but steady loss (up to 40% after 30 cycles) in electroactivity as a result of repeated cycling under comparable conditions. No significant surface coverages were detected for adsorbates **8**–**15** via this method under comparable conditions, Table 1.

Influence of Surface Modification on the Properties and Structure of $YBa_2Cu_3O_{7-\delta}$. An important issue pertains to the effects of surface modification on the normal state, superconductivity, and other bulk properties of the material. To address this issue, AFM, resistivity vs

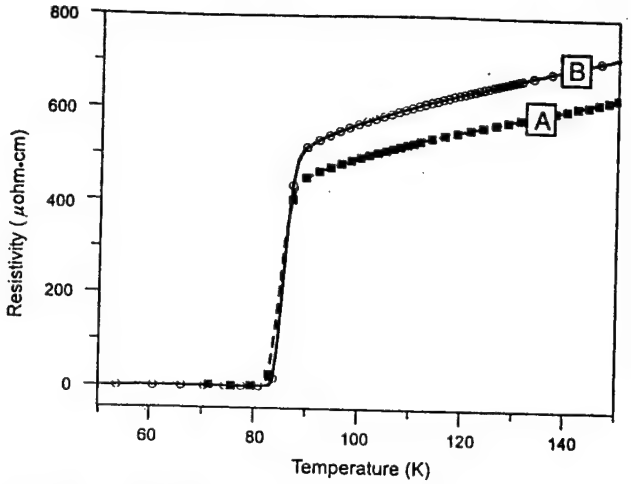

Figure 5. Resistivity vs temperature curves acquired for a $YBa_2Cu_3O_{7-\delta}$ thin film (1500 Å) supported on a MgO (100) substrate. Two plots are shown for the sample (A) before (■) and (B) after (○) 18 h soaking in a 1 mM solution of **1** in dry CH_3CN. The samples were analyzed using the four-point conductivity technique as the film was cooled with liquid helium. The T_c (critical temperature) of the modified material, within experimental error, is unchanged from the untreated film.

temperature, magnetization, and XRD measurements on $YBa_2Cu_3O_{7-\delta}$ were performed before and after surface modification.

The AFM method was employed to study the general surface morphology of $YBa_2Cu_3O_{7-\delta}$ as a function of surface modification. Before modification, $YBa_2Cu_3O_{7-\delta}$ films prepared by the PLD method appeared smooth by optical microscopy and SEM, Figure 2C, but AFM showed they were substantially rough at the micrometer and nanometer length scales. Images of a typical film showed grains and particles with diameters in the ~10–100 nm range scattered over the surface, Figure 3A. When a $YBa_2Cu_3O_{7-\delta}$ film was modified with **1**, there was no apparent change in the surface morphology of the film, at least on the 100 nm length scale.[29] Films modified with other amine adsorbates, such as hexylamine and octadecylamine, also yielded similar results. However, morphology changes must be taking place on the atomic length scale since extended soaking of $YBa_2Cu_3O_{7-\delta}$ in amine solutions is known to result in Cu^{2+} sequestration and the formation of Cu-amine coordination complexes in solution.[30] This issue along with a detailed analysis of the products formed in this reaction are being addressed in a separate study.[31]

Resistivity vs temperature measurements were performed on a *c*-axis-oriented thin film of $YBa_2Cu_3O_{7-\delta}$ before and after modification with **1** to investigate the effect of surface modification on superconductivity. The resistivity vs temperature plots for a representative film before and after surface modification with **1** in CH_3CN show little, if any, measurable decrease in T_c as a result of chemical modification, Figure 5. No noticeable decrease in T_c for the superconductor was noted after modification for short periods of time (3 h), as well as for longer term treatments (48 h). However, the latter exposures were found to increase room-temperature resistivity values by ~5%. Magnetism vs temperature measurements of polycrystalline $YBa_2Cu_3O_{7-\delta}$ powder also displayed unchanged

(29) The initial work, ref 14, was not descriptive with respect to the term "nanometer length scale" and unintentionally may have implied a smaller length scale.

(30) James, P. M.; Thompson, E. J.; Ellis, A. B. *Chem. Mater.*, **1991**, *3*, 1087.

(31) Xu, F.; Piner, R.; Mirkin, C. A., Manuscript in preparation.

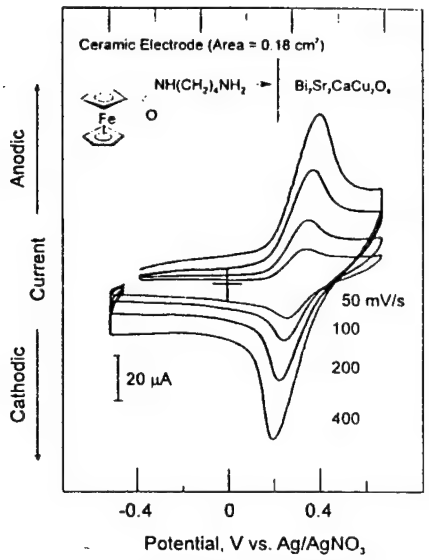

Figure 6. Cyclic voltammetry of adsorbate **1** on an epoxy-encapsulated polycrystalline $Bi_2Sr_2CaCu_2O_8$ ceramic electrode. Electrochemistry was done in 0.1 M n-Bu_4NPF_6/CH_3CN solution.

Meissner signals before and after soaking in solutions of amine adsorbates for 2 days. Under these conditions the bulk superconductivity of $YBa_2Cu_3O_{7-\delta}$ is unaffected by surface modification with alkylamine reagents.

Finally, $YBa_2Cu_3O_{7-\delta}$ powder was characterized by XRD as a function of surface modification. Freshly prepared polycrystalline $YBa_2Cu_3O_{7-\delta}$ pellets were hand-ground in an agate mortar. Powder prepared in this way (0.2 to 10 μm by size) was soaked in a CH_3CN solution of propylamine for 2 days. The powder was filtered and dried under vacuum (~100 μmHg) for 2 h. XRD measurements were taken before and after modification (see Supporting Information for the spectra). No detectable change in the XRD pattern was observed under these conditions with polycrystalline $YBa_2Cu_3O_{7-\delta}$ powder retaining its single-phase orthorhombic structure. $YBa_2Cu_3O_{7-\delta}$ powders soaked in carefully dried organic solvents such as pentane and CH_3CN also produce identical XRD patterns before and after soaking. Therefore, the bulk structure and superconductivity of $YBa_2Cu_3O_{7-\delta}$ are not significantly altered under the conditions used for surface modification.

The Nature of Bonding between Amine Adsorbates and $YBa_2Cu_3O_{7-\delta}$. This amine adsorption chemistry has been extended to another cuprate oxide, $Bi_2Sr_2CaCu_2O_8$. Electrodes prepared from polycrystalline $Bi_2Sr_2CaCu_2O_8$, which were soaked in a 1 mM CH_3CN solution of **1** for 2 days, exhibited stable cyclic voltammetry associated with surface-confined **1**, Figure 6. More than 80% of the current associated with oxidation/reduction of surface-adsorbed **1** was preserved after 30 cycles at 200 mV/s. The surface coverage of **1** on $Bi_2Sr_2CaCu_2O_8$ was determined to be 5×10^{-9} mol/cm^2, which is comparable with that observed for **1** on $YBa_2Cu_3O_{7-\delta}$ ceramic electrodes, Table 1. Unfortunately, due to the complicated microstructure of ceramic superconductors and different preparation methods, cross comparison of surface coverages on different cuprate ceramic superconductors can be misleading. However, qualitatively, all of these data suggest that copper, which is the only common metal element present in these two oxides, is likely involved in amine bonding with the HTSC surface.

The surface active site(s) for adsorbate binding is an important fundamental issue which needs to be addressed. The $YBa_2Cu_3O_{7-\delta}$ compound is a quaternary metal oxide with three different metal ions. For the reactions involving all of these adsorbates, the nature of the adsorbed species could be quite complicated, especially since $YBa_2Cu_3O_{7-\delta}$ is a strongly oxidizing material. Since amines are the best adsorbates of the ones studied thus far (Table 1), we have focused our initial efforts on the characterization of the adsorption reaction between amines and $YBa_2Cu_3O_{7-\delta}$. The observation that primary amine **1**, secondary amine **2**, tertiary amine **3**, and arylamine **4** display strong affinities for $YBa_2Cu_3O_{7-\delta}$ suggests that surface active sites are metal-based, and hydrogen bonding between adsorbate and substrate is not necessary. Amines are strong Lewis bases and common ligands used in Cu coordination chemistry,[32a] although amine–alkaline earth element coordination compounds[32b] and amine lanthanide coordination compounds also are known.[32c] In view of our observations reported in this manuscript and the studies by Ellis et al., which show $YBa_2Cu_3O_{7-\delta}$ reacts with chelating diamines in aqueous solution to form Cu(II)–amine coordination complexes, it is likely that amines are anchoring to Cu sites on the $YBa_2Cu_3O_{7-\delta}$ substrate in these monolayer films. Indeed, secondary ion mass spectrometry (SIMS) studies carried out during the course of writing and reviewing this manuscript have now confirmed this hypothesis.[33]

Conclusion

We have synthesized a series of ferrocenylalkyl and ferrocenylaryl compounds, each possessing a potential surface binding functional group, and tested their chemical affinity for the cuprate HTSC, $YBa_2Cu_3O_{7-\delta}$. Through this survey, we have identified several adsorbate types **1**-**7** which show high affinities for $YBa_2Cu_3O_{7-\delta}$. Although several of these molecule types form stable monolayer films, the functional group of choice, which has emerged from these studies, is the alkylamine group.

This survey is the most extensive study of the surface modification chemistry of the HTSC, and the methodology reported herein provides an alternative to the indirect methods that others have used to modify these important materials.[34] The adsorption of alkylamines on $YBa_2Cu_3O_{7-\delta}$ involves the coordination of amino groups to Lewis acidic Cu sites on the HTSC surface, and hydrogen bonding between the amino groups of the adsorbates and oxygen atom sites on the surface is not required for adsorption since tertiary amines also form stable monolayer films.

Finally the surface and bulk properties of $YBa_2Cu_3O_{7-\delta}$ (both c-axis-oriented thin film and polycrystalline ceramic samples) modified with a variety of amine adsorbates were extensively characterized. On the basis of these studies, we conclude that the modification process is a nondestructive method with respect to the bulk properties of $YBa_2Cu_3O_{7-\delta}$ and superconductivity of the material. Therefore, from a methodology stand point, this is an excellent way of tailoring the surface and interfacial properties of this important class of materials. Surface-sensitive techniques are needed to fully understand the

(32) (a) Fenton, D. E. In *Comprehensive Coordination Chemistry*; Wilkinson, G., Gillard, R. D., McCleverty, J. A., Eds.; Pergamon: New York, 1987; Vol. 3, Chapter 23. (b) Hart, F. A. In *Comprehensive Coordination Chemistry*; Wilkinson, G., Gillard, R. D., McCleverty, J. A., Eds.; Pergamon: New York, 1987; Vol. 3, Chapter 39. (c) Hathaway, B. J. In *Comprehensive Coordination Chemistry*; Wilkinson, G., Gillard, R. D., McCleverty, J. A., Eds.; Pergamon: New York, 1987; Vol. 5, Chapter 53.

(33) Zhu, J.; Mirkin, C. A.; Braun, R. M.; Winograd, N. *J. Am. Chem. Soc.* **1998**, *120*, 5126.

(34) Peck, S. R.; Curtin, L. S.; Tender, L. M.; Carter, M. T.; Terrill, R. H.; Murray, R. W.; Collman, J. P.; Little, W. A.; Duan, H. M.; Dong, C.; Hermann, A. M. *J. Am. Chem. Soc.* **1995**, *117*, 1121.

potentially complex coordination chemistry between amino groups and $YBa_2Cu_3O_{7-\delta}$ and to determine the structure of the monolayers formed on this inorganic oxide. Efforts in this direction are underway.

Acknowledgment. C.A.M., D.K., and J.T.M. acknowledge the AFOSR (F49620-96-1-0133) for support of this work. This work also is supported in part by the NSF (Grant DMR 91-20000) through the Science and Technology Center for Superconductivity. C.A.M. also acknowledges a Camille Dreyfus Teacher Scholar Award, a Beckman Young Investigator Award, a National Science Foundation Young Investigator Award, and a Naval Young Investigator Award. J.T.M. also acknowledges a National Science Foundation Young Investigator Award and an Exxon Education Foundation Award, and thanks the ONR (N00014-94-1-0706), the Welch Foundation (UTA-96-0366) for support of this effort. Professor Kenneth R. Poeppelmeier is thanked for use of his instrumentation, and Dr. K. Otzschi is acknowledged for assistance with superconductor preparation. Dr. Dean J. Campbell and Mr. Joshua R. Farrell are thanked for samples of compounds **7** and **10**.

Supporting Information Available: Text giving synthesis and characterization of compounds **1**–**3** and **11**–**13**; including magnetism measurement and X-ray powder diffraction data of ceramic superconductors before and after modification and a figure showing XRD patterns (5 pages). Ordering and Internet access information is given on any current masthead page.

LA980143N

ADVANCED MATERIALS

Paper 2

Research News

Controlling the Surface Properties of High Temperature Superconductors**

By Chad A. Mirkin,* Feng Xu, and Jin Zhu

1. Introduction

Molecular monolayer-based surface modification chemistry, often referred to in the literature as "self-assembly", has been developed and used extensively for three of the four important classes of electronic materials: metals, semiconductors, and insulators[1] (Table 1). This chemistry, which involves the covalent attachment of adsorbate molecules to a surface of interest and occasionally ordering of those adsorbate molecules into distinct and characterizable surface structures,[2] has been used to address many important fundamental and technological problems. For example, chemical sensors,[3] novel photoresists,[4] materials with enhanced nonlinear optical properties,[5] contact microprinting methods,[6] and optically sensitive interfaces for proof-of-concept molecule-based actinometers[7] have all been developed via monolayer self-assembly methodology. In addition, self-assembled monolayers (SAMs) have been used to address important issues involving interfacial electron transfer,[2a,8] molecular conductivity,[9] adhesion,[10] and surface wetting.[1] Surprisingly, methods to chemically modify the surfaces of the fourth important class of electronic materials, cuprate-based high temperature superconductors (HTSCs), have been notably absent from this field, even though methods to control and tailor the surface and interfacial properties of this class of materials are needed. Indeed, the surface composition of the cuprate HTSCs, especially the commercially most promising material, $YBa_2Cu_3O_{7-\delta}$, is quite complex and susceptible to change due to the reactivity of the material with environmental reagents.[11] For example, $YBa_2Cu_3O_{7-\delta}$ reacts with H_2O to form $Ba(OH)_2$, which subsequently reacts with CO_2 to form a passivating layer of $BaCO_3$. Such reactivity not only presents problems to those interested in making *reproducible* fundamental measurements on HTSCs but also to those interested in commercializing them.[12] The development of chemical methods to cap and stabilize the surface with molecular reagents can have profound consequences with regard to controlling some of the undesirable HTSC chemical reactivity. In addition, it can open new avenues to the preparation and study of unusual and potentially useful hybrid molecular monolayer/HTSC heterostructures.

Table 1. Examples of substrates for which surface modification chemistry has been developed.

Insulators	Semiconductors	Metals	HTSCs*
SiO_2	SnO_2, TiO_2	Au	
Al_2O_3	Ge/GeO	Pt	?
	Si, InP	Ag	
	CdSe, CdS	Cu	
	GaAs		

* High temperature superconductors.

Recently, in a collaborativ effect the McDevitt group and our group discovered the first chemistry to modify the surfaces of HTSCs with monolayers of molecular reagents[13] (Scheme 1). This methodology, which involves the direct chemical attachment of adsorbates to the surface of the underlying HTSC, complements methodology developed by Murray and co-workers that involves the initial deposition of an Au or Ag layer followed by adsorption of the adsorb-

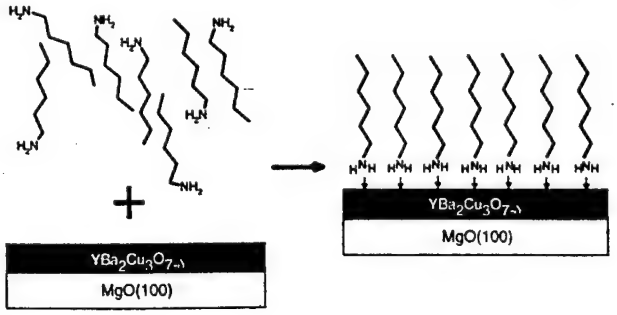

Scheme 1.

[*] Prof. C. A. Mirkin, F. Xu, J. Zhu
Department of Chemistry, Northwestern University
2145 Sheridan Road, Evanston, IL 60208-3113 (USA)

[**] CAM acknowledges the NSF Science and Technology Center for Superconductivity and the AFOSR for support of this work. Professor J. T. McDevitt and Professor L. H. Greene are acknowledged for helpful discussions.

ate molecules onto the noble metal films.[14] However our direct surface modification method has a distinct advantage since it allows one to chemically tailor HTSC surface and interfacial properties without an intermediary metal layer and has a variety of new and exciting implications with regard to understanding fundamental HTSC surface chemistry, controlling HTSC surface degradation reactions, and designing new hybrid molecular monolayer/HTSC materials and devices. Although HTSC surface modification chemistry is only one year old, a great deal of progress has been made in 1) identifying some of the functional groups that will bind to the surfaces of the cuprate HTSCs, 2) characterizing the resulting monolayer structures, 3) investigating some of the monolayer formation kinetics and dynamic exchange processes, and 4) investigating the novel properties of hybrid monolayer/HTSC materials. In this article, we discuss some of the important advances in this new area of surface chemistry.

2. The Surface Coordination Chemistry of Cuprate-Based HTSCs

Before one can begin designing stable molecule-based surface structures on HTSCs in a rational manner, one must first develop an understanding of suitable adsorbate molecules for adsorption onto the surfaces of such materials. Furthermore, ways must be developed to determine the efficiency of the adsorption process (i.e., adsorbate surface coverage and packing density, monolayer growth kinetics, etc.) and the orientations of the adsorbate molecules. Control over adsorbate orientation and packing will provide control over the chemical properties of the HTSC surface. Much of the initial HTSC surface coordination chemistry has been probed by synthesizing a series of redox-active potential adsorbate molecules, reacting them with HTSCs of interest, and characterizing the resulting monolayer structures (if formed) via cyclic voltammetry (Table 2 and Fig. 1). Thirteen redox-active molecules with different functional groups have been examined thus far via this method,[13,15] and it is now known that alkylamines, arylamines, alkylthiols, alkyldisulfides, and alkylselenols adsorb onto $YBa_2Cu_3O_{7-\delta}$ to form stable monolayer films. Linear alkylamines appear to form the most robust structures with the highest surface coverages, which can be determined by integrating the current associated with the one-electron ferrocenyl oxidation/reduction wave (Fig. 1A). Significantly, the real surface areas of $YBa_2Cu_3O_{7-\delta}$ pellets and laser-ablated thin films are substantially greater than their geometric surface areas. Based on the molecular footprint of the ferrocenyl-based adsorbate molecules and electrochemically determined surface coverages, we estimate roughness factors of at least 10 and 5, respectively. Therefore, full monolayer coverages for ferrocenyl-based molecules are ~(4–5) × 10^{-9} mol/cm^2 for ceramic pellet substrates and ~(2–3) × 10^{-9} mol/cm^2 for thin film substrates. These values, of course, are significantly higher than full monolayer coverages for ferrocenylalkanethiols adsorbed onto smoother substrates such as Au(111)/mica (roughness factor ~1.3–1.5; typical surface coverage ~(4–5) × 10^{-10} mol/cm^2). It is important to note that roughness factors will be highly dependent on pellet and film preparation conditions, which can be quite variable.

When $YBa_2Cu_3O_{7-\delta}$ substrates are freshly prepared and the soaking solutions are free of H_2O, robust monolayers are formed. Thus far, there is no evidence that crystal or-

Table 2. Surface coverage values for redox-active "ligands".

"Ligands" (Fc: ferrocenyl)	Surface coverage (mol/cm^2)	
	ceramic	thin film
FcC(O)NH(CH$_2$)$_4$NH$_2$ (*alkyl amine*)	4 x 10^{-9}	2 x 10^{-9}
p-Fc-C$_6$H$_4$-NH$_2$ (*aryl amine*)	4 x 10^{-10}	2 x 10^{-11}
FcC(O)(CH$_2$)$_{10}$SH (*thiol*)	2 x 10^{-9}	9 x 10^{-10}
(FcC(O)(CH$_2$)$_{10}$S)$_2$ (*disulfide*)	5 x 10^{-10}	UT**
Fc(CH$_2$)$_4$SeH (*selenol*)	7 x 10^{-10}	UT
FcCH$_2$OH (*alcohol*)	NS*	NS
(FcC(O)NHCH$_2$)$_2$ (*amide*)	NS	NS
FcO(CH$_2$)$_2$PPh$_2$ (*phosphine*)	NS	NS
FcC(O)(C$_2$H$_2$)$_5$N$_3$ (*azide*)	NS	UT
Fc(CH$_2$)$_4$CN (*nitrile*)	NS	UT
FcC(O)NHCH$_2$C$_5$H$_4$N (*pyridine*)	NS	UT
FcC(O)(CH$_2$)$_5$Br (*bromide*)	NS	UT
FcC(O)(CH$_2$)$_4$Cl (*chloride*)	NS	UT

* No significant surface coverage measured. ** Untested.

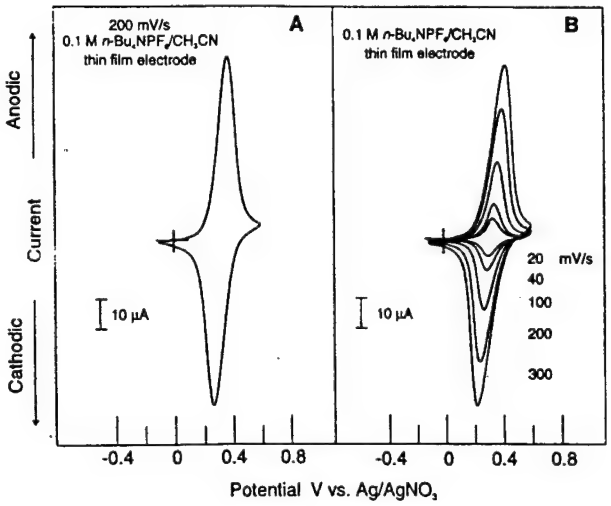

Fig. 1. a) Cyclic voltammetry for a $YBa_2Cu_3O_{7-\delta}$/MgO(100) polycrystalline *c*-axis thin film electrode modified with 4-aminobutylamidoferrocene. b) Sweep rate dependent cyclic voltammetry. Peak current scales linearly with scan rate. which is consistent with a surface-confined redox-active adsorbate.

© VCH Verlagsgesellschaft mbH, D-69469 Weinheim, 1997 0935-9648/97/0202-0168 $ 10.00+.25/0 Adv. Mater. 1997, 9, No. 2

ientation makes a difference in the adsorption process, although this issue has not yet been adequately probed. In dry 0.1 M $^{n}Bu_4NPF_6$/acetonitrile, the monolayers are stable to repeated cycling, but in wet solutions, the monolayers decompose and the surface becomes passivated, as evidenced by cyclic voltammetry.[15b] Under the conditions studied, the monolayer adsorption process does not alter T_c or substantially change substrate morphology on the micrometer length scale. However, it should be noted that Ellis and co-workers have reported evidence for Cu sequestration by amine reagents in aqueous solution, especially at high amine concentrations.[15c]

3. Spectroscopy on Monolayer-Modified HTSCs

Because of the poor optical properties of the $YBa_2Cu_3O_{7-\delta}$, it is difficult to do conventional IR and Raman vibrational spectroscopy on the monolayer structures formed on the surface of the HTSC. However, with regard to Raman spectroscopy this problem has been circumvented via a novel strategy that takes advantage of Au colloids that are deposited onto the monolayer-modified surfaces as Raman enhancers[16] (Scheme 2). By using bifunctional molecules with one end that can bind to the HTSC and one end that can be used for further modification with Au colloids, excellent Raman spectra of monolayers can be obtained. For example, 4-aminopyridine has an NH_2 group that is expected to bind to $YBa_2Cu_3O_{7-\delta}$ and a pyridyl group that does not bind to $YBa_2Cu_3O_{7-\delta}$ (Table 2) but can bind to Au colloids. The FT-Raman spectrum of the HTSC with a 4-aminopyridine monolayer is featureless (λ_{ex} = 1064 nm) (Fig. 2A). However, after the substrate is soaked in a toluene solution of Au colloids for 2 h, an excellent spectrum of the monolayer can be obtained (Fig. 2B). Using this method, and deuterium labeling studies, we have obtained the first evidence for a direct chemical interaction between the NH_2 group of the 4-amino pyridine and the $YBa_2Cu_3O_{7-\delta}$ surface (see Figs. 2B and 2C); a 29 cm^{-1} shift to lower energy for the NH_2 scissoring mode is observed upon the adsorption of 4-aminopyridine onto the HTSC. Significantly, this method should be extremely useful for determining some of the chemical characteristics of the adsorption processes involving other adsorbate molecule types (thiols, disulfides, etc.). It is important to note that this method is based on the work of others, who have previously demonstrated the Raman-enhancing qualities of Au colloids for the study of a variety of organic materials.[17] Interestingly, this appears to be the first Au colloid/surface enhanced Raman scattering (SERS) study of a monolayer on any type of surface.

Although the specific chemical interaction between the amine and the HTSC surface has yet to be determined, based on inorganic coordination chemistry involving amines[18] and the elements that make up the HTSC, the site of binding is likely Cu-based. This is also consistent with the

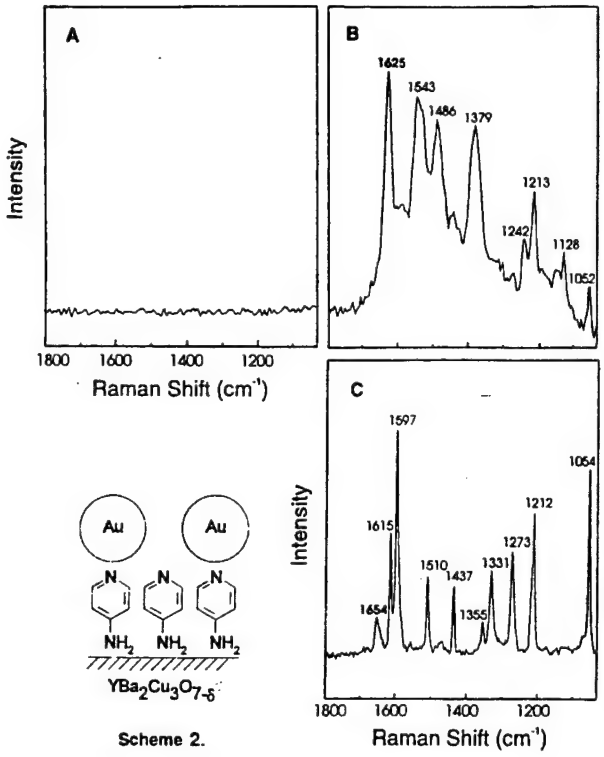

Scheme 2.

Fig. 2. Raman spectra for $YBa_2Cu_3O_{7-\delta}$ modified with a monolayer of 4-aminopyridine: a) before treatment with Au colloids, and b) after 2 h treatment with Au colloids. c) The Raman spectrum of solid 4-aminopyridine.

Cu sequestration data that Ellis and co-workers report for amine reagents (see above).[15c] In addition, preliminary theoretical modeling data support this hypothesis,[19a] and it is likely that this can be tested experimentally via $_{15}N$-labeling studies in conjunction with the SERS experiment described above. The Cu–N stretch is expected to appear in the 300–500 cm^{-1} region of the Raman spectrum.[19]

In some respects, the alkylamine "self-assembly process" on a substrate like $YBa_2Cu_3O_{7-\delta}$ is a less complicated process than alkanethiol adsorption onto noble metals. For example, it is unlikely that the amine chemistry with the HTSC is complicated by the possibility of bridging modes involving the amine ligand and multiple metal sites on the HTSC surface. Inorganic coordination chemistry studies of Cu suggest that amine ligands are not likely to act as bridging ligands between multiple metal sites on the HTSC surface.[18] However, the potential for hydrogen bonding between the amine and the oxygenated surface could add a level of complexity to the ligation properties of this type of adsorbate molecule. Detailed Raman studies will be important in fully characterizing this process. In comparison with the ligating properties of alkyl- and arylamines for the HTSC surface, the ligating properties of thiols, disulfides, and selenols are likely to be quite complex due to their susceptibility to oxidation and the oxidizing properties of the HTSC. For this reason, most initial studies have focused on elucidating the chemistry of the less complicated alkyl- and arylamine systems.

  0935-9648/97/0202-0169 $ 10.00+.25/0

4. Growth Kinetics and Adsorbate–Adsorbate Exchange Processes

For the alkyl- and arylamine systems studied thus far, all data suggest that the monolayer adsorption process is fast, efficient, and results in a durable surface structure consisting of densely packed, highly oriented adsorbate molecules. Although the role that the adsorbate molecule structure plays in determining the resulting monolayer structure is still unknown, we do know that monolayers of linear alkylamines and linear fluorinated alkylamines form densely packed structures, as evidenced by H_2O and hexadecane advancing contact angle measurements[20] (Table 3). Such

Table 3. Contact angle measurements of alkylamines on $YBa_2Cu_3O_{7-\delta}$ thin films and their thiol analogues on Au(111).

Molecules	Contact angle measurements n-$C_{16}H_{34}$ [°]	Water [°]
$CH_3(CH_2)_{17}NH_2$ on $YBa_2Cu_3O_{7-\delta}$	0	122
$CH_3(CH_2)_{17}SH$ on Au(111)	47	112
$CF_3(CF_2)_7(CH_2)_2NH_2$ on $YBa_2Cu_3O_{7-\delta}$	42	118
$CF_3(CF_2)_7(CH_2)_2SH$ on Au(111)	71	118
Unmodified $YBa_2Cu_3O_{7-\delta}$	112	70

data are comparable to data obtained from measurements made on alkanethiol and fluorinated alkanethiol monolayers on Au, which are known to be densely packed, oriented, and highly ordered.[1] The differences in contact angle values can be traced to differences in substrate roughness.[1c]

Using redox-active adsorbate molecules, monolayer growth kinetics can be studied by integrating the current associated with the redox-active adsorbate molecule as a function of soaking conditions (e.g., time, temperature, and solvent).[21] Initial studies show that a full monolayer of aminoalkylamidoferrocene (**A**) forms on a $YBa_2Cu_3O_{7-\delta}$ pellet after soaking for less than 12 h in a 1 mM acetonitrile solution of the adsorbate molecule (Scheme 3) (Case 1). Additional soaking may result in structural changes in the monolayer, but it does not substantially increase adsorbate surface coverage. Significantly, we have determined that the alkylamine adsorption process is dynamic and reversible. Exchange studies using redox-active ferrocenylalkylamine molecules with different $E_{1/2}$ values show that these monolayers undergo exchange reactions with solution adsorbate molecules. The process can be monitored easily as a function of time, temperature, and soaking conditions by cyclic voltammetry. For example, a monolayer can be prepared from an aminoalkylamidoferrocene (**A**) and then exchanged with an aminoalkylferrocene (**B**) (Scheme 3, Case 2, and Fig. 3 A–C). The latter molecule has an $E_{1/2}$ that is 220 mV more negative than the former one and, therefore, they can be easily differentiated by cyclic voltammetry. Note that the exchange process, although slow under these conditions (10 days for complete exchange) and nonlinear, is critical for "self-assembly". In order to form ordered densely packed mono-

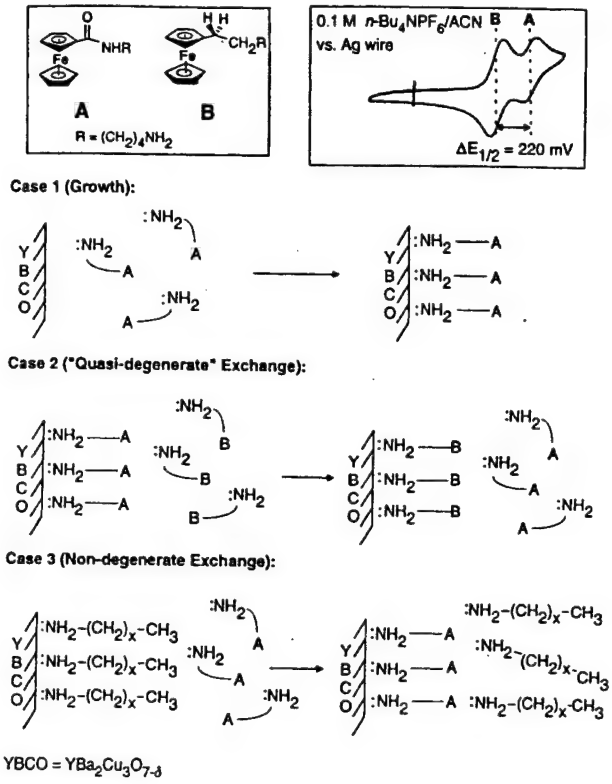

Scheme 3.

layer structures, ways for the film to correct defect structure are necessary.

This electrochemical approach for studying dynamic processes in SAMs has been used to study similar processes involving alkanethiols on Au.[22] Importantly, it can be used to evaluate monolayer growth kinetics, "quasi-degenerate" exchange processes (where the adsorbate head groups are the same and the tail groups only slightly differ as with **A** and **B**) and non-degenerate exchange processes (where the adsorbate head or tail groups differ substantially) (Scheme 3, Cases 1–3). This strategy will be very useful for elucidating some of the mechanistic issues associated with amine monolayers on HTSCs, which are likely to be very different from other SAM systems based on differences in surface coordination chemistry.

5. Applications of Monolayer-Modified HTSCs

There are many applications for monolayer-modified HTSCs. Some of these pertain to basic science issues regarding the physical properties of HTSCs, and others pertain to furthering our understanding of the monolayer self-assembly process. Still others relate to the development of new methods for improving the durability of HTSC materials and devices, as well as the development of new types of hybrid monolayer/HTSC structures. Indeed, Murray has recognized the importance of examining fundamental electron transfer events between immobilized molecule-based

0935-9648/97/0202-0170 $ 10.00+.25/0 Adv. Mater. 1997, 9, No. 2

ADVANCED MATERIALS

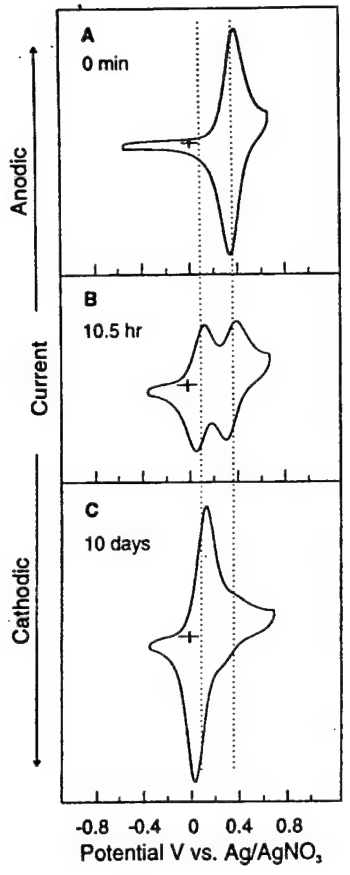

Fig. 3. Exchange of a redox-active compound **B** with a monolayer of redox-active compound **A**. Note that after 10 days, the new surface wave was ~220 mV negative of the initial wave. Cyclic voltammetry a) of a monolayer of compound **A**, b) after 10.5 h in a 1 mM solution of **B**, and c) after soaking for 10 days in a 1 mM solution of **B**.

structures on HTSCs as a function of temperature to determine if there are any special features associated with this type of reaction, such as the involvement of paired electrons.[14] With this new monolayer chemistry, it is now possible to address this issue in detail for a wide range of adsorbate molecules. Through choice of adsorbate molecule, one can vary the electron transfer driving force, the distance between the redox-group and electrode surface, and the chemical composition of the surface tethering group or electron transport medium. Monolayers on HTSCs also can be used as effective hydrophobic blocking layers for small molecules like H_2O. Indeed, perfluorinated monolayers have been shown to be excellent barrier layers for inhibiting the H_2O-induced corrosion reaction.[20] This is not only further evidence for the densely packed monolayer structure, but it also has important implications with regard to stabilizing HTSCs toward environmental corrosion and developing improved packaging methods for these materials. Others have started to use this methodology in attempts to develop passivation methods for commercially viable HTSC structures.[12]

Monolayers also can be used as adhesion promotor layers to interface polymeric materials with the HTSC that normally do not adhere well to the oxide surface.[20] For example, Teflon AF, which is particularly attractive as an HTSC passivation material, does not adhere to an unmodified $YBa_2Cu_3O_{7-\delta}$ substrate. However, when $YBa_2Cu_3O_{7-\delta}$ is modified with a monolayer of $H_2NCH_2CH_2(CF_2)_7CF_3$, Teflon AF adheres quite well to this surface. The passivating properties of this combination of monolayer and polymeric material can be seen quite well in an experiment that examines the conductivity of the HTSC as a function of its exposure to H_2O (Fig. 4). Here, bare $YBa_2Cu_3O_{7-\delta}$ cor-

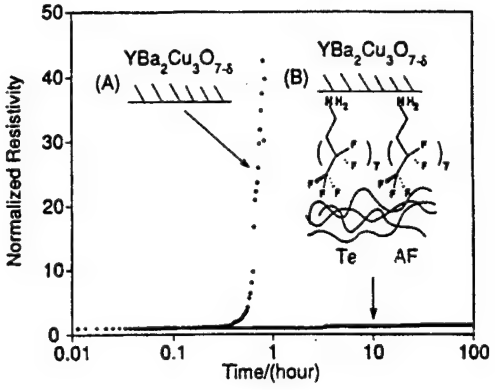

Fig. 4. Resistivity versus time measurements recorded for two $YBa_2Cu_3O_{7-\delta}$ (1500 A) thin-film samples on MgO(100) substrates that were exposed to 75 °C water vapor and ~98% humidity. Data are provided for an uncoated film and for a similar film that was coated with a monolayer of $CF_3(CF_2)_7CH_2CH_2NH_2$ onto which a 4 mm thick Teflon AF polymer layer was coated. (Reproduced with permission from *Chem. Mater.* **1996**, *8*, 811.)

rodes quickly, as evidenced by a catastrophic increase in resistance after short H_2O exposure times (< 1 h). The Teflon AF/flourinated monolayer modified materials are stable for substantially longer periods of time and do not exhibit significant increases in resistance within the time frame of the experiment (100 h).

In addition, monolayers of *N*-(3-aminopropyl)pyrrole have been used as nucleation layers for polypyrrole growth on $YBa_2Cu_3O_{7-\delta}$ substrates.[23] These studies suggest that electrochemically deposited polypyrrole grows faster at defect sites on *c*-axis oriented $YBa_2Cu_3O_{7-\delta}$. Like graphite,[24] the defect sites on *c*-axis oriented $YBa_2Cu_3O_{7-\delta}$ have higher conductivies than the non-defect sites and are responsible for much faster film growth; the result is non-uniform polypyrrole film growth. On the other hand, $YBa_2Cu_3O_{7-\delta}$ with a monolayer of *N*-(3-aminopropyl)pyrrole forms extremely smooth polypyrrole films under identical electrochemical deposition conditions and solution pyrrole concentrations. It is believed that initial oxidation of the pyrrole monolayer generates a conducting polymer film with more uniform conductivity than the underlying HTSC surface, thereby resulting in more uniform polypyrrole growth. Therefore, this experiment not only reveals an interesting way to use monolayers to nucleate polymer film growth but also some of the surface/electronic characteristics of the HTSC.

  0935-9648/97/0202-0171 $ 10.00+.25/0

Another application for monolayers on HTSCs pertains to the development of artificial tunnel junctions. The superconductor/insulator/superconductor tunnel junction can be used to fabricate a range of devices that can be commercially useful as SQUIDs, submillimeter wave detectors, and, possibly, ultrafast digital logic circuits (e.g., SFETs).[25] Tunnel junctions also can be used to determine some of the important fundamental physical properties of HTSCs, such as the superconducting gap (shape and magnitude), tunneling density of states, and other intrinsic electronic properties of superconductors. Both inorganic and organic materials have been used in attempts to fabricate this type of tunnel junction.[26] However, it has proved difficult to control the thickness and uniformity of the inorganic layers studied thus far, and organic films formed via the Langmuir–Blodgett technique still constitute a major challenge because of their fragility. Since the monolayer assembly process described herein provides easy control over the chemical composition, uniformity, stability, and thickness of the organic surface structures generated, such films are promising candidates for high T_c tunnel junction devices. Indeed, the Greene and Mirkin groups have constructed the first such device, which utilizes $YBa_2Cu_3O_{7-\delta}$ and Pb as the two superconducting materials and a monolayer of octadecylamine as the insulating tunneling layer.[27] Although the results are promising, problems still exist with monolayer damage occurring during Pb evaporation. It is likely that these problems can be overcome by capping the monolayers with functional groups that adhere to the lead and slow down diffusion into the monolayer structure. Such strategies have proven useful for impeding metal migration through organic monolayers on other substrates,[28] and indeed, others have shown that organic monolayers can constitute exceptional insulators at the nanometer length scale.[29]

6. Summary

HTSC surface modification with molecular monolayers is a straightforward method to chemically tailor the surface and interfacial properties of this important class of electronic materials. The amine and thiol adsorption chemistries reported herein extend to a wide range of cuprate-based superconductors (Table 4), and provide new ways to address important fundamental science and technological issues pertaining to this class of materials. Finally, the monolayer/surface chemistry of these ionic HTSCs represents a distinct departure from such studies on the surfaces of covalent, delocalized, bound noble metal substrates. Therefore, it is not only likely that new advances in HTSC processing and packaging and device fabrication will come from such studies, but also a rich set of surface coordination chemistries and new mechanisms for adsorbate self-assembly on these types of ionic lattices.

Table 4. HTSCs for which surface modification chemistry has been developed

HTSCs
$YBa_2Cu_3O_{7-\delta}$
$Tl_{1.4}Ba_2CaCu_2O_7$
$Y_{0.6}Ca_{0.4}Ba_{1.6}La_{0.4}Cu_3O_7$

[1] For reviews on monolayer films, see: a) A. Ulman, *Chem. Rev.* **1996**, *96*, 1533. b) L. H. Dubois, R. G. Nuzzo, *Annu. Rev. Phys. Chem.* **1992**, *43*, 437. c) A. Ulman, *An Introduction to Ultrathin Organic Films: From Langmuir–Blodgett to Self-assembly*, Academic, Boston **1991**.

[2] a) W. B. Caldwell, D. J. Campbell, K. Chen, B. R. Herr, C. A. Mirkin, A. Malik, M. K. Durbin, K. G. Huang, P. Dutta, *J. Am. Chem. Soc.* **1995**, *117*, 6071. b) X. Shi, W. B. Caldwell, K. Chen, C. A. Mirkin, *J. Am. Chem. Soc.* **1994**, *116*, 11598. c) A.-A. Dhirani, R. W. Zehner, R. P. Hsung, P. Guyot-Sionnest, L. R. Sita, *J. Am. Chem. Soc.* **1996**, *118*, 3319. d) G. Liu, P. Fenter, C. E. D. Chidsey, D. F. Ogletree, P. Eisenberger, M. Salmeron, *J. Chem. Phys.* **1994**, *101*, 4301. e) C. A. Alves, M. D. Porter, *Langmuir* **1993**, *9*, 3507. f) C. A. Alves, E. L. Smith, M. D. Porter, *J. Am. Chem. Soc.* **1992**, *114*, 1222.

[3] a) C. A. Mirkin, M. A. Ratner, *Annu. Rev. Phys. Chem.* **1992**, *43*, 719. b) C. A. Mirkin, J. R. Valentine, D. Ofer, J. J. Hickman, M. S. Wrighton, in *Biosensors and Chemical Sensors* (Eds: P. G. Edelman, J. Wang), ACS Symposium Series 487, American Chemical Society, Washington, DC **1992**, Ch. 17. c) J. J. Hickman, D. Ofer, P. E. Laibinis, G. M. Whitesides, M. S. Wrighton, *Science* **1991**, *252*, 688. d) M. Wells, R. M. Crooks, *J. Am. Chem. Soc.* **1996**, *118*, 3988.

[4] a) E. W. Wollman, D. Kang, C. D. Frisbie, I. M. Lorkovic, M. S. Wrighton, *J. Am. Chem. Soc.* **1994**, *116*, 4395. b) E. W. Wollman, C. D. Frisbie, M. S. Wrighton *Langmuir* **1993**, *9*, 1517. c) M. J. Tarlov, D. R. F. Burgess, Jr., G. Gillen, *J. Am. Chem. Soc.* **1993**, *115*, 5305.

[5] T. J. Marks, M. A. Ratner, *Angew. Chem., Int. Ed. Engl.* 1995, *34*, 155.

[6] a) A. Kumar, N. L. Abbott, E. Kim, H. A. Biebuyck, G. M. Whitesides, *Acc. Chem. Res.* **1995**, *28*, 219. b) Y. Xia, G. M. Whitesides, *J. Am. Chem. Soc.* **1995**, *117*, 3274. c) A. Kumar, G. M. Whitesides, *Appl. Phys. Lett.* **1993**, *63*, 2002.

[7] a) Y. Kawanishi, T. Tamaki, M. Sakuragi, T. Seki, Y. Suzuki, K. Ichimura, *Langmuir* **1992**, *8*, 2601. b) K. Ichimura, Y. Suzuki, T. Seki, A. Hosoki, K. Aoki, *Langmuir* **1988**, *4*, 1214.

[8] a) H. O. Finklea, in *Electroanalytical Chemistry*, Vol. 19 (Ed: A. J. Bard), Marcel Dekker, New York **1995**, p. 109. b) B. R. Herr, C. A. Mirkin, *J. Am. Chem. Soc.* **1994**, *116*, 1157. c) D. J. Campbell, B. R. Herr, J. C. Hulteen, R. P. Van Duyne, C. A. Mirkin, *J. Am. Chem. Soc.*, **1996**, *118*, 10211.

[9] a) L. A. Bumm, J. J. Arnold, M. T. Cygan, T. D. Dunbar, T. P. Burgin, L. Jones II, D. L. Allara, J. M. Tour, P. S. Weiss, *Science* **1996**, *271*, 1705. b) M. P. Samanta, W. Tian, S. Datta, J. I. Henderson, C. P. Kubiak, *Phys. Rev. B* **1996**, *53*, 7626.

[10] L. F. Rozsnyai, M. S. Wrighton, *Chem. Mater.* **1996**, *8*, 309.

[11] a) M. F. Yan, R. L. Barns, Jr., H. M. O'Bryan, P. K. Gallagher, R. C. Sherwood, S. Jin, *Appl. Phys. Lett.* **1987**, *51*, 532. b) A. Barkatt, H. Hojaji, V. R. W. Amarakoon, J. G. Fagan, *MRS Bull.* **1993**, *18*, 45.

[12] a) B. D. Thorson, *Supercond. Ind.* **1995**, *8*, 31. b) A. D. Hibbs, *Chem. Eng. News* **1996**, *74(23)*, 59.

[13] K. Chen, C. A. Mirkin, R. Lo, J. Zhao, J. T. McDevitt, *J. Am. Chem. Soc.* **1995**, *117*, 6374.

[14] S. R. Peck, L. S. Curtin, L. M. Tender, M. T. Carter, R. H. Terrill, R. W. Murray, J. P. Collman, W. A. Little, H. M. Duan, C. Dong, A. M. Hermann, *J. Am. Chem. Soc.* **1995**, *117*, 1121.

[15] a) F. Xu, K. Chen, J. Zhu, D. J. Campbell, C. A. Mirkin, R.-K. Lo, J. Zhao, J. T. McDevitt, in *Proc. – Electrochem. Soc.*, in press. b) K. Chen, F. Xu, R. Lo, K. S. Nanjundaswamy, J.-P. Zhou, J. T. McDevitt, *Langmuir* **1996**, *12*, 2622. c) P. M. James, E. J. Thompson, A. B. Ellis, *Chem. Mater.* **1991**, *3*, 1087.

[16] J. Zhu, F. Xu, S. J. Schofer, C. A. Mirkin, J. Am. Chem. soc. in press.

[17] a) R. G. Freeman, K. C. Grabar, K. J. Allison, R. M. Bright, J. A. Davis, A. P. Guthrie, M. B. Hommer, M. A. Jackson, P. C. Smith, D. G. Walter, M. J. Natan, *Science* **1995**, *267*, 1629. b) K. C. Grabar, R. G. Freeman, M. B. Hommer, M. J. Natan, *Anal. Chem.* **1995**, *67*, 735. c)

0935-9648/97/0202-0172 $ 10.00+.25/0

ADVANCED MATERIALS

K. C. Grabar, P. C. Smith, M. D. Musick, J. A. Davis, D. G. Walter, M. A. Jackson, A. P. Guthrie, M. J. Natan, *J. Am. Chem. Soc.* **1996**, *118*, 1148.

[18] F. A. Cotton, G. Wilkinson, *Advanced Inorganic Chemistry*, 5th ed., Wiley, New York **1988**, Ch. 18.

[19] a) D. R. Kanis, private communication. b) K. Nakamoto, *Infrared and Raman Spectra of Inorganic and Coordination Compounds*, Wiley, New York **1986**.

[20] J. T. McDevitt, C. A. Mirkin, R. Lo, K. Chen, J. Zhou, F. Xu, S. G. Haupt, J. Zhao, D. C. Jurbergs, *Chem. Mater.* **1996**, *8*, 811.

[21] F. Xu, J. Zhu, C. A. Mirkin, unpublished results.

[22] a) D. M. Collard, M. A. Fox, *Langmuir* **1991**, *7*, 1192. b) C. E. D. Chidsey, C. R. Bertozzi, T. M. Putvinski, A. M. Mujsce, *J. Am. Chem. Soc.* **1990**, *112*, 4301.

[23] R. Lo, J. Zhao, J.-P. Zhou, J. T. McDevitt, F. Xu, C. A. Mirkin, *J. Am. Chem. Soc.*, J. E. Ritchie **1996**, *118*, 11295.

[24] M. T. McDermott, K. Kneten, R. L. McCreery, *J. Phys. Chem.* **1992**, *96*, 3124.

[25] M. C. Foote, B. D. Hunt, L. J. Bajuk, *Proc. SPIE* **1991**, *1477*, 192.

[26] a) K. Hirata, K. Yamamoto, K. Iijima, J. Takada, T. Terashima, Y. Bando, H. Mazaki, *Appl. Phys. Lett.* **1990**, *56*, 683. b) N. Rando, P. Videler, A. Peacock, A. van Dordrecht, P. Verhoeve, R. Venn, A. C. Wright, J. Lumley, *J. Appl. Phys.* **1995**, *77*, 4099. c) C. M. Fischer, M. Burghard, S. Roth, *Synth. Met.* **1996**, *76*, 237.

[27] M. Covington, F. Xu, C. A. Mirkin, W. L. Feldmann, L. H. Greene, in *Czech. J. Phys.* **1996**, *46*, 53:1341.

[28] a) D. R. Jung, A. W. Czanderna, *Crit. Rev. Solid State Mater. Sci.* **1994**, *19*, 1. b) D. R. Jung, A. W. Czanderna, G. C. Herdt, *J. Vac. Sci. Technol. A* **1996**, *14*, 1779. c) D. R. Jung, A. W. Czanderna, *J. Vac. Sci. Technol. A* **1995**, *13*, 1337.

[29] C. Boulas, J. V. Davidovits, F. Rondelez, D. Vuillaune, *Phys. Rev. Lett.* **1996**, *76*, 4797.

Paper 3

Infrared and Computational Studies of Spontaneously Adsorbed Amine Reagents on $YBa_2Cu_3O_7$: Structural Characterization of Monolayers atop Anisotropic Superconductor Surfaces

Jason E. Ritchie, Cyndi A. Wells, Ji-Ping Zhou, Jianai Zhao, John T. McDevitt, Carl R. Ankrum, Luckner Jean, and David R. Kanis

Contribution from the Department of Chemistry and Biochemistry, The University of Texas at Austin, Austin, Texas 78712, and Department of Chemistry and Physics, Chicago State University, Chicago, Illinois 60628

JOURNAL OF THE AMERICAN CHEMICAL SOCIETY®

Reprinted from
Volume 120, Number 12, Pages 2733–2745

Infrared and Computational Studies of Spontaneously Adsorbed Amine Reagents on $YBa_2Cu_3O_7$: Structural Characterization of Monolayers atop Anisotropic Superconductor Surfaces

Jason E. Ritchie,† Cyndi A. Wells,† Ji-Ping Zhou,† Jianai Zhao,† John T. McDevitt,*,† Carl R. Ankrum,‡ Luckner Jean,‡ and David R. Kanis*,‡

Contribution from the Department of Chemistry and Biochemistry, The University of Texas at Austin, Austin, Texas 78712, and Department of Chemistry and Physics, Chicago State University, Chicago, Illinois 60628

Received March 4, 1997

Abstract: Methods capable of forming highly organized monolayers on top of $YBa_2Cu_3O_7$ (YBCO), a high-T_c superconductor, have been identified and are described for the first time. Here, grazing reflectance infrared fourier transform spectroscopy (GRIFTS) is employed to evaluate the degree of order for these monolayer structures. Through these investigations, it is found that while octadecylamine forms a well-ordered, crystalline-like monolayer on the surface of *c*-axis-oriented $YBa_2Cu_3O_7$ thin films, the same reagent adsorbed onto polycrystalline $YBa_2Cu_3O_7$ pellets affords disordered, liquid-like monolayers. Computational studies of alkylamine packing, using a molecular mechanics methodology, reveal two plausible structures for the crystalline-like monolayer. A GRIFTS comparison of primary, secondary, and tertiary alkylamine reagents also has been completed, and the substitution pattern dependence of the monolayer order has been assessed experimentally. Moreover, comparisons between amine monolayers on top of $YBa_2Cu_3O_7$ and alkyl thiol reagents on gold surfaces are made using GRIFTS and thermal desorption experiments. This work documents the initial report of the assembly and characterization of organized monolayers supported on high-T_c superconductor surfaces, the most complex substrate yet reported capable of fostering ordered adsorbate layers.

Introduction

Since the discovery of high-temperature superconductivity over a decade ago,[1,2] there has been a tremendous amount of excitement in the scientific and industrial communities in anticipation of the practical utilization of these remarkable materials. Unfortunately, the cuprate compounds are plagued by a number of parasitic chemical degradation reactions such as water reactivity, oxygen loss, and oxide ion electromigration. These degradation pathways have drastically slowed progress in the area of high-T_c research and product development.[3−6] Many of the envisioned technological applications and fundamental studies involving high-T_c systems rely on a firm understanding of the interfacial properties of these cuprate compounds. While initial applications using high-T_c materials approach the market place in the form of NMR pick-up coils, microwave devices, and SQUID sensors,[7−12] the true potential of this area cannot be realized until new processing methods are identified that are capable of controlling the interfacial properties of these reactive high-T_c systems.[13] To date, variations in the local chemical structure of high-T_c thin film structures have made it impossible to prepare large arrays of high-T_c junctions suitable for digital applications.[14] While the advantages of intrinsic speed and power dissipation are clearly recognized for superconductor devices relative to their semiconducting counterparts, the high-T_c digital revolution awaits further developments in areas related to the chemical processing of high-T_c systems. Clearly, the development of reliable procedures to control the local structure and interfacial properties of high-T_c materials will have an important influence on the area of high-T_c superconductivity.

Of the four classes of electronic materials (insulators,

* Author to whom correspondence should be addressed (email mcdevitt@huckel.cm.utexas.edu).

† The University of Texas at Austin.

‡ Chicago State University.

(1) Kresin, V. Z.; Wolf, S. A. *Fundamentals of Superconductivity*; Plenum Press: New York, 1990.

(2) Poole, C. P.; Farach, H. A.; Creswick, R. J. *Superconductivity*; Academic Press: San Diego, CA, 1995.

(3) Zhou, J.-P.; Savoy, S. M.; Zhao, J.; Riley, D. R.; Zhu, Y. T.; Manthiram, A.; Lo, R.-K.; Borich, D.; McDevitt, J. T. *J. Am. Chem. Soc.* **1994**, *116*, 9389−9390.

(4) McDevitt, J. T.; Riley, D. R.; Haupt, S. G. *Anal. Chem.* **1993**, *65*, 535A−545A.

(5) McDevitt, J. T.; Haupt, S. G.; Jones, C. E. In *Electrochemistry of High-T_c Superconductors*; McDevitt, J. T., Haupt, S. G., Jones, C. E., Eds.; Marcel Dekker: New York, 1996; Vol. 19, pp 355−481.

(6) McDevitt, J. T.; Haupt, S. G.; Clevenger, M. B. In *Conductive Polymer/High-Temperature Superconductor Assemblies and Devices*; McDevitt, J. T., Haupt, S. G., Clevenger, M. B., Eds.; Marcel Dekker: New York, 1996; pp 1029−1058.

(7) Berkowitz, S. J.; Zhang, Y. M.; Mallison, W. H.; Char, K.; Terzioglu, E.; Beasley, M. R. *Appl. Phys. Lett.* **1996**, *69*, 3257−3259.

(8) Berkowitz, S. J.; Hirahara, A. S.; Char, K.; Grossman, E. N. *Appl. Phys. Lett.* **1996**, *69*, 2125−2127.

(9) Katz, A. S.; Sun, A. G.; Dynes, R. C.; Char, K. *Appl. Phys. Lett.* **1995**, *66*, 105−107.

(10) Koelle, D.; Miklich, A. H.; Dantsker, E.; Ludwig, F.; Nemeth, D. T.; Clarke, J.; Ruby, W.; Char, K. *Appl. Phys. Lett.* **1993**, *63*, 3630−3632.

(11) Mallison, W. H.; Berkowitz, S. J.; Hirahara, A. S.; Neal, M. J.; Char, K. *Appl. Phys. Lett.* **1996**, *68*, 3808−3810.

(12) Martens, J. S.; Pance, A.; Char, K.; Lee, L.; Whiteley, S.; Hietala, V. M. *Appl. Phys. Lett.* **1993**, *63*, 1681−1683.

(13) McDevitt, J. T.; Lo, R.-K.; Zhou, J.; Haupt, S. G.; Zhao, J.; Jurbergs, D. C.; Chen, K.; Mirkin, C. A. *Chem. Mater.* **1996**, *8*, 811−813.

(14) Talvacchio, J.; Forrester, M. G.; Hunt, B. D.; McCambridge, J. D., M.; Young, R. M.; Zhang, X. F.; Miller, J. D. *IEEE Trans. Appl. Supercond.* **1997**, *7*, 2051−2056

S0002-7863(97)00692-6 CCC: $15.00
Published on Web 03/13/1998

semiconductors, metals, and superconductors), methods for surface modification of these systems have been extensively studied in all cases except for superconductors.[15] For example, the spontaneous adsorption of monolayer films has been demonstrated for a large number of adsorbate molecules with varying functional groups; selected examples include: alkyl thiols,[16] dialkyl disulfides,[17,18] and dialkyl sulfides,[19] on Au (111), carboxylic acids on metal oxides,[20,21] trichloro- and trialkoxysilanes on oxide surfaces,[22−26] thiols on GaAs,[27] CdSe, CdS, Cu,[28,29] and Ag,[28,30] and thiols, olefins, alcohols, amines, and isonitriles on Pt.[19,31−33] Importantly, spontaneously adsorbed monolayer films have been used to examine fundamental processes involving interfacial electron transfer, adhesion, and surface wetting.[15,34] Furthermore, a variety of interesting practical applications for the adsorbed monolayers have been reported in areas such as microcontact printing,[35,36] chemical sensing,[37] corrosion protection,[29,38] nonlinear optical materials,[39] organization of nanoscale particles,[40] and high-density memory devices.[41]

Like superconductivity, the field of self-assembled monolayers (SAMs) has attracted a significant amount of attention over the past decade. Currently, the number of highly organized monolayer systems are limited to alkylsiloxanes on SiO_2, *n*-alkanoic acids on oxidized silver and aluminum, dialkyl disulfides, dialkyl sulfides, alkyl thiols on gold, and alkyl thiols on pristine silver, copper, and GaAs.[27] To date, there is no literature precedent for organized monolayers supported on anisotropic conductors and none on systems containing more than one metal binding site.[5]

Recently, we described the first effective method capable of adsorbing persistent monolayer structures onto the high-T_c superconductors: $YBa_2Cu_3O_7$, $Y_{0.6}Ca_{0.4}Ba_{1.6}La_{0.4}Cu_3O_7$ (TX-YBCO), and $Tl_{1.4}Ba_2CaCu_2O_7$.[42,43] Here, molecular reagents possessing reactive functional groups were tagged with redox-active ferrocene reagents to electrochemically assay which reagents spontaneously adsorb to the high-T_c materials. Alkylamines, arylamines, alkyl thiol, alkyl disulfides, and alkyl selenols were shown to adsorb and form stable and electroactive superconductor-localized monolayers.[42,43] Primary *n*-alkylamines were found to form to the most rugged and persistent monolayers. Electrochemically assayed surface coverages (corrected for surface roughness values), scan rate dependence of voltammetric current, contact angle, and X-ray photoelectron spectroscopy measurements together yield convincing evidence for the presence of the superconductor-localized monolayer structures. Importantly, very little change is noticed in the superconductor's electrical properties following the adsorption of the monolayer reagents. Furthermore, adsorbed electroactive monolayers display voltammetry consistent with a surface-localized monolayer (i.e., small ΔE_p values and approximately equal current for the anodic and cathodic waves). All of these factors point to the conclusion that the amine monolayer adsorption occurs through "soft chemistry", causing little damage to the fragile high-T_c substrate.

While recent reports have described the use of alkylamine, arylamine, and alkyl thiol species for the formation of persistent monolayers atop a variety of cuprate phases,[42−45] the degree of order for such superconductor-localized monolayers has yet to be reported. Indeed, comparisons with other metal oxide systems such as Al_2O_3 and SiO_2 might suggest that ordered monolayers anchored atop the complex, reactive, and anisotropic high-T_c superconductors would be difficult to obtain.[20] Indeed, for the creation of effective corrosion barriers,[13] tunnel junctions,[46] adhesion layers,[13] and molecular spacer layers for energy transfer studies, it is essential that procedures be identified that are capable of producing organized superconductor-localized monolayers.

The method of grazing reflectance infrared fourier transform spectroscopy (GRIFTS) has been used by many researchers to acquire useful qualitative and quantitative information related to the order of spontaneously adsorbed monolayers.[16,18,20,28,31,47−49] The peaks in the C−H stretching region are particularly diagnostic for the degree of crystallinity of the adsorbed monolayer. Specific frequencies and peak intensities of the various C−H vibrations yield useful information regarding the local chemical environment within the SAM layer. For the case of highly ordered, long-chain alkyl thiol monolayers on gold

(15) Ulman, A. *An Introduction to Ultrathin Organic Films, From Langmuir−Blodgett to Self-Assembly*; Academic Press: Boston, MA, 1991.
(16) Porter, M. D.; Bright, T. B.; Allara, D. L.; Chidsey, C. E. D. *J. Am. Chem. Soc.* **1987**, *109*, 3559−3568.
(17) Nuzzo, R. G.; Allara, D. L. *J. Am. Chem. Soc.* **1983**, *105*, 4481−4483.
(18) Nuzzo, R. G.; Fusco, F. A.; Allara, D. L. *J. Am. Chem. Soc.* **1987**, *109*, 2358−2368.
(19) Troughton, E. B.; Bain, C. D.; Whitesides, G. M.; Nuzzo, R. G.; Allara, D. L.; Porter, M. D. *Langmuir* **1988**, *4*, 365.
(20) Allara, D. L.; Nuzzo, R. G. *Langmuir* **1985**, *1*, 52−66.
(21) Schlotter, N. E.; Porter, M. D.; Bright, T. B.; Allara, D. L. *Chem. Phys. Lett.* **1986**, *132*, 93−98.
(22) Tripp, C. P.; Hair, M. L. *Langmuir* **1992**, *8*, 1120−1126.
(23) Parikh, A. N.; Allara, D. L.; Azouz, I. B.; Rondelez, F. *J. Phys. Chem.* **1994**, *98*, 7577−7590.
(24) Kessel, C. L.; Granick, S. *Langmuir* **1991**, *7*, 532−538.
(25) Savig, J. *J. Am. Chem. Soc.* **1980**, *102*, 92.
(26) Moaz, R.; Sagiv, J. *J. Colloid Interface Sci.* **1984**, *100*, 465−496.
(27) Sheen, C. W.; Shi, J.-X.; Martensson, J.; Parikh, A. N.; Allara, D. L. *J. Am. Chem. Soc.* **1992**, *114*, 1514−1515.
(28) Laibinis, P. E.; Whitesides, G. M.; Allara, D. L.; Tao, Y. T.; Parikh, A. N.; Nuzzo, R. G. *J. Am. Chem. Soc.* **1991**, *113*, 7152−67.
(29) Laibinis, P. E.; Whitesides, G. M. *J. Am. Chem. Soc.* **1992**, *114*, 9022−9028.
(30) Walczak, M. M.; Chung, C.; Stole, S. M.; Widrig, C. A.; Porter, M. D. *J. Am. Chem. Soc.* **1991**, *113*, 2370−2378.
(31) Hickman, J. J.; Laibinis, P. E.; Auerbach, D. I.; Zou, C.; Gardner, T. J.; Whitesides, G. M.; Wrighton, M. S. *Langmuir* **1992**, *8*, 357−359.
(32) Stern, D. A.; Laguren-Davidson, L.; Frank, D. G.; Gui, J. Y.; Lin, C.-H.; Lu, F.; Salaita, G. N.; Walton, N.; Zapien, D. C.; Hubbard, A. T. *J. Am. Chem. Soc.* **1989**, *111*, 877−891.
(33) Mebrahtu, T.; Berry, G. M.; Bravo, B. G.; Michelhaugh, S. L.; Soriaga, M. P. *Langmuir* **1988**, *4*, 1147−1151.
(34) Bard, A. J.; Abruna, H. D.; Chidsey, C. E. D.; Faulkner, L. R.; Feldberg, S. W.; Itaya, K.; Majda, M.; Melroy, O.; Murray, R. M.; Porter, M. D.; Soriaga, M. D.; White, H. S. *J. Phys. Chem.* **1993**, *97*, 7147−7173.
(35) Kumar, A.; Whitesides, G. M. *Science* **1994**, *263*, 60−62.
(36) Xia, Y.; Mrksich, M.; Kim, E.; Whitesides, G. M. *J. Am. Chem. Soc.* **1995**, *117*, 9576−9577.
(37) Dermody, D. L.; Crooks, R. M.; Kim, T. *J. Am. Chem. Soc.* **1996**, *118*, 11912−11917.
(38) Feng, Y.; Teo, W.-K.; Siow, K.-S.; Gao, Z.; Tan, K.-L.; Hsieh, A.-K. *J. Electrochem. Soc.* **1997**, *144*, 55−64.
(39) Lin, W.; Lee, T.-L.; Lyman, P. F.; Lee, J.; Bedzyk, M. J.; Marks, T. J. *J. Am. Chem. Soc.* **1997**, *119*, 2205−2211.
(40) Freeman, R. G.; Grabar, K. C.; Allison, K. J.; Bright, R. M.; Davis, J. A.; Guthrie, A. P.; Hommer, M. B.; Jackson, M. A.; Smith, P. C.; Walter, D. G.; Natan, M. J. *Science* **1995**, *267*, 1629−1632.
(41) Kawanishi, Y.; Tamaki, T.; Sakuragi, M.; Seki, T.; Suzuki, Y.; Ichimura, K. *Langmuir* **1992**, *8*, 2601.
(42) Chen, K.; Mirkin, C. A.; Lo, R.-K.; Zhao, J.; McDevitt, J. T. *J. Am. Chem. Soc.* **1995**, *117*, 1121−1122.
(43) Chen, K.; Xu, F.; Mirkin, C. A.; Lo, R.-K.; Nanjundaswamy, K. S.; Zhou, J.-P.; McDevitt, J. T. *Langmuir* **1996**, *12*, 2622−2624.
(44) Lo, R.-K.; Ritchie, J. E.; Zhou, J.-P.; Zhao, J.; McDevitt, J. T. *J. Am. Chem. Soc.* **1996**, *118*, 11295−11296.
(45) Zhu, J.; Xu, F.; Schofer, S. J.; Mirkin, C. A. *J. Am. Chem. Soc.* **1997**, *119*, 235−236.
(46) Clevenger, M. B.; Zhao, J.; McDevitt, J. T. *Chem. Mater.* **1996**, *8*, 2693−2696. Covington, M.; Xu, F.; Mirkin, C. A.; Feldman, W. L.; Greene, L. H. *Czech. J. Phys.* **1996**, *46*, 1341.
(47) Camillone, N. I.; Chidsey, C. E. D.; Liu, G.-y.; Scoles, G. *J. Chem. Phys.* **1993**, *98*, 4234−4245.
(48) Chidsey, C. E. D.; Loiacono, D. N. *Langmuir* **1990**, *6*, 682−691.
(49) Porter, M. D. *Anal. Chem.* **1988**, *60*, 1143A−1155A.

(111) surfaces, the observed frequencies for d^- (asymmetric (asym) CH_2) of 2917 cm^{-1} and d^+ (symmetric (sym) CH_2) of 2850 cm^{-1} agree well with those observed for crystalline alkanes. In addition, these results correspond well with the vibrational features observed at 2918 and 2851 cm^{-1}, which are associated with solid samples of $CH_3(CH_2)_{21}SH$ in KBr.[16] Liquid alkyl thiol samples are shown to exhibit methylene stretches at 2924 and 2855 cm^{-1}. These observations suggest that spontaneously adsorbed alkyl thiol monolayers atop gold (111) possess an extended linear structure containing very few gauche defects. Moreover, the intensities of the various $-CH_2$ and $-CH_3$ vibrations deviate markedly from those observed for the isotropic samples. From an analysis of the IR data using the transition dipole orientation with respect to the polarization vector, an estimate for the monolayer tilt angle of 20−35° has been made.[16,18,50] The calculated angle, based on the IR analysis, agrees well with data obtained from other experimental methods such as ellipsometry, He diffraction, and electron diffraction.[16,48,50,51]

While ordered monolayers have been shown to form on surfaces such as noble metal single crystals and evaporated films of metals (Ag,[21,28] Cu,[28] Au,[16,18,28] Pt), disordered monolayers are observed to form on the more complex substrates such as Al_2O_3, Al with a native oxide surface, Ag_2O, and SiO_2.[20,52] In the highly studied case of siloxane monolayers on SiO_2 surfaces, it has been found that there is a critical adsorption temperature at which the surface energy is minimized. Below this critical temperature, monolayers of octadecyltrichlorosilane with d^- (asym CH_2) values of 2917 cm^{-1} and d^+ (sym CH_2) of 2849 cm^{-1} are obtained.[23] Above this critical temperature, the methylene stretches increase in frequency, indicating that the monolayer is being deposited in a disordered manner.

A recent report describing the use of gold colloids in the context of a surface enhanced raman spectroscopy (SERS) study has yielded direct spectroscopic evidence for the association of the amine functional group with the high-T_c cuprate lattice. Using a strategy developed my Natan,[40] Mirkin and co-workers[45] have confirmed prior indirect evidence for the existence of a strong amine headgroup interaction.[13,42−44,46] Unfortunately, the 4-aminopyridine reagent (used for this study because of its high Raman cross-section) does not provide structural features analogous to hydrocarbon species commonly used to generate adsorbate monolayers and no information was reported related to its ordering characteristics.

While many metal oxide surfaces have been successfully modified with alkylsiloxane or alkylcarboxlyic acid reagents, high-T_c superconductors represent a more complex system than those previously examined. Most of the previously studied systems have had the advantage of supporting hydrated surfaces, which could then be modified with siloxane type reagents. Unfortunately, $YBa_2Cu_3O_7$ is very susceptible to corrosion by water and acids.[4,5,53−56] When exposed to the atmosphere, $YBa_2Cu_3O_7$ rapidly reacts to form nonsuperconductive corrosion products such as $BaCO_3$, Y_2BaCuO_5, and CuO.[57]

Indeed, there are several differences that set $YBa_2Cu_3O_7$ apart from prior metal oxides shown to support adsorbate monolayers. These differences include the following: (1) $YBa_2Cu_3O_7$ has a water reactive surface which is readily corroded, (2) $YBa_2Cu_3O_7$ possesses a complex and anisotropic structure composed of CuO, BaO, CuO_2, and Y 2-dimensional layers, (3) the adsorption chemistry at $YBa_2Cu_3O_7$ is complicated by the fact that the lattice is composed of three cations (Y^{3+}, Ba^{2+}, Cu^{n+}), (4) the intrinsically poor reflectivity exhibited by $YBa_2Cu_3O_7$ makes classical reflectance IR structural analysis difficult. Thus, the surface modification of $YBa_2Cu_3O_7$ does not simply represent the modification of a new metal oxide surface, but a fundamentally new class of electronic materials which presents its own set of new challenges.

There are several issues related to the structure of monolayers spontaneously adsorbed to high-T_c materials that remain unaddressed at this juncture. Important questions yet to be answered include the following: (1) Can organized monolayers be created atop real samples of anisotropic cuprate superconductors? (2) Does the sample type (i.e., ceramic vs oriented thin film) influence the degree of monolayer order? (3) Can monolayers be adsorbed onto the different crystallographic faces of $YBa_2Cu_3O_7$ [i.e., (001) vs (100) orientation]? (4) What are the structural features of these self-assembled monolayer structures, and can these be systematically altered by tailoring the substrate? (5) Can the monolayers be thermally desorbed without damage to the high-T_c lattice? (6) What role does etching play in the establishment of monolayer structures? (7) How are the superconductor properties influenced by the monolayer adsorption process?

In this paper, the GRIFTS method is used to explore the degree of ordering of amine monolayers on $YBa_2Cu_3O_7$ samples. Both polycrystalline ceramic samples as well as (001) and (100) oriented thin films are examined in this context. Moreover, the studies are extended to an analysis of the ordering properties for primary, secondary, and tertiary amine reagents. Using the IR data combined with computational studies, plausible structures for selected monolayers are proposed and discussed.

Experimental Section

Sample Preparation and Treatment. Gold film samples were deposited as 2000 Å thick layers, prepared by resistive evaporation (Edwards Auto 306 Metal Evaporator equipped with cryodrive pump) onto a 50 Å Cr adhesion layer. Film thickness values were monitored with an in-situ quartz crystal microbalance. Silicon and glass substrates were used to support the metal layers. Both of these substrates were cleaned with pihrana solution, H_2O_2/H_2SO_4 (1:3) (*CAUTION! extremely corrosive*), immediately prior to deposition. Evaporated gold samples were used soon after their evaporation. Gold evaporated onto glass and silicon substrates were examined by X-ray powder diffraction. These gold samples exhibited only the (111) diffraction peak indicating a >95% (111) orientation. On the other hand, gold samples evaporated onto $YBa_2Cu_3O_7$ pellets were shown to yield a relatively strong (002) diffraction peak in addition to the (111) reflection, indicating the presence of alternative orientations in these films. From these experiments, it is clear that polycrystalline gold films are prepared when the metal is deposited atop the polycrystalline cuprate surface.

Ceramic pellets of $YBa_2Cu_3O_7$ were prepared by standard solid-state synthesis methods.[58] Here, Y_2O_3, CuO, and $BaCO_3$ were combined and ground for 45 min using an agate mortar and pestle. The resulting gray mixture was then placed into an alumina crucible and fired for 24 h at 900 °C in a box-type furnace. The resulting black powder was

(50) Strong, L.; Whitesides, G. M. *Langmuir* **1988**, *4*, 546−558.
(51) Nuzzo, R. G.; Dubois, L. H.; Allara, D. L. *J. Am. Chem. Soc.* **1990**, *112*, 558−569.
(52) Golden, W. G.; Snyder, C. D.; Smith, B. *J. Phys. Chem.* **1982**, *86*, 4675−4678.
(53) Zhou, J.-P.; Lo, R.-K.; Savoy, S. M.; Arendt, M.; Armstrong, J.; Yang, D.-Y.; Talvacchio, J.; McDevitt, J. T. *Phys. C* **1997**, *273*, 223−232.
(54) Riley, D. R.; Jurbergs, D. J.; Zhou, J.-P.; Zhao, J.; Markert, J. T.; McDevitt, J. T. *Solid State Commun.* **1993**, *88*, 431−434.
(55) Riley, D. R.; McDevitt, J. T. *J. Electroanal. Chem.* **1990**, *295*, 373−384.
(56) Zhou, J.-P.; McDevitt, J. T. *Chem. Mater.* **1992**, *4*, 953−959.
(57) Barkatt, A.; Hojaji, H.; Amarakoon, V. R. W.; Fagan, J. G. *MRS Bull.* **1993**, *18*, 45−52.
(58) Schneemeyer, L. F. In *Crystal Growth and Solid State Synthesis of Oxide Superconductors*; Schneemeyer, L. F., Ed.; Noyes: Park Ridge, NJ, 1992.

then reground for 45 min, pressed into 1 cm diameter pellets, and sintered for 24 h at 900 °C. These pellets were then broken up in a porcelain mortar and ground for the final time into a very loose powder. The $YBa_2Cu_3O_7$ powder was repressed into a 2.5 cm diameter pellets (5 g of $YBa_2Cu_3O_7$) and fired for 24 h at 900 °C. These pellets were then annealed in a tube furnace at 550 °C under flowing oxygen for 12 h. The use of large pellets is necessary to maximize the signal from the infrared measurement (*vide infra*).

Thin films of both (001) and (100) oriented $YBa_2Cu_3O_7$ were prepared by the pulsed laser ablation method.[59] Here, a $YBa_2Cu_3O_7$ ceramic target was mounted in a deposition chamber which was evacuated to a base pressure of 1×10^{-7} Torr. A KrF excimer laser beam (248 nm, 20 ns pulse width) was focused onto the target at an angle of 45° to produce a 2 J cm^{-2} energy density on the surface of the target. The substrates (typically $LaAlO_3$ single crystals) were mounted 5 cm from the target. The resulting crystallographic orientation of $YBa_2Cu_3O_7$ thin films are dependent on the substrate temperature used during the pulsed laser ablation. To prepare a (001) oriented thin film, a substrate temperature of 760 °C is maintained during the deposition, while a (100) oriented film is obtained when a substrate temperature of 680 °C is used. Optimal results were obtained when a deposition rate of 1 Å per pulse, and a 100 mTorr oxygen partial pressure were used. After deposition the samples were cooled to 450 °C where they were maintained for approximately 20 min in a 1 Torr oxygen atmosphere. The film samples were then cooled to room temperature in the same oxygen atmosphere.

The thin film superconductor samples were fully characterized by X-ray powder diffraction and four probe conductivity measurements. All superconductor specimens used in these experiments showed metallic temperature dependence of resistivity, and a superconducting critical temperature of 90 K. The (001) oriented film samples were shown by X-ray diffraction to exhibit nearly exclusive *c*-axis orientation, while the (100) oriented films were shown to contain 95% (100) oriented material. The $YBa_2Cu_3O_7$ thin films used in these experiments were 3000 Å in thickness and were supported on single-crystal $LaAlO_3$ (100) substrates (2 cm × 2 cm × 1 mm). It was necessary to use the large films to maximize the signal from the infrared measurement, as well as achieving reproducible sample alignment.

Monolayer adsorption experiments were carried out by soaking the substrates in a 1 mM solution of the adsorbate molecule in hexanes. Typically, samples were allowed to remain in the solution for 18−24 h. Upon removal from the adsorption bath, substrates were sequentially washed by immersion in four baths of hexanes to remove any physisorbed amine reagent. After the final washing step, samples were blown dry in a stream of dry nitrogen. Film specimens were immediately characterized by infrared measurements.

Infrared Measurements. Grazing reflectance infrared fourier transform spectra (GRIFTS) were acquired on a Nicolet 550 Fourier-transform spectrometer equipped with a liquid nitrogen cooled mercury−cadmium−telluride (MCT) detector. This spectrometer was adapted with a spectral reflectance attachment, which was aligned so that radiation was delivered to the sample at an angle of 79° to the surface normal for the majority of the experiments.[60] In selected cases, alternative incident angles were employed resulting in qualitatively similar spectral features. No attempt is made here to utilize measured absorbance values along with dipole analysis to estimate tilt angles as per previously described method of Allara and Nuzzo.[20] Before such measurements are possible, complete characterization of the optical constants of $YBa_2Cu_3O_7$ is necessary. Complications related to reactivity properties of the cuprate compound presently preclude an accurate and reliable analysis of this type. Future detailed studies may overcome this limitation. The incident radiation was polarized perpendicular to the plane of the substrate (i.e., p-polarized). Spectra were acquired at 4 cm^{-1} resolution with a mirror speed of 1.4 cm/s. Typically, 4000 scans were obtained so as to achieve a spectrum with an adequate signal-to-noise ratio. Background spectra were acquired on the substrate immediately after deposition and prior to adsorption of the monolayer reagent. Atmospheric exposure of the film samples was minimized.

Transmission FT-IR spectra were acquired for selected samples using a second Nicolet 550 spectrometer that was equipped with a deuterated triglycerine sulfate (DTGS) pyroelectric detector. Spectra of liquid samples were acquired using drops of the liquid confined between KBr salt plates, whereas solid samples were incorporated into pressed KBr pellets.

Computational Studies. All molecular mechanics computations reported in this work employed an MM2 force field with standard MM2 parameters.[61−63] Specifically, the Molecular Mechanics algorithm in the CAChe (Computer-Aided Chemistry) package was used with default parameters specified. The rigid molecule chosen for the majority of the studies was an energy-minimized geometry of a five-carbon primary amine ($NH_2(CH_2)_4CH_3$). The geometry of the prototype amine was optimized at an ab initio level (6-311G** basis set) using the Mulliken algorithm in the CAChe software package.[64] The free energy of each monolayer assembly was explored by comparing two different geometries of monolayers. The first geometry was composed of four duplicate amines placed over a 3 × 3 copper lattice, aligned in one plane and spatially separated from one another by a distance corresponding to the $\sqrt{2}\times\sqrt{2}$R45° adlayer separation of (001) oriented $YBa_2Cu_3O_7$, with the chains occupying the four corner adsorption sites. Note that the middle copper site is left vacant in this geometry. The second geometry was identical to the first except that the previously vacant middle copper site is occupied by a fifth chain. These geometries are schematically illustrated in Figure 8. This technique minimizes artificial variations in the computed energies due to edge effects. In addition, studies of alkyl thiol reagents adsorbed on to gold (111) surfaces were completed to determine the reliability of the described computational studies. Energy terms related to the lattice and the headgroup−substrate interaction were not evaluated in this study.

Plausible structures were identified on the basis of the minimized intermolecular energy between the amines in the various test sets. Within the framework of molecular mechanics, the total potential energy of a system can be partitioned into bond stretches, angle bends, torsion bends, van der Waals' interactions, and electrostatic interactions. The last two terms are the intermolecular contributions to the potential energy. Because van der Waals' forces were cut off at 9 Å in our model, the energy differences between the four- and five-chain systems were determined primarily by interaction of the center chain with its nearest neighbors. These van der Waals' 6−12 terms dominate the electrostatic terms in the molecule−molecule potential energy of our system.

To ensure that the MM2 computations were providing reliable results, we also carried out PM3 computations on a representative series of orientations. All PM3 computations were performed using the MOPAC algorithm in the CAChe software package, with none of the semi-empirical parameters modified.[65,66] The ab initio and MOPAC computations were carried out on an Apple Work Group 500 Server (256 MB of RAM) using CAChe for Workgroups,[63] whereas the mechanics computations were carried out using the Personal CAChe software on a Power Macintosh.[67]

Molecular Reagents. Octadecylamine, trioctylamine, and dioctylamine compounds were obtained as reagent grade from Aldrich and were used as received. Reagent grade hexanes was used as received. High-T_c starting materials, yttria, barium carbonate, and copper oxide were purchased from Alfa Aesar, all as high purity (99.99%) compounds.

(59) Miyazawa, S.; Tazoh, Y.; Asano, H.; Nagai, Y.; Michikami, O. *Adv. Mater.* **1993**, *5*, 179.

(60) Finklea, H. O.; Melendez, J. A. *Spectroscopy* **1986**, *1*, 47−48.

(61) Allinger, N. L. *J. Am. Chem. Soc.* **1977**, *99*, 8127−8134.

(62) Berkert, U.; Allinger, N. L. *Molecular Mechanics*; American Chemical Society: Washington, DC, 1982.

(63) Clark, T. *A Handbook of Computational Chemistry*; Wiley: New York, 1985.

(64) CAChe/IBM, Oxford Molecular/IBM, CAChe Workgroup Software Package containing Mulliken Version 3.7.2, Beaverton, Oregon.

(65) Stewart, J. J. P. *J. Comput. Chem.* **1989**, *10*, 209−220.

(66) Dewar, M. J. S.; Thiel, W. I. *J. Am. Chem. Soc.* **1977**, *99*, 4899−4907.

(67) CAChe/MOPAC, Oxford Molecular, Personal CAChe Software Package containing MOPAC Version 6.0, Beaverton, Oregon.

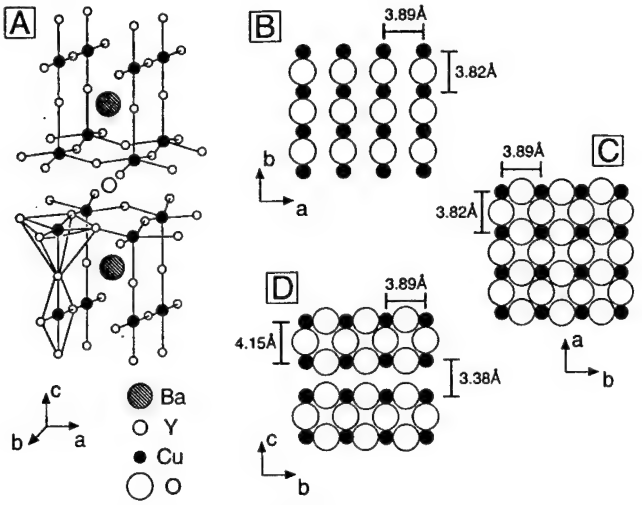

Figure 1. The unit cell of $YBa_2Cu_3O_7$ and the copper-containing layers are illustrated. Shown in (A) is the unit cell of $YBa_2Cu_3O_7$, in (B) the structure of the copper chain layer of (001) oriented $YBa_2Cu_3O_7$, in (C) the copper sheet layer of (001) oriented $YBa_2Cu_3O_7$, and in (D) the expected copper containing termination for a (100) oriented $YBa_2Cu_3O_7$ sample.

Results and Discussion

The high-T_c superconductor, $YBa_2Cu_3O_7$, was chosen for the monolayer adsorption studies for a number of reasons. First, the material can be prepared easily as a single phase both in ceramic (i.e., polycrystalline) and thin film form. Moreover, the compound represents one of the most technologically and scientifically important high-T_c phases, making its use in monolayer adsorption chemistry particularly relevant.

The compound, $YBa_2Cu_3O_7$, possesses a number of interesting and important structural features that are highlighted in Figure 1. The lattice of $YBa_2Cu_3O_7$ is composed of six sheets which are stacked along the *c*-axis in the order of Cu(1)O, BaO, $Cu(2)O_2$, Y, Cu(2)O, and BaO (Figure 1A). In principle, any of the metal cations could support the adsorption of the amine reagents. However, there are a number of factors which support the presumption that amines adsorb only at copper sites. First, copper/amine coordination chemistry is more prevalent than for any of the other metal cations present in the lattice.[68] Second, prior studies by Ellis and co-workers have documented copper cations leaching away from the high-T_c lattice upon its exposure to high concentrations of chelating amine reagents.[69] We have also obtained UV−vis and atomic adsorption spectral data consistent with copper/amine complexes when high-T_c samples have been soaked in amine reagents (i.e., hexylamine) for extended periods of time.

Monolayer adsorption onto $YBa_2Cu_3O_7$ surfaces has a large dependence on the type of sample onto which the molecule is adsorbed. Here, both polycrystalline and various thin film structures are considered (Figure S1, Supporting Information). Polycrystalline $YBa_2Cu_3O_7$ is composed of individual grains, 2−10 μm in size, which are fused together as a sintered ceramic pellet to create a sample having good mechanical integrity. Very little long-range crystallographic order is seen in such specimens.

Deposition of $YBa_2Cu_3O_7$ thin films onto a variety of single-crystal substrates allows for the creation of oriented and ordered superconductor samples. Matching between the superconductor lattice parameters and those of the substrate allow for the preparation of $YBa_2Cu_3O_7$ samples having both (001) and (100) orientations. A substrate temperature of 760 °C is used here to prepare $YBa_2Cu_3O_7$ samples having (001) orientations. These samples display relatively smooth surface morphologies (*vide infra*). Samples of this type have surfaces which expose the *a*−*b*-plane of the lattice. High-T_c films with $YBa_2Cu_3O_7$ having (100) orientations are produced by using a lower deposition temperature of 680 °C. These samples display a rougher, more textured surface (*vide infra*). The dependence of the monolayer adsorption and ordering characteristics on crystallographic surfaces can be assayed by investigating the behavior fostered by these three types of surfaces.

Most $YBa_2Cu_3O_7$ single crystals are prepared at elevated temperatures in which they are formed in a tetragonal environment.[58] Upon cooling, extra oxygen is taken up by the lattice leading to the formation of an orthorhombic material. To relieve lattice stress, twinning along the (110) plane occurs. Thus, most $YBa_2Cu_3O_7$ single crystals possess twinned microstructures which may influence the monolayer ordering characteristics. The same behavior is also prevalent for the *c*-axis-oriented high-T_c films described below.

Before alkylamine monolayers can be reliably and reproducibly adsorbed to $YBa_2Cu_3O_7$, several problems related to the complex cuprate substrate must be overcome: (1) Samples having relatively low surface roughness values must be used. Here, we employed smooth *c*-axis-oriented films of $YBa_2Cu_3O_7$ as prepared by pulsed laser ablation for the majority of our studies. (2) Surface reactivity problems must be minimized. This objective is accomplished by using the superconductor samples immediately following their deposition, and by using only rigorously dried solvents for the monolayer adsorption steps. (3) Samples of $YBa_2Cu_3O_7$ exhibit poor reflectivity values in the infrared as compared to more conventional metals such as Au, Ag, and Al.[70] To overcome this limitation, it is necessary to use high-T_c samples having large thickness values relative to the optical penetration depth. Likewise, ceramic pellets of $YBa_2Cu_3O_7$ can be evaluated when disks with 2 cm diameter and 0.5 cm thickness are used, but the quality of the resulting spectra are inferior to those obtained with films. For $YBa_2Cu_3O_7$ films, samples with thicknesses greater than 3000 Å are used to achieve adequate reflectivity properties.

Important information related to the structural properties of the superconductor-localized monolayers can be obtained through comparisons made with the thoroughly studied alkyl thiol system on gold (111), upon which well-ordered monolayers are known to form.[16,18] Thus, both alkyl thiols on gold and alkylamines on $YBa_2Cu_3O_7$ are studied here. To evaluate the contribution of surface roughness to the monolayer structure, data is also acquired for alkyl thiol monolayers on smooth gold (111) surfaces as well as for rough polycrystalline gold deposited atop ceramic $YBa_2Cu_3O_7$ pellets.

Smooth, Oriented $YBa_2Cu_3O_7$ Surfaces. Prior work on metal oxides (SiO_2, Al_2O_3) has focused mainly on the coupling of monolayers to the oxide surfaces using Si−O−R linkages. Monolayers resulting from this type of chemistry have been shown to be disordered.[20] Attempts to employ similar chemistry for high-T_c superconductors resulted in a significant amount of

(68) Cotton, F. A.; Wilkinson, G. *Advanced Inorganic Chemistry*; Wiley-Interscience: New York, 1988.

(69) James, P. M.; Thompson, E. J.; Ellis, A. B. *Chem. Mater.* **1991**, *3*, 1087−1092.

(70) A comparison of the IR reflectivity of $YBa_2Cu_3O_7$ and gold samples, recorded in the mid-IR, showed important thickness and morphology dependencies. At 1600 cm^{-1}, a 1000 Å $YBa_2Cu_3O_7$ (001) film showed a reflectivity, relative to 2500 Å gold film, of 41%. Whereas, a 2500 Å $YBa_2Cu_3O_7$ (001) film showed a relative reflectivity of 52%. Under identical conditions, a ceramic pellet of $YBa_2Cu_3O_7$ displayed a relative reflectivity of only 8%. To maximize the signal obtained from $YBa_2Cu_3O_7$ samples, it is necessary to maximize the reflectivity and the sample size.

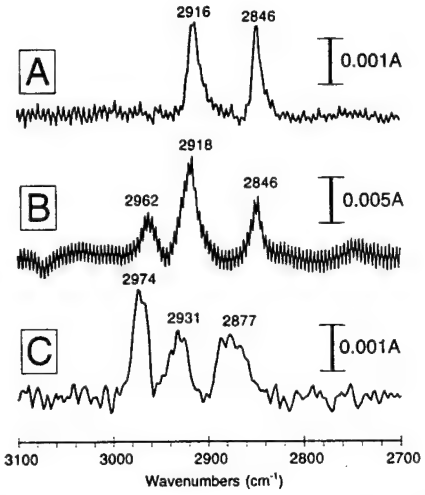

Figure 2. Shown are GRIFTS spectra obtained for octadecylamine monolayers which are supported on top of various types of $YBa_2Cu_3O_7$ surfaces: (A) a smooth (001) oriented $YBa_2Cu_3O_7$ film prepared by laser ablation, (B) a smooth (100) oriented $YBa_2Cu_3O_7$ film prepared by the same method, and (C) a polycrystalline ceramic pellet of $YBa_2Cu_3O_7$ made by a solid-state route.

damage done to the cuprate material.[71] However, octadecylamine spontaneously adsorbs to $YBa_2Cu_3O_7$ (001) films samples from a 1 mM solution in hexanes. When the resulting octadecylamine monolayer is examined by GRIFTS, two peaks are seen in the CH stretching region (Figure 2A). The frequencies of the peaks are 2916 and 2846 cm^{-1}. These peaks are assigned as the asymmetric and symmetric methylene stretching modes, respectively.

When comparing the GRIFTS spectra of octadecylamine on $YBa_2Cu_3O_7$ (001) and octadecyl thiol on gold (111), it is immediately apparent that although the methylene vibrational modes are similar in appearance, the methyl vibrations from the modified $YBa_2Cu_3O_7$ sample are conspicuously absent (Figure 2A). These infrared characteristics for octadecylamine on $YBa_2Cu_3O_7$ (001) are very reminiscent of the spectral features of alkyl thiols adsorbed to GaAs (100) acquired by Allara and co-workers.[27] The alkyl thiol/GaAs system was found to exhibit a very large molecular tilt angle of 57° from surface normal. A qualitative comparison of the GRIFTS data for the thiol/GaAs system with that observed at high-T_c adsorbate layer suggests a large tilt angle is also present for the cuprate system. This lack of methyl signal can be explained by an analysis of the vibrational dipoles (Figure S2, Supporting Information).

In addition to the position of the peaks in the GRIFTS spectra, the width of the vibrational modes can be used to diagnose the crystallinity of the hydrocarbon-based monolayer.[72] Shown in Table 1 is a compilation of peak positions and full width at half maximum (fwhm) spectral widths for all of the monolayer systems investigated in this report. The asymmetric methylene stretch of octadecylamine adsorbed to a $YBa_2Cu_3O_7$ (001) oriented thin film shows a fwhm of the asymmetric methylene stretch of 12 cm^{-1} (Table 1). Crystalline octadecyl thiol monolayers adsorbed to gold (111) surfaces show fwhm of 10 cm^{-1}, while disordered monolayers of hexadecanoic acid adsorbed to Al_2O_3 show fwhm of 34 cm^{-1}.[20] From this highly reproducible measurement, it may be inferred that octadecylamine monolayers adsorb onto $YBa_2Cu_3O_7$ (001) films in such manner that structures exhibiting a high degree of average chain-conformational order are obtained.

(71) Ritchie, J. E.; Murray, W.; McDevitt, J. T. Manuscript in preparation.
(72) Byrd, H.; Pike, J. K.; Talham, D. R. *Chem. Mater.* **1993**, *5*, 709–715.

Table 1. Comparison of the Antisymmetric Methylene Stretches for a Variety of Substrates, Monolayers, and Substitution Patterns

substrate	monolayer	frequency (cm^{-1})	fwhm (cm^{-1})
gold/silicon	$CH_3(CH_2)_{17}SH$	2917	10
gold/glass	$CH_3(CH_2)_{17}SH$	2918	9
gold/YBCO pellet	$CH_3(CH_2)_{17}SH$	2928	33
YBCO film (001)	$CH_3(CH_2)_{17}NH_2$	2916	12
YBCO film (001)	$(CH_3(CH_2)_7)_2NH$	2931	14
YBCO film (001)	$(CH_3(CH_2)_7)_3N$	2929	23
YBCO film (100)	$CH_3(CH_2)_{17}NH_2$	2918	20
YBCO pellet	$CH_3(CH_2)_{17}NH_2$	2931	22
YBCO pellet	$(CH_3(CH_2)_7)_2NH$	2929	29
YBCO pellet	$(CH_3(CH_2)_7)_3N$	2933	19
alumina[a]	$CH_3(CH_2)_{14}COOH$	2926	34
neat solid	$CH_3(CH_2)_{17}NH_2$[c]	2917	24
neat solid[a]	$CH_3(CH_2)_{14}COOH$[c]	2918	11
neat liquid[b]	$CH_3(CH_2)_7SH$[c]	2924	*d*
neat solid[b]	$CH_3(CH_2)_{21}SH$[c]	2918	*d*

[a] Adapted from Allara, D.L., et al., *Langmuir*, **1985**, *1*, 52–66 [b] Adapted from Porter, M.D., et al., *J. Am. Chem. Soc.*, **1987**, *109*, 3559–3568. [c] Indicates that measurement was made in transmission mode without the use of a substrate. [d] These data were not supplied for these cases.

Shown in Figure 2B is a GRIFTS spectrum of octadecylamine adsorbed to (100) oriented $YBa_2Cu_3O_7$ film.[73] These data displays similar features seen when the same molecule is adsorbed to (001) oriented $YBa_2Cu_3O_7$, including the presence of the asymmetric methylene stretch at 2918 cm^{-1}. However, the in-plane asymmetric methyl stretch is also seen at 2962 cm^{-1} for this substrate. The reappearance of the methyl vibration may be caused by a smaller tilt angle in the adsorbate layer fostered by the presence of short Cu–Cu separations for the exposed (100) surface (*vide infra*).

While the asymmetric methylene stretch of octadecylamine adsorbed to $YBa_2Cu_3O_7$ (100) films is observed to be centered in the same place as the (001) oriented samples, the spectral width is this peak is slightly greater than that of the (001) oriented sample (20 cm^{-1} vs 8–12 cm^{-1}, see Table 1). This behavior is most likely due to the decreased order of the copper spacing in the (100) oriented film samples. Although the surface copper–copper distances in the *a* and *b* lattice directions are nearly the same for (001) oriented $YBa_2Cu_3O_7$ film (Figure 1B,C), there is a significant difference in the copper–copper spacings for (100) oriented $YBa_2Cu_3O_7$ samples (Figure 1D). This difference in spacing may lead to a decrease in the chemical homogeneity of the resulting monolayer on (100) oriented samples. While the spectral width of the asymmetric methylene stretch of the monolayer atop (100) oriented $YBa_2Cu_3O_7$ is somewhat broader than seen in other "ordered" monolayers, the positioning of the peak is good evidence that the monolayer adopts a relatively ordered structure on this substrate. Due to the width of this peak, it is probable that this structure possesses more defects than previously seen in other ordered cases.

Having identified vibrational characteristics consistent with the formation of crystalline monolayer structures,[16] it now becomes important to consider possible packing structures for the adsorbed hydrocarbon monolayers. The surface structure

(73) Note also that this sample displays periodic features that appear to be present as "background noise." However, more careful analysis of the frequency of such peaks suggests they are caused by an interference phenomenon. Likewise, the frequency dependence of these peaks/troughs corresponds exactly with constructive/destructive wave combinations reflected from exterior and interior surfaces of the high-T_c film. Roughening of the substrate with etching and thermal annealing steps reduces the magnitude of these interference fringes and can improve the appearance of the spectral features.

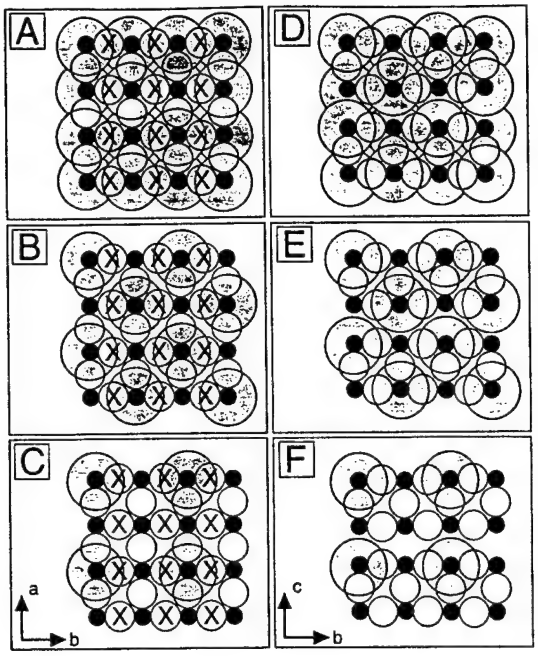

Figure 3. Possible packing structures for primary linear alkylamine monolayers on $YBa_2Cu_3O_7$. For this simplistic diagram, the footprint of the hydrocarbon is shown as a circle with dimensions corresponding to a van der Waals' radius of 4.5 Å.[16] Shown in (A) and (D) are the 1×1 monolayer adlayers for the (001) surface (A) and for the (100) oriented surface (D). Likewise, (B) and (E) show the $\sqrt{2}\times\sqrt{2}R45°$ adlayer for the (001) surface (B) and the (100) oriented surface (E). Shown in (C) and (F) are the 2×2 adlayer for (001) (C) and (100) (F) oriented samples. Oxygen atoms marked with "X" indicate oxygens that are not present in the copper chain layer of the (001) oriented film but that are present in the copper sheet layer of (001) oriented $YBa_2Cu_3O_7$ films (see Figure 1).

of $YBa_2Cu_3O_7$ is somewhat complicated, having several layers that could support spontaneous adsorption of alkylamines. The unit cell of $YBa_2Cu_3O_7$ contains six distinct layers along the *c*-axis. While three of these layers do not contain copper, their presence may complicate the analysis. In (001) oriented samples of $YBa_2Cu_3O_7$, spontaneous adsorption of alkylamines is likely to occur at either the copper chain (CuO) or copper sheet (CuO_2) layer (Figure 1B,C, respectively). For (100) oriented $YBa_2Cu_3O_7$ samples, there is only one unique copper-containing layer (Figure 1D).

Shown in Figure 3 is the spatial distribution for the CuO_2 and CuO sheet layers as well as the molecular "footprint" for the hydrocarbon reagent. These diagrams illustrate the features of the docking sites for both the (001) and (100) exposed surfaces of $YBa_2Cu_3O_7$. The van der Waals' distance within paraffin crystals of 4.5 Å[16] would seem to preclude the adsorption of the amine reagents at every exposed copper site. The adsorption of alkylamines at every exposed copper site (Figure 3A) would lead to a 1×1 adlayer with a 3.8 Å separation between hydrocarbon chains; far too compact to represent a realistic packing motif. On the other hand, a $\sqrt{2}\times\sqrt{2}R45°$ adlayer (Figure 3B) yields a good monolayer coverage with a headgroup separation of 5.4 Å. The adsorption of alkylamine at every other copper site without using diagonal sites leads to a 2×2 adlayer with a 7.4 Å distance separating the alkyl chains. This packing motif is probably too diffuse to promote strong chain−chain interactions (*vide infra*).

The separation achieved for the $\sqrt{2}\times\sqrt{2}R45°$ case is about 10% larger than previously observed for alkyl thiol reagents on Au (111).[16] To compensate for the larger separation, an increase in the molecular tilt axis (θ_m) is expected. Molecular space filling models predict a θ_m value of 27° for alkyl thiol on gold (111),[16] which is in good agreement with experimental data. Likewise, a value of at least 35° is predicted for alkylamine monolayers on $YBa_2Cu_3O_7$ (001) (Figures S3 and S4, Supporting Information). This tilt angle prediction is based on a tilting of the monolayer chains in the (110) plane of $YBa_2Cu_3O_7$. If the monolayer chains were to be tilted in the (100) or (010) plane of the lattice, the predicted tilt angle is found to increase to 50° due to the larger copper−copper distance in the (100) and (010) lattice dimensions (Figure 1B).

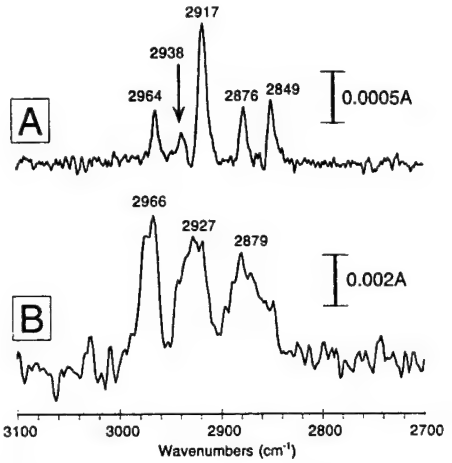

Figure 4. Shown here are GRIFTS spectra for octadecyl thiol monolayers that are adsorbed to two different gold surfaces: (A) a smooth (111) oriented gold film prepared by the evaporation onto glass and (B) a rough, polycrystalline gold surface prepared by the evaporation of gold onto a ceramic pellet of $YBa_2Cu_3O_7$.

Polycrystalline $YBa_2Cu_3O_7$ and Au Surfaces. Polycrystalline ceramic samples of $YBa_2Cu_3O_7$, when exposed to octadecylamine, are found to support the adsorption of monolayers as shown in Figure 2C. While both (100) and (001) oriented films of $YBa_2Cu_3O_7$ serve as templates for growth of ordered monolayers of the primary amine reagent, the same molecule adsorbed on ceramic surfaces is found to be highly disordered as evidenced by the asymmetric methylene stretching frequency of 2931 cm^{-1} as well the peak width of 22 cm^{-1} (Table 1).

To further explore the role of surface roughness on a more classical substrate, alkyl thiol reagents were adsorbed onto smooth and polycrystalline gold surfaces. For the former, Au (111) was evaporated onto smooth glass substrates according to standard literature procedures.[50,74] Shown in Figure 4A is a GRIFTS spectra showing the C−H stretching region for octadecyl thiol adsorbed onto an evaporated film of gold (111). This spectra replicates the five main C−H vibrational modes noted previously for this system.[16,18] Three of the modes (2964, 2938, 2876 cm^{-1}) are assigned to the CH_3 modes, and the other two modes (2917, 2849 cm^{-1}) are attributed to the CH_2 vibrations.[20]

As mentioned above, the frequencies of the alkyl modes are diagnostic of the crystallinity of the hydrocarbon-based monolayer. Spectra of octadecyl thiol adsorbed onto Au (111) show the antisymmetric methylene stretch at 2917 cm^{-1} (Figure 4A), the frequency of which corresponds nicely to solid paraffin. A crystalline-like monolayer structure is suggested from these data.[16,18]

While XRD experiments showed that gold evaporated onto glass substrates exhibited exclusive (111) orientation, gold that

(74) Willicut, R. J.; McCarley, R. L. *Langmuir* **1995**, *11*, 296−301.

is evaporated onto a rough $YBa_2Cu_3O_7$ ceramic samples adopts rough morphological characteristics and yields polycrystalline orientations. Use of this roughened gold as a substrate for monolayer adsorption allows the dependence of the substrate roughness to be studied for the well-characterized adsorbate system. Accordingly, shown in Figure 4B is a GRIFTS spectrum of octadecyl thiol adsorbed to this roughened gold system. These data shows the typical signature of a disordered monolayer, that is, the asymmetric methylene stretch appears at 2927 cm^{-1} with a spectral width of 33 cm^{-1}. These results demonstrate that there is a strong dependence on the quality (i.e., the smoothness and the orientation) of the monolayer adsorption substrate.

Poirier has extensively studied the role of substrate defects and their affect on the crystallinity of the adsorbed monolayer.[75] These prior studies concluded that small concentrations (<5%) of defects in the substrate do not affect the crystallinity of the resulting monolayer. However, substrates that have larger concentrations of defects, or are highly roughened, do not possess the long-range order necessary to produce a well-ordered monolayer film. Defects in the $YBa_2Cu_3O_7$ lattice primarily occur at the grain boundaries. While grain sizes within the films are actually smaller than those observed for the ceramic specimens, the relative orientation grain-to-grain is much more controlled for the films relative to the ceramics.

Atomic force microscopy (AFM) was used to quantify the surface roughness properties of these substrates. Using AFM, dramatic differences in the root-mean-square (RMS) roughness values were measured for evaporated gold on glass (4.39 nm), a (001) oriented $YBa_2Cu_3O_7$ thin film (17.0 nm), a (100) oriented $YBa_2Cu_3O_7$ thin film (30.9 nm), and a particularly smooth polycrystalline $YBa_2Cu_3O_7$ pellet (293 nm). In general, ceramic pellets of $YBa_2Cu_3O_7$ are much too rough to evaluate by AFM instrumentation. Shown in Figure 5 are typical AFM images of the surfaces examined in this report. Also included is a profilometry measurement of the surface of a typical polycrystalline $YBa_2Cu_3O_7$ pellet (Figure 5D). The two different $YBa_2Cu_3O_7$ samples seen in Figure 5 are of comparable roughness, whereas the gold film is significantly smoother and the ceramic pellet is significantly rougher.

From these images it is clear that oriented $YBa_2Cu_3O_7$ thin film samples are relatively smooth as are evaporated gold specimens. The surface morphological characteristics allow for the formation of compact and crystalline monolayers. The roughness of the $YBa_2Cu_3O_7$ ceramic pellet, and the gold surface that was deposited thereon, precludes any long-range order, which would be necessary for the formation of compact and crystalline monolayers. Given the results for the polycrystalline $YBa_2Cu_3O_7$ and the data from the polycrystalline gold case, a strong argument can be made that the smoothness, orientation, and defect density of the substrate are critical factors for producing compact, ordered, and defect-free monolayers.

Alkylamine Substitution Pattern Dependence. Amines offer the capability of being substituted to various degrees allowing for studies involving the substitution pattern dependence of monolayer ordering characteristics. We find that the substitution pattern of the monolayer reagent plays a vital role in the crystallinity of the resulting monolayer. While, monothiol-based reagents can accommodate only one alkyl substituent directly attached to the sulfur headgroup, amines can possess up to three alkyl substituents. Interestingly, we observe that primary (octadecylamine), secondary (dioctylamine), and tertiary amines (trioctylamine) all spontaneously adsorb to $YBa_2Cu_3O_7$.

(75) Poirier, G. E. *Langmuir* **1997**, *13*, 2019−2026.

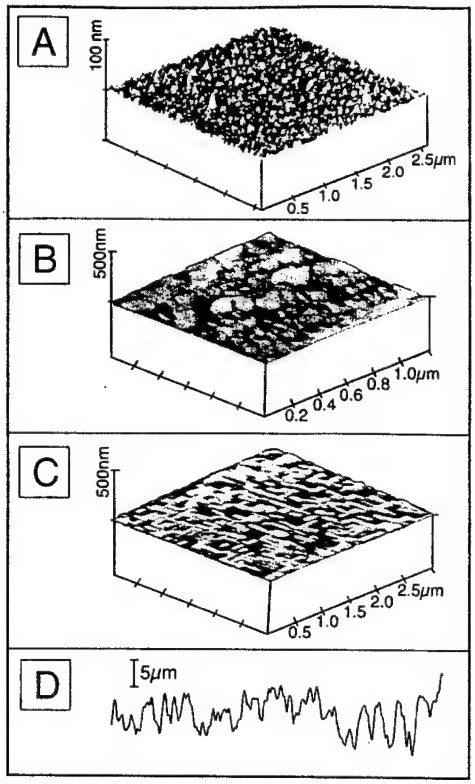

Figure 5. Shown are AFM images and a profilometry trace for the four substrates studied herein. Included here are AFM images of (A) a typical evaporated gold film, (B) a (001) oriented $YBa_2Cu_3O_7$ film, (C) a (100) oriented $YBa_2Cu_3O_7$ film, and (D) a profilometer trace of a typical polycrystalline $YBa_2Cu_3O_7$ pellet. For the last case, the length over which the profilometry trace was recorded was 2000 μm. The large Z range for the $YBa_2Cu_3O_7$ pellet prevented an AFM measurement on this surface.

However, the secondary and tertiary amines do not form crystalline monolayers on $YBa_2Cu_3O_7$ (001) films or pellets (Table 1) as do the above-described primary amines. Rather, the GRIFTS spectra obtained for these samples are very similar to the primary amine reagents adsorbed on rough substrates. Shown in Figure 6 is a comparison of trioctylamine, dioctylamine, and octadecylamine adsorbed to $YBa_2Cu_3O_7$ (001) oriented thin films. In addition, spectra of these same three amine reagents were taken on rough $YBa_2Cu_3O_7$ ceramic samples (not shown). These spectra are very similar to those shown in Figure 6, and the results of such studies are summarized in Table 1.

It is apparent from the peak position and peak width measurements that the secondary and tertiary amines form disordered monolayers when adsorbed to both rough and smooth substrates. This behavior indicates that the crystallinity of the resulting monolayer is strongly dependent on the substitution pattern of the amine monolayer reagent.

Thermal Desorption. The GRIFTS technique was also employed to follow the thermal desorption and subsequent readsorption of alkylamines to a $YBa_2Cu_3O_7$ thin film. GRIFTS spectra were taken at each iteration. Initially, a $YBa_2Cu_3O_7$ film was modified with a monolayer of trioctylamine which yielded an IR signature consistent with a disordered monolayer (Figure 7A). The modified film was then annealed in flowing oxygen at 550 °C for 12 h, and the loss of C−H vibrational characteristics were noted (Figure 7B). Immediately after the annealing step and GRIFTS characterization, the film was exposed to a 1 mM solution of octadecylamine to reestablish the monolayer (Figure 7C). From an analysis of the peak

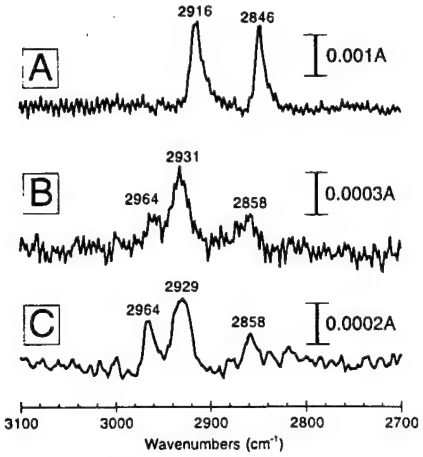

Figure 6. Provided are GRIFTS spectra for three different amine reagents adsorbed to $YBa_2Cu_3O_7$ (001) films. Shown here is data for primary, secondary, and tertiary substituted linear alkylamines: (A) octadecylamine, (B) dioctylamine, and (C) trioctylamine. While the dioctylamine and the trioctylamine samples show disordered or liquid-like behavior, it is apparent that ordered monolayers are obtained with octadecylamine.

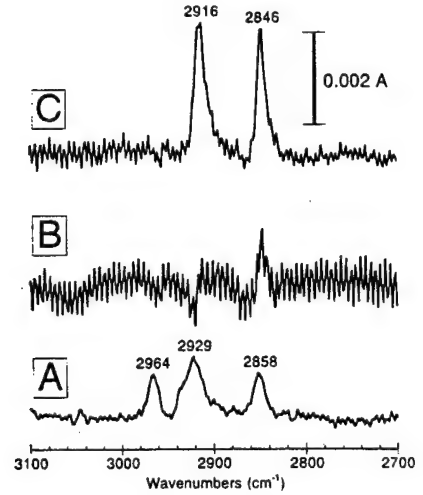

Figure 7. The adsorption and thermal desorption followed by readsorption of various amine reagents atop a single $YBa_2Cu_3O_7$ (001) thin film sample are followed by GRIFTS measurements. (A) Initially, the high-T_c sample is exposed to trioctylamine resulting in the formation of a disordered monolayer. (B) The same sample is subsequently heated to 550 °C in flowing O_2 for 12 h, and the resulting sample shows no infrared signature for adsorbed hydrocarbon. (C) Finally, the same sample was then exposed to octadecylamine and the appearance of an ordered monolayer is observed.

positions, it is clear that the noncrystalline trioctylamine monolayer was removed by the annealing procedure and replaced by the crystalline octadecylamine monolayer. Moreover, it is clear that the surface of the $YBa_2Cu_3O_7$ after monolayer desorption remains receptive to further monolayer adsorption. Thus, thermal desorption appears to be an effective processing procedure that can be exploited to remove the organic layer after its utility is no longer required. This behavior may have important implications in the context of developing "soft chemistry" methods for processing/packaging of high-T_c conductors and devices.

Molecular Modeling. While the above infrared experiments yield essential qualitative information about the ordering characteristics of the amine monolayers on various types of $YBa_2Cu_3O_7$ surfaces, it is desirable to consider in more detail the structural features of the adsorbate layer. Prior successful methodologies for monolayer ordering of the more conventional adsorbate systems such as alkyl thiols on gold (111) have been fully described using popular methods such as ellipsometry and dipolar analysis by polarized infrared data. For the ellipsometric experiments, a number of attempts have been completed and disagreement remains in the literature related to the intrinsic optical constants for $YBa_2Cu_3O_7$.[76] Further work is required here before this technique can be applied to yield reliable information regarding superconductor monolayer structures. Likewise, calculations of molecular tilt angles via the method pioneered by Allara, Chidsey, and Nuzzo[16,18] await more complete characterization of the optical characteristics of $YBa_2Cu_3O_7$ surfaces.

With the advent of powerful computer hardware and efficient software methodologies, computational chemistry is able to provide important structural information for complicated systems.[77,78] Indeed, there is a large body of literature describing computational studies on self-assembled monolayers (SAMs) using molecular mechanics,[79,80] molecular simulations,[81-83] molecular dynamics,[81,84-90] and various other methodologies,[91,92] with the majority of these studies focusing on alkyl thiols adsorbed onto gold (111). Structural information can be obtained through all of these techniques. However, complicated dynamic information on the formation of these monolayers can only be obtained through the more sophisticated techniques, such as molecular dynamics simulations. In this study, our goal is to identify the prominent structural features of the superconductor-localized monolayers. Therefore, we have chosen to employ an efficient molecular mechanics technique for evaluating the favorability of packing arrangements afforded by the permitted degrees of freedom. Although the headgroup−substrate interaction is energetically important for the formation of monolayers, the overall SAM structure is also highly dependent on interchain interactions. The cumulative interactions for the contributing CH_2 groups play an essential role in dictating the structural characteristics of the surface-localized monolayers and is the focus of the modeling studies discussed here. The headgroup−substrate interaction in SAM modeling often serves to keep the chemisorbed molecules in two dimensions and in registry with the substrate.[93] Because this registry is accomplished artificially in our model, the exclusion of the headgroup interaction is not expected to significantly affect the results presented here. More sophisticated molecular dynamic modeling, which incorporates

(76) Gibbons, B. J.; Trolier-McKinstry, S.; Schlom. D. G.: Eom, C. B. *Mater. Res. Soc. Symp.* **1996**, *401*, 333−338.
(77) Davidson, E. R. *Chem. Rev.* **1991**, *91*, 649−1108.
(78) Lipkowitz, K. B.; Boyd, D. B. *Reviews in Computational Chemistry*; VCH: New York, 1990−1997; Vol. 1−10.
(79) Ulman, A.; Eilers, J. E.; Tillman, N. *Langmuir* **1989**, *5*, 1147−1152.
(80) Ulman, A. *Chem. Rev.* **1996**, *96*, 1533−1554.
(81) Shnidman, Y.; Ulman, A.; Eilers, J. E. *Langmuir* **1993**, *9*, 1071−1081.
(82) Siepmann, J. I.; McDonald, I. R. *Langmuir* **1993**, *9*, 2351−2355.
(83) Siepmann, J. I.; McDonald, I. R. *Mol. Phys.* **1992**, *75*, 255−259.
(84) Hautman, J.; Klein, M. L. *J. Chem. Phys.* **1989**, *91*, 4994−5001.
(85) Hautman, J.; Klein, M. L. *J. Chem. Phys.* **1990**, *93*, 7483−7492.
(86) Hautman, J.; Bareman, J. P.; Mar, W.; Klein, M. L. *J. Chem. Soc., Faraday Trans.* **1991**, *87*, 2031−2039.
(87) Bhatia, R.; Garrison, B. *Langmuir* **1997**, *13*, 765−769.
(88) Tupper, K. J.; Brenner, D. W. *Langmuir* **1994**, *10*, 2335−2338.
(89) Tupper, K. J.; Colton, R. J.; Brenner, D. W. *Langmuir* **1994**, *10*, 2041−2043.
(90) Sellers, H.; Ulman, A.; Shnidman, Y.; Eilers, J. E. *J. Am. Chem. Soc.* **1993**, *115*, 9389−9401.
(91) Gerdy, J. J.; Goddard, W. A. I. *J. Am. Chem. Soc.* **1996**, *118*, 3233−3236.
(92) Felix, O.; Hosseini, M. W.; Decian, A.; Fisher, J. *Angew. Chem., Int. Ed. Engl.* **1997**, *36*, 102−104.
(93) Pertsin, A. J.; Grunze, M. *J. Chem. Phys.* **1997**, *106*, 7343−7351.

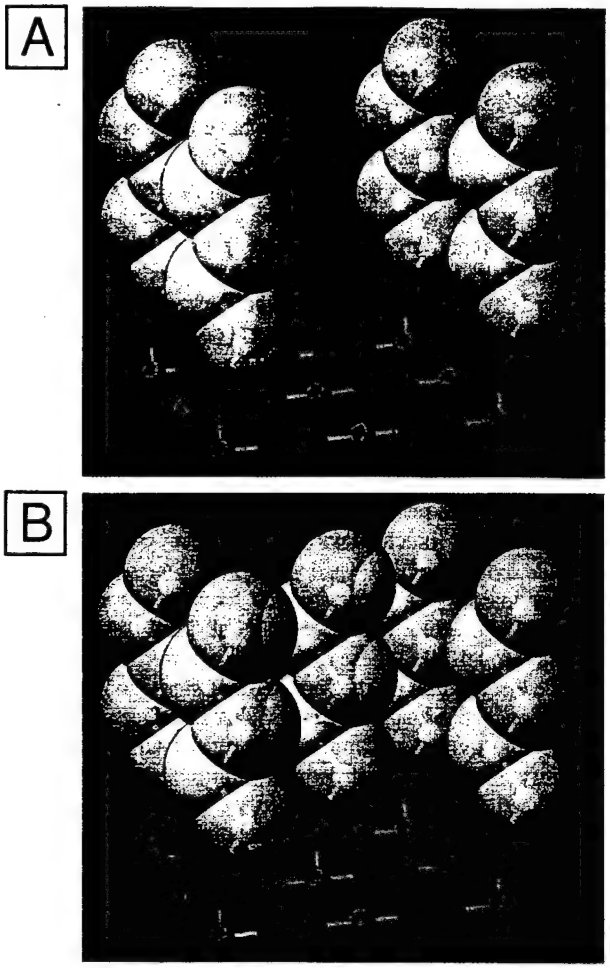

Figure 8. Schematic illustrations showing two clusters of amine reagents adsorbed to a copper oxide table. The amine headgroups are shown in blue, the copper ions in the lattice are shown in green, and the oxygen atoms of the lattice are shown in red. The hydrocarbon layer is shown with 100% van der Waals' radii. Hydrogen atoms are omitted for clarity. The copper oxide "table" in this figure corresponds to the surface of (001) oriented $YBa_2Cu_3O_7$, with the monolayer in a $\sqrt{2}\times\sqrt{2}$R45° adlayer geometry. In case A, four amines at the corners of the table. In case B, the amine located at the center of the table is also included.

the headgroup−substrate interaction, is currently underway and will be the subject of a future report.

To reduce errors associated with edge effects and to create a computationally efficient method to assay the energetic features of the various geometries, two molecular clusters of the type shown in Figure 8 were evaluated. One cluster contains four amine molecules at the corners of a "cuprate table". Note that the middle copper adsorption site is left vacant in this cluster. The second cluster differs by the presence of a fifth amine in the central, previously vacant site. Thus, the amine headgroups are aligned in one plane and spatially separated from one another by a distance corresponding to the $\sqrt{2}\times\sqrt{2}$R45° adlayer separation of (001) oriented $YBa_2Cu_3O_7$.[94] Other arrangements, such as 1×1 or 2×2 adlayers, show less favorable energies.

(94) Energies for 1×1, 2×2, and $\sqrt{2}\times\sqrt{2}$R45° amine adlayers were calculated for various plausible geometries. Here, tables analogous to those described in the text were created to evaluate the energy of amine reagents in environments having all the nearest neighbors present. For the 1×1 case, overlap between neighboring chains precluded any molecular tilt. For the 2×2 case, large separation between sites limited favorable molecular interactions. Comparison of the energies for the various optimized monolayer structures suggests that the $\sqrt{2}\times\sqrt{2}$R45° adlayer is more stable than either the 1×1 or 2×2 arrangements.

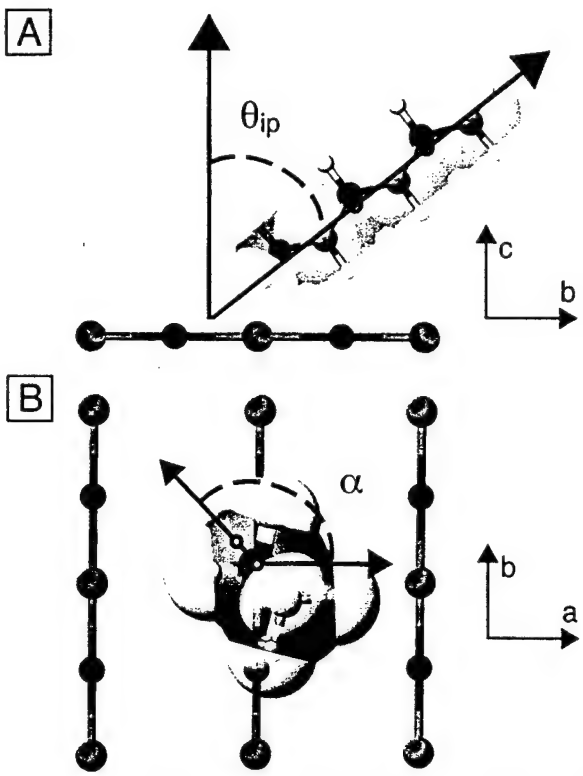

Figure 9. Schematic illustration which details the (A) in-plane tilt (θ_{ip}) and (B) the molecular twist angle (α). For A, θ_{ip} is a measure of the angle between the *c*-axis and the molecular axis projection into the *bc*-plane. The out-of-plane tilt (θ_{op}) is similarly obtained. For B, the twist angle is measured between the plane of the C−C backbone and the *a*-axis of the substrate. The amine headgroups are shown in blue, the copper ions in the lattice are shown in green, and the oxygen atoms of the lattice are shown in red.

The energy of both clusters are evaluated using an MM2 force field. Only the chain interactions are considered; the lattice and headgroup−substrate interaction are not included in these energy calculations. By subtracting the four amine cluster energy from the five amine cluster energy, the contribution for the single amine present with all its nearest neighbors can be obtained. Since the clusters contain a differing number of chains, the intramolecular energy for one chain was removed from the energy difference between the two clusters; only the intermolecular energies were considered. While this model is simple and would not be sufficient for a thorough understanding of the dynamics of monolayer formation, it has the advantages of being a computationally efficient method for evaluating the favorability of packing arrangements afforded by the permitted degrees of freedom.

In this study, three degrees of freedom of molecular orientation were permitted: an in-plane tilt (θ_{ip}), an out-of-plane tilt (θ_{op}), and a twist (α) around the molecular axis of each molecule. A schematic illustrating two of these degrees of freedom is shown in Figure 9. Here, the amine chain orientation will be described in terms of local $YBa_2Cu_3O_7$ lattice parameters. The amine nitrogens are coplanar in the *ab*-plane (substrate plane). Tilt angles were measured using the angle formed by the molecular axis, as defined by the line bisecting the first and last carbon−carbon bonds on the chain, and the *c*-axis (surface normal). The in-plane tilt (θ_{ip}) is defined as the angle between the projection of the molecular axis into the *bc*-plane and the *c*-axis of the lattice. Similarly, the out-of-plane tilt (θ_{op}) is defined as the angle between the projection of the molecular axis into the *ac*-plane and the *c*-axis of the cuprate lattice. The

twist angle is defined as the angle formed by the *b*-axis and the projection from the middle methylene carbon (i.e., the γ carbon to the amine headgroup) through the midpoint of its two hydrogens onto the *ab*-plane. Here, a zero degree twist angle ($\alpha = 0°$) is defined as the projection lying in the *bc*-plane (i.e., along the positive *b*-axis).

Since spectroscopic evidence indicates that the adsorbed monolayer is crystalline, it is reasonable to assume that the chemical homogeneity of the system is relatively high. Therefore, all of the alkyl chains in the clusters are treated as being identical in conformation and orientation relative to the underlying lattice. Also, the favored molecular conformation in the monolayer and the molecular conformation for an isolated molecule are not expected to differ significantly, because of the simplicity of the rodlike molecular shape and the dominance of van der Waals' interactions among the chains.[95] Thus, exact duplicates of a chain which was *ab initio* optimized as an isolated molecule were used to construct the modeled patterns. Once the molecules were in the modeled pattern, the molecules were not permitted to change their intramolecular geometry characteristics.

To justify the use of an MM2 force field in these computations, we carried out identical MNDO-PM3 and MM2 studies on a representative system. Specifically, we examined the energy difference between the five- and four-amine clusters as a function of the in-plane tilt. The results indicated that both the MNDO-PM3 model and the less-sophisticated MM2 model predict a 53° in-plane angle for the representative system. Moreover, the curves are virtually identical in magnitude of energy difference and functional shape.

The above-described procedure possesses an advantage over some prior studies on other SAM systems in which clusters were used with incomplete nearest neighbor arrangements. For example, a linear patch of three alkyl thiols spaced at the gold (111) separation distance was found to exhibit an optimal tilt angle of 32°.[96] When our cluster arrangement and computational procedure is applied to the alkyl thiol case to extract the energy for a single thiol with its six nearest neighbors, we find the largest energy difference between the two clusters and, thus, the best packing arrangement occurs with an alkyl thiol molecular tilt of 29° away from the gold surface normal along with twist about the molecular axis of 63° (Figure S5, Supporting Information). These values agree nicely with the experimentally reported values of molecular tilt and twist angles of 27° and 55°, respectively,[51] and provide credence to the described computational method. Thus, the use of the complete set of nearest neighbors combined with the identification of the energetic characteristics of single adsorbate reagents appears to be an effective procedure for the modeling of ordered adsorbate layers systems.

Although Kitaigorodoskii did extensive studies on the possible forms of packing of infinite hydrocarbon chains,[97] the degree to which monolayer tilting influences the energy for orthorhombic $YBa_2Cu_3O_7$ supported monolayers has yet to be reported. Therefore, the energy of a series of clusters having different combinations of the two tilt angles and twist angle were investigated. To reduce the amount of computational time required to complete this study, logical assumptions were made and tilt angle combinations that would clearly not yield minimum energies were discarded. Also in the interests of reduced computational time, five-carbon amine chains were used to search for plausible structures. However, strategically important areas were also evaluated using 10-carbon-chain amines; all of the optimal angles obtained with these longer chains agreed nicely (±1°) with the shorter chain results. A series of two-dimensional slices through the three-dimensional energy difference surface are presented here.

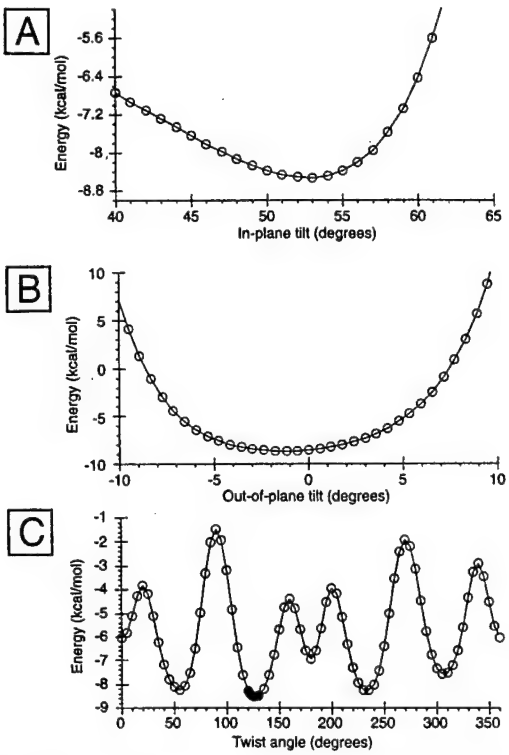

Figure 10. Energy characteristics of uniformly organized adsorbate layers having various structures. A multidimensional energy contour map is created where values of θ_{ip} (A), θ_{op} (B), and α (C) are varied. Two-dimensional slices are obtained through the energy surface near the energy minimum which focus on curves associated with lowest identified energy minimum, $\theta_{ip} = 53°$, $\theta_{op} = 0°$, and $\alpha = 126°$. Three curves are provided: (A) energy vs θ_{ip} where fixed values of $\theta_{op} = 0°$ and $\alpha = 126°$ are used, (B) energy vs θ_{op} where $\theta_{ip} = 53°$ and $\alpha = 126°$, and (C) energy vs α where $\theta_{ip} = 53°$ and $\theta_{op} = 0°$ are used.

Two plausible monolayer geometries corresponding to two minima located on the energy difference surface were identified. The deepest minimum occurs at $\theta_{ip} = 53°$, $\theta_{op} = 0°$, and $\alpha = 126°$. The graphs of energy differences as a function of these variables are shown in Figure 10. Space-filling diagrams of the five-amine cluster of this best packing geometry is shown in Figure 11A,B. It is apparent from careful inspection of the optimized geometry that excellent van der Waals' contacts occur in this system by interdigitation of the hydrogens with the central amine (Figure 11B). The large in-plane tilt in this geometry precludes any significant out-of-plane tilting of the amine reagents toward the diagonal direction of the lattice (i.e., along the 110 plane). With this geometry, the molecular tilt occurs in a direction which coincides nicely with the *b*-axis direction of the high-T_c substrate. Note that in this direction, the amine reagents seek out the association with their next nearest neighbors. Tilting along the principal axis directions allows for this large value for the molecular tilt axis.

Careful evaluation of the energetic characteristics of alternative geometries reveals a second minimized structure occurring at $\theta_{ip} = 32°$, $\theta_{op} = 14°$, and $\alpha = 120°$ (Figure S6, Supporting Information). This favorable five-amine cluster is shown in

(95) Nuzzo, R. G.; Korenic, E. M.; Dubois, L. H. *J. Chem. Phys.* **1990**, *93*, 767–775.

(96) Ulman, A.; Eilers, J. E.; Tillman, N. *Langmuir* **1989**, *5*, 1147–1152.

(97) Kitaigorodskii, A. I. *Organic Chemical Crystallography*; Consultants Bureau Enterprises, Inc.: New York, 1961.

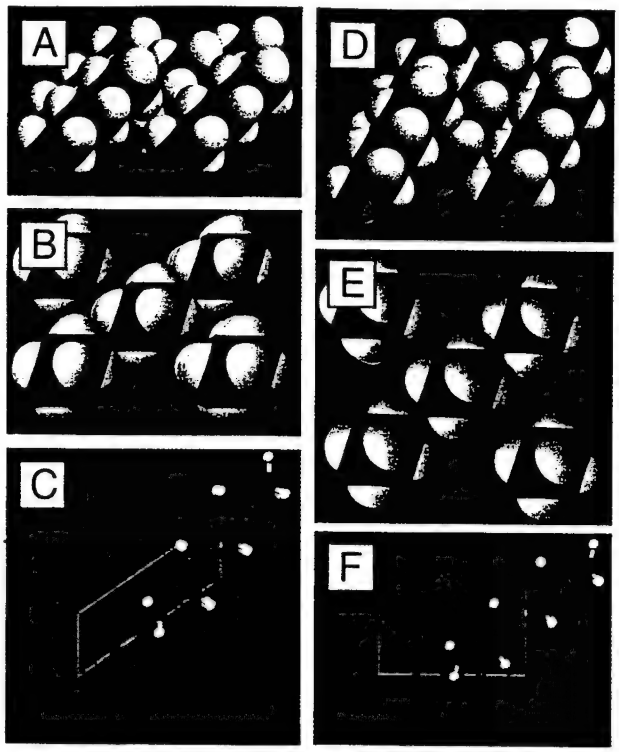

Figure 11. Molecular models showing the packing and orientational properties of the lowest energy system: $\theta_{ip} = 53°$, $\theta_{op} = 0°$, and $\alpha = 126°$. Included are three different views: (A) side perspective of the space filling structure, (B) similar structure viewed from the top surface down the molecular axis, and (C) a single adsorbate molecule is isolated and shown with respect to the crystallographic axes of the $YBa_2Cu_3O_7$ (001) superconductor substrate. Shown in (D), (E), and (F) are analogous views for the minimum encountered at $\theta_{ip} = 32°$, $\theta_{op} = 14°$, and $\alpha = 120°$.

Figure 11D,E,F. Again, the interdigitation of the hydrogens with the central amine provides good van der Waals' contacts. By viewing down the molecular axes of these clusters (Figure 11B,E), the superiority of the 53°, 0°, 126° geometry's packing can be seen; the gaps between the chains in this geometry are much smaller than the 32°, 14°, 120° geometry.

As expected for a rectangular substrate system, the twist angle (α) in both geometries exhibits a 4-fold periodicity. The twist angle plays a significant role in both geometries, exhibiting a calculated barrier to rotation of about 1.5 kcal mol^{-1} per methylene unit in the 53°, 0°, 126° case. For comparison, using the same computational method, the barrier to rotation found for the alkyl thiol/gold system is about 1.8 kcal mol^{-1}. The high-energy twist angle geometries result from extremely close chain contacts. Because of the rigidity found in the alkyl thiol/gold (111) system[98] and the similarity of rotational energy barriers between the two systems, we expect that there will be little rotation about the molecular axes for the superconductor-localized reagents. The barrier to rotation is lowered in the 32°, 14°, 120° case as the amines have more space available before encountering their neighbor. However, the barrier is still significant for this geometry. It is important to note that the absolute values of the calculated energies are not meant to provide an accurate measure of the energetic characteristics of real systems. Rather, meaningful comparisons are made with respect to the relative calculated values.

While these minima appear significant in our assay of the energy difference surface, certain precautions must be heeded when evaluating these results. As mentioned previously, this model can neither account for the dynamics of monolayer formation nor include interactions with the substrate. Thus, the tilt and twist angles described here are representative of the best packing as influenced by chain interaction for the prescribed spacing. More sophisticated molecular dynamics calculations involving this interaction are underway. Also, these two minima are not the only ones on the energy difference surface. Because the lattice constants for the *a*- and *b*-axes are similar for $YBa_2Cu_3O_7$, we expect that the minima at both these geometries have "mirror" minima, i.e., $\theta_{ip} = 0°$, $\theta_{op} = 53°$, $\alpha = 126°$ would be close to another minimum. Furthermore, the energy differences between the $\theta_{ip} = 53°$, $\theta_{op} = 0°$, and $\alpha = 126°$ and $\theta_{ip} = 32°$, $\theta_{op} = 14°$, and $\alpha = 120°$ geometries are modest. Thus, it is likely that both structural types can exist simultaneously atop real samples of $YBa_2Cu_3O_7$ (001) which are modified with long alkyl chain primary amine reagents.

Importantly, the rather large tilt angles predicted by these computational studies are consistent with experimental evidence. To couple to the incident radiation in a GRIFTS experiment, it is necessary to have a component of the vibrational dipole that is perpendicular to the substrate. Assuming that the monolayer assumes a tilt angle of 53°, the dipole of the methyl symmetric stretching mode lies at an angle of 87° away from the substrate normal (Figure S2, Supporting Information). The dipole projection is nearly parallel to the substrate surface where coupling to the incident radiation is expected to be very weak. In addition, the vibrational dipole of the out-of-plane asymmetric methyl stretch lies in the plane of the substrate. The vibrational dipole of the in-plane asymmetric methyl stretch has a component that lies perpendicular to the substrate. Interestingly, this mode has not been identified in the $YBa_2Cu_3O_7$/alkylamine system when adsorbed to (001) oriented $YBa_2Cu_3O_7$. This mode is also not observed in the alkyl thiol/GaAs (100) system.[27] Allara and co-workers ascribed the high tilt angle of this system as being responsible for the low signal from this vibration. The large tilt angle predicted by computer modeling of the $YBa_2Cu_3O_7$/alkylamine system combined with the low absorbance value observed for the one methyl group per adsorbate molecule adequately explains the observed low signal intensity for this vibration.

Summary

New procedures have been developed for the preparation and analysis of superconductor-localized monolayers structures. Here, the following important information has been acquired: (1) GRIFTS methods have been successfully employed for the first time to evaluate the structural characteristics of cuprate monolayers. Such measurements have become possible only following the identification of important experimental variables such as superconductor sample thickness, substrate roughness, and monolayer formation procedures. (2) Likewise, a large substrate orientation dependence is noted for this system. Oriented films of $YBa_2Cu_3O_7$ (001) are shown to support crystalline-like monolayers, while polycrystalline samples yield disordered adsorbate layers. (3) Furthermore, a substitution pattern dependence for amine reagents is observed. Primary amines form crystalline monolayers, while secondary and tertiary amines form disordered monolayers on $YBa_2Cu_3O_7$ (001). (4) A plausible adsorbate layer structure of $\sqrt{2}\times\sqrt{2}R45°$ has been proposed, and calculations examining alkylamine packing support this adsorbate layer structure as the favored one for long linear chain reagents. (5) An efficient and simple computational method has been devised for the evaluation of

(98) Karpovich, D. S.; Blanchard, G. J. *Langmuir* **1996**, *12*, 5522−5524.

the energies of adsorbate layer structures. Although this new method does not incorporate the headgroup−substrate interaction, it has been tested on the well studied alkyl thiol/gold (111) system and found to yield results which agree extremely well with the accepted experimental values. The method has been applied also to the alkylamine/$YBa_2Cu_3O_7$ (001) adsorbate structure where two distinct, stable structures have been identified. The most energetically stable system found from the computational experiments would be expected to yield reflectance IR characteristics consistent with the observed experimental data. (6) Methods for the thermal desorption of the amine reagents from the high-T_c surface have been developed as have strategies for the subsequent readsorption of similar reagents. The reversible adsorption/desorption process noted here suggest that the described "soft chemistry" procedures may be effective for the molecular-level control of superconductor interfacial properties.

Acknowledgment. J.T.M. and D.R.K. acknowledge the Air Force Office of Scientific Research and the National Science Foundation for support of this work. J.T.M. acknowledges the Office of Naval Research for support of this work. J.E.R. acknowledges the support of a University of Texas Continuing Fellowship. D.R.K. acknowledges the Camille and Henry Dreyfus Foundation for support of this work. Professors Al Bard and James Whitesell are thanked for use of their instrumentation. Professors David Allara and Chad Mirkin, and Dr. Atul Parik are thanked for useful discussions.

Supporting Information Available: Supplementary Figures S1−S6 (8 pages). See any current masthead page for ordering information and Web access instructions.

Note Added in Proof. From our studies of a variety of hydrocarbon amine and fluorocarbon amine reagents by X-ray photoelectron spectroscopy, we have obtained important information regarding the nature of the adsorbate−surface headgroup interaction. Likewise, convincing evidence has now been obtained which suggests a strong interaction occurs between the amine lone pair and the copper ions from the high-T_c lattice. A more detailed description of this work will soon be published elsewhere (J. E. Ritchie, J. T. McDevitt, manuscript in preparation). This new information provides the direct experimental evidence which defines the location of the adsorbate docking site and supports the adsorbate−surface binding mode hypothesized in this manuscript.

JA9706920

The First Raman Spectrum of an Organic Monolayer on a High-Temperature Superconductor: Direct Spectroscopic Evidence for a Chemical Interaction between an Amine and $YBa_2Cu_3O_{7-\delta}$

Jin Zhu, Feng Xu, Susan J. Schofer, and Chad A. Mirkin*

Department of Chemistry, Northwestern University Evanston, Illinois 60208

Received July 25, 1996

Since the first reported example of the preparation of an organic monolayer on a cuprate-based high-temperature superconductor (HTSC),[1] a great deal has been learned about the utility of these new surface structures for tailoring HTSC surface and interfacial properties. Monolayers on HTSCs have been used as hydrophobic layers for corrosion passivation[2] and as prelayers for polymer adhesion[2] and nucleation.[3] In addition, they have been used in attempts to prepare a new class of artificial tunnel junctions for studying the fundamental physical properties of the HTSCs.[4] Although the modes of adsorbate surface binding are still undetermined, it is known that alkylamines, arylamines, alkylthiols, alkyldisulfides, and alkylselenols spontaneously adsorb onto the surfaces of a wide range of cuprate superconductors to form robust monolayer films.[1b]

Although organic monolayers on HTSCs have been characterized by a series of surface analytical techniques,[1-3] vibrational spectroscopic methods, which have been crucial to the characterization of other monolayer structures, have yet to be reported for this class of monolayer. Because of its extraordinary sensitivity, surface-enhanced Raman spectroscopy (SERS) has been extremely useful in characterizing monolayer structures on a variety of substrates with accessible surface plasmon resonances, including Au, Ag, and Cu.[5]

Herein, we report a method to do SERS on cuprate superconductors modified with organic monolayers. Using this method, we have obtained the first direct spectroscopic evidence for a chemical interaction between an arylamine and the underlying cuprate superconductor. This method takes advantage of the work of Natan and Murray involving the use of colloids[6] and evaporated metal films,[7] respectively, to enhance the Raman spectra of organic films on a variety of substrates. Natan has shown that Au and Ag nanoparticles will assemble onto surfaces with the appropriate organic functionality to yield SERS-active substrates.[6] The Natan method has been used to gain spectroscopic information regarding organic thin films that were subsequently deposited onto the layer of colloid particles. Apparently, under the conditions employed, the underlying organic monolayer is never spectroscopically observed. Similarly, Murray has shown that Ag metal can be vapor-deposited onto monolayers to gain spectroscopic information regarding the underlying organic structure.[7] Our method, which is a modification of the Natan method and designed to be compatible with the hygroscopic nature and chemical reactivity of the HTSC, yields outstanding Raman spectra of many organic monolayers on $YBa_2Cu_3O_{7-\delta}$. Furthermore, these spectra can be collected from a commercially available FT-Raman spectrometer with a Nd:YAG laser (λ_{ex} = 1064 nm, ~70 mW), making it a very versatile and straightforward approach for the study of organic monolayer films on HTSCs.

Scheme 1

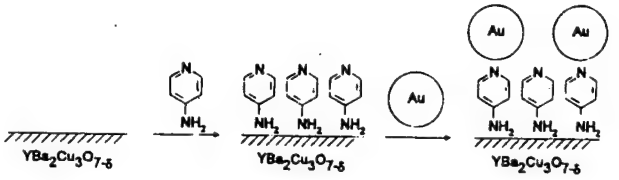

The schematic representation of the monolayer preparation and colloid self-assembly process is shown in Scheme 1. First, a monolayer of 4-aminopyridine is formed on $YBa_2Cu_3O_{7-\delta}$ by immersion of the HTSC in a 1 mM acetonitrile solution of the adsorbate molecule. This molecule was chosen because it has one functional group, an arylamine, that is proposed to have a chemical affinity for the $YBa_2Cu_3O_{7-\delta}$ and a pyridine group that is expected to have an affinity for Au colloids. Both of these assumptions are verified spectroscopically (*vide supra*) and by prior electrochemical data which suggests that the pyridine group *does not* have an affinity for the $YBa_2Cu_3O_{7-\delta}$ under these conditions.[1b] Once the monolayer is formed, its exposure to a solution of Au colloids is expected to result in the adsorption of colloids and the formation of a SERS-active surface.

Unlike the other substrates studied thus far for monolayer purposes,[8ab] $YBa_2Cu_3O_{7-\delta}$ is water sensitive and corrodes in air to form an insulating layer of $Ba(OH)_2$, which subsequently reacts with CO_2 to form $BaCO_3$.[9] This process not only is damaging to the superconductor but it also degrades, and eventually, desorbs the monolayer. To circumvent this problem, Au colloids (5 ± 2 nm) were prepared and dispersed in toluene in the absence of stabilizing alkylthiol.[10] The 5.2 mM colloid solution was subsequently used to modify the HTSC surface-immobilized monolayers, Scheme 1. In toluene solution, the UV-vis spectra of the dispersed colloids exhibit a characteristic absorption band at 520 nm, but when aggregated, this band is red-shifted and responsible for their SERS activity.[5]

In our first experiment, which was designed to test the suitability of the proposed method (Scheme 1), a polycrystalline $YBa_2Cu_3O_{7-\delta}$ pellet[11] was treated with a 1 mM acetonitrile solution of 4-aminopyridine. After soaking the substrate for 48 h, the electrode was thoroughly rinsed with acetonitrile, and the Raman spectrum of the chemically modified surface was acquired. No signal associated with the monolayer was detectable (Figure 1A). Significantly, when the same substrate was immersed in a solution of Au colloids for 2 h and then rinsed several times with pentane to remove the physisorbed colloids,

* Author to whom correspondence should be addressed.

(1) (a) Chen, K.; Mirkin, C. A.; Lo, R.-K.; Zhao, J.; McDevitt, J. T. *J. Am. Chem. Soc.* **1995**, *117*, 6374. (b) Xu, F.; Chen, K.; Zhu, J.; Campbell, D. J.; Mirkin, C. A.; Lo, R.; Zhao, J.; McDevitt, J. T. *Proc. Electrochem. Soc.* **1996**. In press.

(2) McDevitt, J. T.; Mirkin, C. A.; Lo, R.-K.; Chen, K.; Zhou, J.-P.; Xu, F.; Haupt, S. G.; Zhao, J.; Jurbergs, D. C. *Chem. Mater.* **1996**, *8*, 811 and references therein.

(3) Lo, R.-K.; Ritchie, J. E.; Zhou, J. P.; Zhao, J.; McDevitt, J. T.; Xu, F.; Mirkin, C. A. *J. Am. Chem. Soc.* **1996**, *118*, 11295.

(4) Covington, M.; Xu, F.; Mirkin, C. A.; Feldmann, W. L.; Greene, L. H. *Proc. Int. Conf. Low Temp. Phys. (LT-21), 21st*, **1996**.

(5) For a recent review, see: Nabiev, I. R.; Sokolov, K. V.; Manfait, M. In *Biomolecular Spectroscopy, Part A*; Clark, R. J. H., Hester, R. E., Eds.; John Wiley: Chicester, U.K., 1993; Vol. 20, Chapter 7.

(6) Freeman, R. G.; Grabar, K. C.; Allison, K. J.; Bright, R. M.; Davis, J. A.; Guthrie, A. P.; Hommer, M. B.; Jackson, M. A.; Smith, P. C.; Walter, D. G.; Natan, M. J. *Science* **1995**, *267*, 1629.

(7) Murray, C. A.; Allara, D. L.; Rhinewhine, M. *Phys. Rev. Lett.* **1980**, *46*, 138.

(8) (a) Bain, C. D.; Whitesides, G. M. *Angew. Chem., Int. Ed. Engl.* **1989**, *28*, 506. (b) Dubois, L. H.; Nuzzo, R. G. *Annu. Rev. Phys. Chem.* **1992**, *43*, 437.

(9) Barkatt, A.; Hojaji, H.; Amarakoon, V. R. W.; Fagan, J. G. *MRS Bull.* **1993**, *18*, 45.

(10) (a) Brust, M.; Walker, M.; Bethell, D.; Schiffrin, D. J.; Whyman, R. *J. Chem. Soc., Chem. Commun.* **1994**, 801. (b) Brust, M.; Bethell, D.; Schiffrin, D. J.; Kiely, C. J. *Adv. Mater.* **1995**, *7*, 795.

(11) Prepared according to literature methods: Riley, D. R.; McDevitt, J. T. *J. Electroanal. Chem.* **1990**, *295*, 373 and references cited therein.

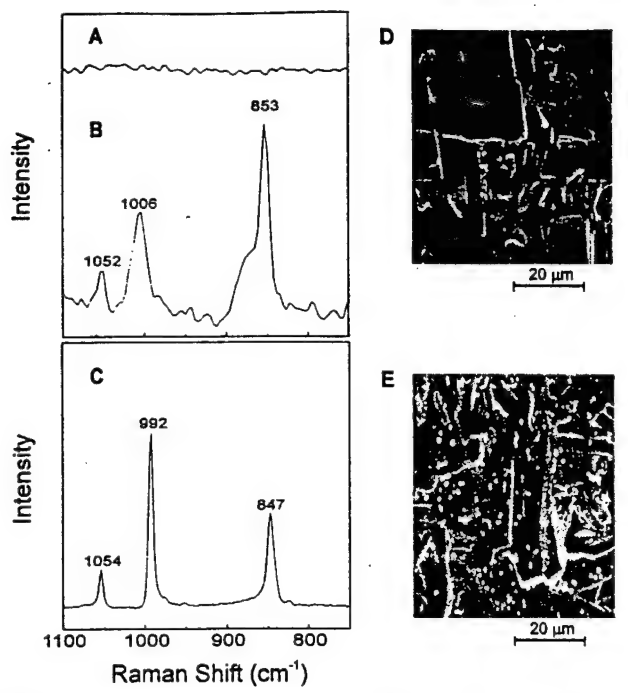

Figure 1. The Raman spectra for $YBa_2Cu_3O_{7-\delta}$ modified with a monolayer of 4-aminopyridine: (A) before treatment with Au colloids (band pass, 4 cm^{-1}, integration time, 160 s) and (B) after 2 h treatment with Au colloids (band pass, 4 cm^{-1}, integration time, 320 s). (C) The Raman spectrum of solid 4-aminopyridine (band pass, 4 cm^{-1}, integration time, 20 s). SEM photographs of $YBa_2Cu_3O_{7-\delta}$ modified with a monolayer of 4-aminopyridine: (D) before treatment with Au colloids, and (E) after soaking in the Au colloid solution for 2 h (white spots are colloid aggregates).

a Raman spectrum with an excellent signal-to-noise ratio was obtained (Figure 1B), which compared well with the spectrum of solid 4-aminopyridine (Figure 1C). The assembly of the Au colloids on the HTSC/monolayer surface was confirmed by scanning electron microscopy (SEM), which clearly shows the surface adsorption of the colloidal particle aggregates (compare panels D and E, Figure 1). Note that the surface coverage of the colloids is soaking-time dependent and, therefore, controllable. Indeed, when the same substrate is soaked in the colloid solution for an additional 12 h, increased colloid surface coverage is observed by SEM. Three strong bands were observed in the 1100−750 cm^{-1} region of the SERS spectrum of the 4-aminopyridine monolayer (Figure 1B). On the basis of the band assignments made by Spinner for solid 4-aminopyridine,[12] we assign the two monolayer bands centered at 1006 and 1052 cm^{-1} to the ring-breathing and deformation modes of the pyridinal ring, respectively. The out-of-plane C−H bending vibration mode also is observed at 853 cm^{-1}.[12a]

Importantly, new information about HTSC monolayers can be obtained via the SERS methodology reported herein. By deuterium labeling the amine group of the 4-aminopyridine, adsorbing the deuterated 4-aminopyridine onto $YBa_2Cu_3O_{7-\delta}$, and characterizing it via SERS, we were able to identify the NH_2 scissoring band for the monolayer at 1625 cm^{-1} (Figure 2). This band, which appears at 1654 cm^{-1} in the Raman spectrum of solid 4-aminopyridine (Figure 2A), experiences a 29 cm^{-1} shift upon adsorption onto $YBa_2Cu_3O_{7-\delta}$ (Figure 2B). Note that these bands were unambiguously assigned to the NH_2 scissoring mode as they experience the expected shift to lower energy when labeled with deuterium (Figure 2C,D). The shift of the NH_2 scissoring band upon adsorption is indicative of the strong chemical interaction between the amine moiety and the underlying HTSC.

(12) (a) Spinner, E. *J. Chem. Soc.* **1962**, 3119. (b) Jakupca, M. R.; Dutta, P. K. *Anal. Chem.* **1992**, *64*, 953.

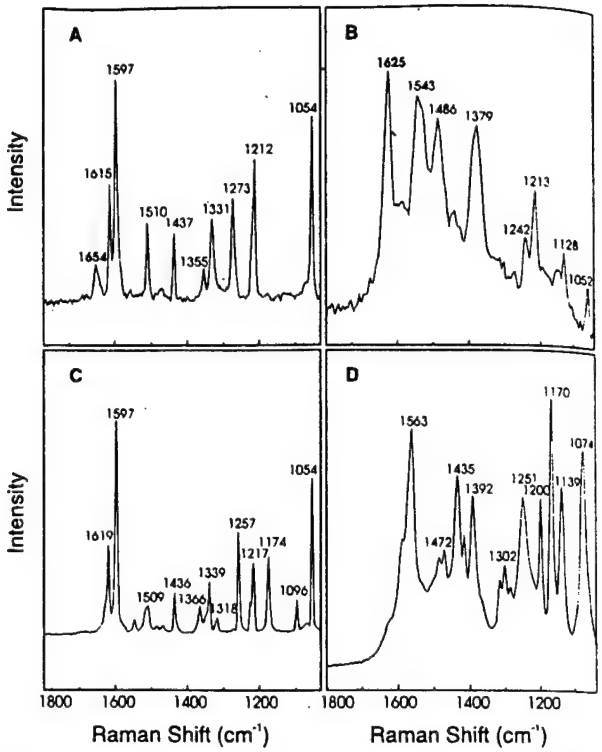

Figure 2. The Raman spectra of (A) solid 4-aminopyridine (band pass, 4 cm^{-1}, integration time, 20 s) (NH_2 scissoring mode in bold, 1654 cm^{-1}), (B) $YBa_2Cu_3O_{7-\delta}$ modified with a monolayer of 4-aminopyridine (band pass, 4 cm^{-1}, integration time, 320 s) (note the NH_2 scissoring mode at 1625 cm^{-1}), (C) solid N-deuterated 4-aminopyridine (band pass, 4 cm^{-1}, integration time, 20 s) (note the disappearance of the band at 1654 cm^{-1} when compared with the Raman spectrum of the unlabeled material, see A), and (D) $YBa_2Cu_3O_{7-\delta}$ modified with a monolayer of N-deuterated 4-aminopyridine (band pass, 4 cm^{-1}, integration time, 320 s) (note the disappearance of the band at 1625 cm^{-1} when compared with the Raman spectrum of the unlabeled material).

To make sure that all of the bands in the monolayer spectra were due to the 4-aminopyridine and not the Au colloids or the $YBa_2Cu_3O_{7-\delta}$, a similar set of spectroscopic experiments were carried out with a monolayer of $NH_2(CH_2)_{10}NH_2$, a molecule with very low Raman cross section bands. This film, which also binds Au colloids, exhibits one barely detectable band centered at 1100 cm^{-1} in the 1800−750 cm^{-1} region of the spectrum in the presence of colloids and no bands in the absence of colloids. This experiment shows that under these conditions (1) the Raman spectrum of the 4-aminopyridine monolayer (Figure 1B) is not complicated by the Raman spectra of the colloids or HTSC and (2) the spectroscopic signal for the monolayer is benefitting from the choice of the large Raman cross section of the 4-aminopyridine adsorbate molecule.

This work (1) documents the first vibrational spectroscopic study of a monolayer on a cuprate superconductor, (2) extends the utility of Au colloids as Raman enhancement tools to the important class of cuprate HTSCs, and (3) provides the first evidence for the direct interaction between the amine group of an adsorbate molecule and the underlying HTSC surface. It is likely that this approach can be used to determine the chemical nature of the adsorption of adsorbate molecules with functional groups other than amines on HTSCs.

Acknowledgment. C.A.M. acknowledges the NSF Science and Technology Center for Superconductivity and the AFOSR for support for this work. C.A.M. also acknowledges use of the NU MRC (Award no. DMR-9120521). Professors J. T. McDevitt, K. R. Poeppelmeier, D. J. Schiffrin, and R. P. Van Duyne and Mr. D. J. Campbell are acknowledged for helpful discussions.

JA962556L

Paper-5

ELSEVIER

Synthetic Metals 84 (1997) 407-408

SYNTHETIC METALS

Molecular Engineering of Organic Conductor / High-Tc Superconductor Assemblies

John T. McDevitt*[a], Jason E. Ritchie[a], Marvin B. Clevenger[a], Rung-Kuang Lo[a], Ji-Ping Zhou[a], Feng Xu[b], Chad A. Mirkin*[b]

a Department of Chemistry & Biochemistry, The University of Texas at Austin, Austin, TX, 78712, USA

b Department of Chemistry, Northwestern University, 2145 Sheridan Road, Evanston IL 60208, USA

Abstract

Organic monolayers on high-Tc superconductors have allowed for the precise structural control of composite organic conductor / high-Tc superconductor assemblies. These hybrid systems display a number of novel electronic and structural properties. This paper discusses the utility of the monolayer self-assembly procedure for the preparation of both conductive polymer and crystalline charge transfer salt layers which are supported directly on top of cuprate superconductor thin film samples.

Keywords: Self-Assembly, Superconductor Composites, Charge Transfer Salts

1. Introduction

A number of researchers have begun to prepare polymer / superconductor composites with the hope of improving the processability and properties of these hybrid materials.[1] Initial studies designed to explore conductive polymer systems in the context of high-Tc applications have now been initiated.[2] Such polymers offer both the prospects for enhanced processability, as well as a wide range of electrical conductivities. Polymeric systems of this type can be doped reversibly from neutral, non-conducting forms to oxidized states which display high electrical conductivity. In their non-conducting form, the electronic interactions between conductive polymers and superconductors should be minimal. Electrochemically deposited polymers may find utility as passivation layers for the protection of high-Tc structures against corrosion or as an insulating dielectric barriers for active devices. However, a doped polymer in intimate contact with a superconductor is expected to display interesting electronic interactions, such as the proximity effect, in an analogous manner to the well documented behavior that has been observed for metal / superconductor and semiconductor / superconductor systems.[1,2]

The important challenge in this area is to define conditions that can be exploited to assemble, in a chemically compatible manner, the hybrid conductive polymer / cuprate superconductor, and organic superconductor / cuprate superconductor structures. Furthermore, it will be necessary to develop techniques which can be utilized to explore the physical and electrical properties of the composite systems. This paper describes two methods for the preparation of hybrid organic conductor / cuprate superconductor assemblies.[3,4]

2. Results

2.1 Polypyrrole/YBa2Cu3O7 composites

The spontaneous adsorption of molecular assemblies onto the surfaces of superconductor films provides an effective and simple method for controlling the interfacial properties of high-Tc structures and devices.[3,5,6] Here, we show that electroactive self-assembled monolayers (i.e. SAMs) based on alkylamine substituted pyrrole functionalities can be used to alter the growth of polypyrrole onto c-axis oriented films of YBa2Cu3O7 . For these studies, polypyrrole was electrochemically polymerized using a potential step technique (1.1V vs. SCE reference) in a 0.1M solution of Bu4NBF4 in 1% pyrrole / acetonitrile. Information relevant to the mechanism of polymerization was explored by varying the deposition times and the applied biases. Data presented in Figure 1 was acquired with a 5 second polymerization time so that details related to the nucleation and initial polymerization can be readily ascertained.

Interestingly, AFM and SEM images of polypyrrole layers grown under identical conditions onto films of c-axis oriented YBa2Cu3O7 thin films, with and without the pyrrole self-assembled monolayer, reveal that the SAM modified surface produces both thicker and more uniform layers (Figure 1). Polypyrrole grown onto the modified superconductor is observed to have >98% surface coverage with feature sizes of approximately 0.20 to 0.25μm width and a surface roughness of <0.05μm. In fact, polymer layers grown onto N-(3-aminopropyl) pyrrole modified YBa2Cu3O7 compare favorably with the smoothest layers of polypyrrole reported in the literature.[7] On the other hand, polymer grown directly onto bare cuprate superconductor leads to the creation of remotely spaced polymer nodules. Here, polymer nodules 0.4μm - 0.6μm in width and 0.3μm - 0.5μm high are observed to cover appx. 4% of the surface.[2]

The observation that ultra-smooth polymer layers are obtained with the pyrrole self-assembled monolayer is consistent with the conclusion that polymer growth proceeds through rapid and uniform nucleation on the pyrrole modified superconductor surface. These studies provide the initial results related to the mapping of the surface conductivity and electrochemical activity of high-Tc materials. Thus, the described method provides a powerful means to evaluate the local surface conductive properties of high-Tc systems.

2.2 (BEDT-TTF)2I3 / YBa2Cu3O7 composites

From theoretical considerations, it is apparent that conductors which exhibit high carrier mobilities, large carrier concentrations, and low effective masses might be expected to support superconductivity over large dimensions.[8] Although some conductive polymers have been shown to exhibit excellent low temperature properties, most polymeric conductors suffer from carrier freeze out at cryogenic temperatures. To a large extent, local inhomogenieties, which are normally present in these disordered polymeric systems, are responsible for this behavior.

* Corresponding author.

PII S0379-6779(96)03960-4

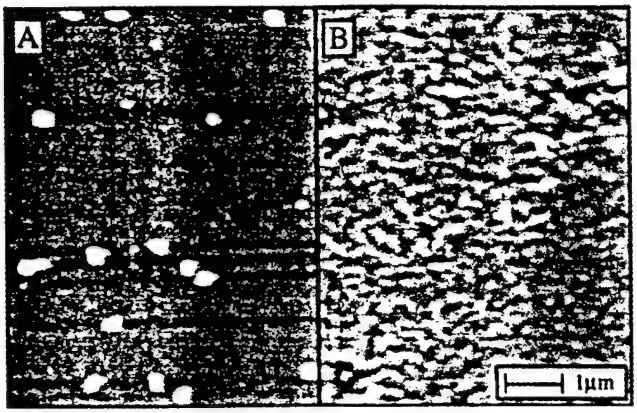

Fig 1 — AFM image acquired for $YBa_2Cu_3O_7$ (c-axis oriented) thin films supported on MgO (100) substrates. Data is provided for (A) bare superconductor as well as (B) superconductor onto which a monolayer of N-(3-aminopropyl)pyrrole was coated. Polypyrrole was polymerized onto both films by a potential step procedure in which the samples were brought from a resting potential of 0.0V vs. SCE to a value of 1.1V vs. SCE for a period of 5 seconds.

Crystalline organic metals, such as those based on bis(ethylenedithio) tetrathiafulvalene (BEDT-TTF), are less susceptible to these effects. Our calculations have shown that crystalline conductors of this type are expected to exhibit large superconducting coherence lengths.[8] Based on this expectation, recent efforts have been devoted to search for methods that can be used to prepare well ordered BEDT-TTF / cuprate superconductor structures. Although there are now a large number of conductors and superconductors based on BEDT-TTF salts, the majority of these materials have been prepared only as single crystals via electrochemical methods. In order to make functional systems which can be readily interfaced with high-Tc structures, it is necessary to prepare thin films of these organic conductors. Recently, methods have been developed for the vapor phase deposition of thin films of (BEDT-TTF)2I3.[9]

We have developed and refined methods for the preparation of well ordered, single phase thin film layers of α, α_T, and β phases of (BEDT-TTF)2I3 using sublimation and thermal anneal methods. A variety of substrates such as Al_2O_3, MgO, $LaAlO_3$, and glass have been used to support the ordered deposition of these films. High quality x-ray diffraction signals document the phase purity and exclusive ordered c-axis orientation for such (BEDT-TTF)2I3 films. Interestingly, organic superconductor layers deposited directly onto YBa2Cu3O7 lead to non-crystalline (BEDT-TTF)2I3 layers by XRD.

In an effort to improve the crystallinity of the organic layer, a self-assembled monolayer composed of a linear alkylamine reagent was created on the surface of YBa2Cu3O7 prior to the vapor phase processing step. Thus, trilayer assemblies incorporating a SAM buffer layer were prepared. Here a three step process was used to create the desired structure. First, YBa2Cu3O7 was deposited onto MgO (100) via the laser ablation method. Second, a self-assembled monolayer of dodecylamine or octadecylamine was formed on the surface of the cuprate compound using our previously reported procedure.[3,5] Third, the (BEDT-TTF)2I3 was sublimed onto the derivatized superconductor.

The importance of the inclusion of the SAM buffer layer is evident from the data presented in Figure 2. Here the direct deposition of (BEDT-TTF)2I3 onto YBa2Cu3O7 leads to a non-crystalline layer of the organic superconductor (Figure 2A). Evidence that the (BEDT-TTF)2I3 is coating the YBa2Cu3O7 comes from x-ray fluorescence, AFM, and optical reflectivity studies. Although the (BEDT-TTF)2I3 is present with the expected elemental composition, the sample is lacking the sharp crystal facets and x-ray powder diffraction signals which would indicate the presence of the crystalline organic material. This unusual effect is highly reproducible having been observed in over 100 carefully prepared samples. However, the inclusion of the SAM buffer layer serves to improve the crystallinity of the (BEDT-TTF)2I3 layer. Figure 2B shows a SEM image of a typical (BEDT-TTF)2I3 sample deposited onto the SAM coated cuprate film where crystalline organic material is apparent. X-ray diffraction studies confirm the crystalline signature of such samples. Studies are now in progress to explore the electrical and superconducting characteristics of these hybrid organic superconductor/cuprate superconductor structures. Furthermore, prospects for creating organic superconductor tunnel junctions are currently being evaluated.

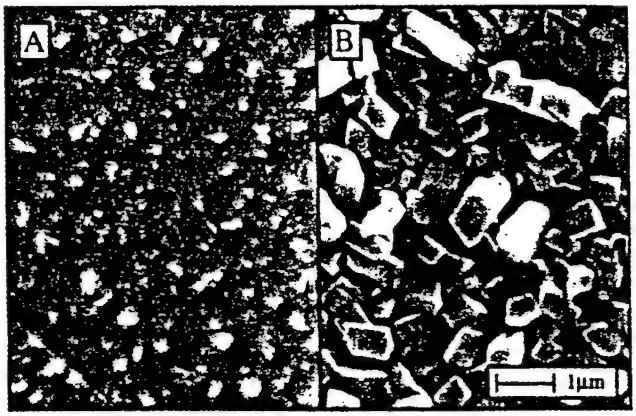

Fig 2 — SEM of (A) $(BEDT\text{-}TTF)_2I_3$ deposited directly onto $YBa_2Cu_3O_7$. (B) $(BEDT\text{-}TTF)_2I_3$ deposited onto octadecylamine modified $YBa_2Cu_3O_7$

3. Conclusions

In summary, this paper describes the construction and study of hybrid assemblies based on conductive polymer and crystalline charge transfer salts which are supported on cuprate superconductor platforms. In the conducting polymer area, a monolayer of N-(3-aminopropyl) pyrrole is used as a template layer for the controlled growth of polypyrrole on YBa2Cu3O7. Large increases in the polymer growth rates and radically smoother polymer layers are obtained using this adsorbed monolayer. Moreover, dramatic improvements in the polymer / superconductor adhesion properties are noted. In the charge transfer salt area, spontaneous adsorption of an alkylamine monolayer onto the cuprate superconductor surface is used to control the crystalline properties of thereon deposited (BEDT-TTF)2I3. Work in the second area represents an important step in the direction of developing organic superconductor / insulator / high-T_c superconductor structures.

4. Acknowledgments

JTM and CAM both thank the AFOSR and ONR for support of this work. CAM wishes to thank the Science and Technology Center for Superconductivity and JTM wishes to thank the NSF and Welch foundation for financial support.

References

(1) McDevitt, J. T.; Haupt, S. G.; Clevenger, M. B. In *Handbook of Conductive Polymers*; 2 ed.; T. A. Skotheim, R. L. Elsenbaumer and J. R. Reynolds, Eds.; Marcel Dekker: New York, ; *accepted.*
(2) Haupt, S. G.; Riley, D. R.; Grassi, J. H.; Lo, R.-K.; Zhao, J.; Zhou, J.-P.; McDevitt, J. T. *JACS* 1994, *116*, 9979-9986.
(3) McDevitt, J. T.; Mirkin, C. A.; Lo, R.-K.; Chen, K.; Zhou, J.-P.; Xu, F.; Haupt, S. G.; Zhao, J.; Jurbergs, D. C. *Chem. Mater.* 1996, *8*, 811-813.
(4) Lo, R.-K.; Ritchie, J. E.; Zhou, J.-P.; Zhao, J.; McDevitt, J. T.; Xu, F.; Mirkin, C. A. *JACS submitted.*
(5) Chen, K.; Mirkin, C. A.; Lo, R.-K.; Zhao, J.; McDevitt, J. T. *JACS* 1995, *117*, 1121-1122.
(6) Chen, K.; Xu, F.; Mirkin, C. A.; Lo, R.-K.; Nanjundaswamy, K. S.; Zhou, J.-P.; McDevitt, J. T. *Langmuir* 1996, *12*,
(7) Willicut, R. J.; McCarley, R. L. *Langmuir* 1995, *11*, 296-301.
(8) Haupt, S. G.; McDevitt, J. T. *Syn. Met.* 1995, *71*, 1539-1542.
(9) Kawabata, K.; Tanaka, K.; Mizutani, M. *Solid State Comm.* 1990, *74*, 83-86.

Paper 6

Observation of Surface-Induced Broken Time-Reversal Symmetry in $YBa_2Cu_3O_7$ Tunnel Junctions

M. Covington,* M. Aprili, E. Paraoanu, and L. H. Greene
Department of Physics, University of Illinois at Urbana-Champaign, Urbana, Illinois 61801

F. Xu, J. Zhu, and C. A. Mirkin
Department of Chemistry, Northwestern University, Evanston, Illinois 60208
(Received 6 March 1997)

Data from *ab*-oriented $YBa_2Cu_3O_7$/I/Cu tunnel junctions are presented. Self-assembled monolayers form the insulating tunnel barrier, I. The $YBa_2Cu_3O_7$ features in the tunneling conductance match those of low-leakage *ab*-oriented $YBa_2Cu_3O_7$/Pb junctions. Results show that the zero-bias conductance peak is an Andreev bound state (ABS) of a *d*-wave order parameter. In *zero* magnetic field, the ABS splits below ~7 K, consistent with the presence of a subdominant order parameter at the surface. An applied magnetic field induces further splitting that grows nonlinearly with increasing field. [S0031-9007(97)03529-1]

PACS numbers: 74.50.+r, 74.72.Bk

Tunneling spectroscopy provides unsurpassed sensitivity and resolution in the measurement of the superconducting quasiparticle density of states, yielding information on the superconducting mechanism and gap [1]. However, the $YBa_2Cu_3O_7$ (YBCO) features reproducibly observed in the conductance of $YBa_2Cu_3O_7$/Pb tunnel junctions are quite puzzling because they are qualitatively different than those expected for a conventional superconductor [2–6]. One particularly intriguing feature is the zero bias conductance peak (ZBCP) observed when tunneling into *ab*-oriented thin films [2–5]. This feature was originally analyzed in terms of spin-flip scattering of the tunneling electrons from magnetic impurities speculated to exist in the insulating barrier [3]. The temperature and voltage dependence of the ZBCP and its splitting upon application of a magnetic field showed some qualitative agreement with this model [7,8]. However, quantitative analysis showed major discrepancies. According to the spin-flip scattering model, the splitting of the ZBCP is linear with field and proportional to the Landé *g* factor of the scattering centers. In *ab*-plane YBCO tunneling, the ZBCP splitting is nonlinear with field, and its magnitude implies an anomalously large *g* factor [3]. A further observation that challenges the spin-flip scattering analysis for YBCO is the absence of the ZBCP in the tunneling conductance of *c*-axis-oriented YBCO/Pb junctions.

Zero-bias quasiparticle bound states in the tunneling density of states of *p*-wave superconductors have been proposed [9]. For the same physical reason, Hu [10] showed that a quasiparticle bound state forms at the Fermi energy (defined to be zero) when the node of a *d*-wave order parameter [11] is normal to a specularly reflecting surface, regardless of any proximity effects. Quasiparticles reflecting from the surface experience a change in the sign of the order parameter along their trajectory and subsequently undergo Andreev reflection. Constructive interference between incident and Andreev reflected quasiparticles leads to bound states confined to the surface. These bound states can carry current and will produce a ZBCP in a tunneling spectrum [12–14]. Further calculations have considered $d_{x^2-y^2}$ symmetry gaps at surface orientations ranging from (100) to (110). These have shown that the Andreev bound state is a robust feature existing for any specular surface misoriented from (100) (the lobe direction of the $d_{x^2-y^2}$ gap), albeit with variable spectral weight [12,13,15]. In a broken time reversal symmetry (BTRS) state, the Andreev bound state shifts to finite energy, resulting in a split ZBCP [14,16].

It is generally agreed that the bulk state of YBCO does not exhibit BTRS [17]. However, a state with two order parameters with a $\pi/2$ relative phase difference has been proposed to exist at the surface of YBCO, giving rise to BTRS [18]. The phase diagram of this BTRS state has recently been calculated by Fogelström *et al.* [14] who discuss the origin of a surface-induced BTRS state and make several predictions in quantitative agreement with our measurements. The essence of their theory follows: Andreev scattering near the surface of a $d_{x^2-y^2}$ superconductor causes strong pair breaking. The quasiparticles may then be paired by a subdominant pairing interaction that is less sensitive to surface pair breaking than the dominant *d* wave. Calculations minimizing the free energy show that the *d*-wave and subdominant order parameters can coexist with a $\pi/2$ relative phase difference at low temperature. This phase difference between the two order parameters leads to a spontaneous supercurrent, and a surface phase transition to a BTRS state is achieved. The bound states are shifted to finite energy in *zero* applied magnetic field. Application of an external magnetic field to the spontaneous BTRS state will further shift the bound state energy *nonlinearly* with increasing field. The predicted splitting of the ZBCP in *zero* magnetic field and its evolution with increasing field distinguishes the BTRS state. Furthermore, this zero field splitting is a unique

0031-9007/97/79(2)/277(4)$10.00

feature of the Andreev bound state that is incompatible with spin-flip scattering.

In this Letter, we present the results of reproducible measurements of YBCO/insulator/Cu planar tunnel junctions in which the ZBCP is observed to split in *zero* magnetic field at low temperature. The measured temperature dependence of the ZBCP gives good quantitative agreement with the calculated phase diagram for surface-induced BTRS phases of a $d_{x^2-y^2}$ superconductor [14]. The observed nonlinear evolution of the ZBCP splitting with increasing magnetic field is also in agreement with these calculations.

The tunnel junctions measured in this experiment are fabricated on YBCO thin films grown by off-axis magnetron sputter deposition that typically exhibit zero resistance at $T_c = 89$ K. Four different film orientations are grown, with details of the deposition conditions published elsewhere [4,19]. After a film is grown, it is soaked in a 1 mM dry acetonitrile solution of 1,12 diaminododecane for $2\frac{1}{2}$ days. This method results in the formation of a densely packed monolayer of 1,12 diaminododecane on the YBCO surface. Although these particular films have not been extensively characterized, this general type of organic monolayer/YBCO structure has been extensively studied and characterized [20,21]. Notably, this is the first use of such structures for preparing tunnel junctions on a cuprate superconductor. The Cu counter electrodes are subsequently evaporated through a stainless steel shadow mask. The resulting tunnel junctions typically have an area of ~ 0.2 mm^2 and a resistance that varies between 4 and 100 Ω. Note that although tunnel junctions are formed, the state of the organic monolayer in the fabricated junction is not yet known.

Conventional I-V and dI/dV-V tunneling measurements are performed in a standard four-lead arrangement as a function of temperature and magnetic field. No attempts are made to shield the ~ 1 G field of the Earth, but this field is insignificant compared to the ~ 0.1 T field required to produce a measurable ZBCP splitting. The junctions are nominally aligned so that the magnetic field is parallel to the film's surface. However, this alignment is imprecise, and it is expected that demagnetization effects produce a diamagnetic signal perpendicular to the junction.

For YBCO/Pb junctions, the observation of the well-known Pb superconducting density of states is used to verify that elastic tunneling is the dominant transport mechanism through the junction. Since Cu has a featureless density of states, more indirect, though no less rigorous, means are required to characterize transport through the YBCO/Cu junctions. These are the observation of YBCO tunneling characteristics and the measurement of the junction resistance versus temperature. First, the YBCO/Cu junctions exhibit all the usual features attributable to the YBCO electrode that are observed in low-leakage ab-oriented-YBCO/Pb tunnel junctions [3,4]. These YBCO features are so well characterized that they are a strong indication that tunneling is the transport current and that it is directed predominantly along the copper oxide planes. Second, the junction resistance is almost independent of temperature. As a typical example, the resistance of a junction biased at 80 mV increases by only 4% from 77 to 4.2 K. This is consistent with the behavior of low-leakage YBCO/Pb junctions and in agreement with the expected behavior of a tunnel junction with a high barrier. Taken together, these reproducible observations provide strong support that elastic tunneling is the dominant transport mechanism through the junctions.

Typical conductance data from a YBCO/Cu junction are shown in Fig. 1. No significant anisotropy is observed between (100)-, (110)-, and (103)-oriented YBCO films, just like YBCO/Pb junctions. In addition, ab-plane characteristics are observed in junctions fabricated on chemically modified (001)-oriented films. We believe this indicates deeper penetration of the counter electrode material into chemically modified YBCO films compared to junctions fabricated by Pb deposition on unmodified films. This would allow tunneling current to flow in the direction of the copper oxide planes in junctions fabricated on nominally c-axis films.

The YBCO/Cu junctions exhibit a gaplike feature (GLF) at the same energy as that measured in ab-oriented YBCO/Pb junctions, ~ 16 meV $= 2.1 k_B T_c$. The GLF energy has also been shown to scale with T_c in ab-oriented Pr-doped YBCO thin films from $T_c = 90$ to 20 K, proving that the superconducting state is being probed when tunneling in the ab-plane direction [5]. Without such proof, the relation of the ZBCP to the Andreev bound state is suspect.

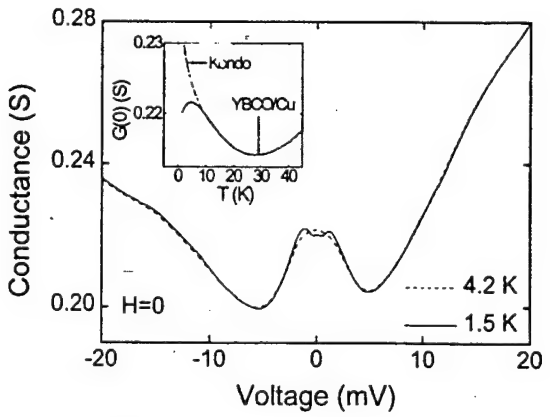

FIG. 1. Temperature-dependent conductance data from a YBCO/Cu tunnel junction. The conductance exhibits the same GLF and ZBCP observed in low-leakage ab-oriented-YBCO/Pb tunnel junctions. The ZBCP is observed to split in zero magnetic field at low temperature. Voltage is defined to be the voltage of Cu with respect to YBCO. Inset: Zero bias conductance, $G(0)$, versus temperature for the same junction, also in zero field. The downturn in $G(0)$ at low temperature corroborates the observation of zero field splitting and is in striking contrast to the $G(0) \sim \ln(T)$ behavior expected from Kondo-type spin-flip scattering, which is indicated by the dotted line.

The YBCO GLF is significantly different from the gaps observed in conventional low-T_c superconductors. It appears that there is a large amount of pair breaking in YBCO near the tunnel junction, resulting in a large number of states within the GLF, as expected for a d-wave order parameter. It is further significant to note that the depth of the GLF in YBCO/Cu junctions is typically twice as small as that measured in YBCO/Pb junctions. This smaller gap depth is also reproducibly observed in ab-oriented Pr-doped YBCO/Pb junctions [5], suggesting that it may be an indication of more disorder and quasiparticle scattering near the interface of YBCO/Cu junctions compared to YBCO/Pb junctions [22].

The most significant experimental observation is the temperature dependence of the ZBCP: It is reproducibly observed to split in zero magnetic field at low temperature, as presented in Fig. 1. To our knowledge, Geerk *et al.* [2] provide the only other possible evidence for a zero field ZBCP splitting in ab-oriented YBCO tunneling. Corroborating evidence comes from the zero-bias conductance, $G(0)$, versus temperature, shown in the inset to Fig. 1. Below about 30 K, the ZBCP begins to appear in the conductance with a concomitant increase in $G(0)$. The $G(0)$ increases with decreasing temperature until the onset of splitting in the density of states, below which it decreases.

Numerical simulations of thermal broadening on the low temperature data show that the conductance cannot be explained by thermal population effects alone, implying that the density of states is temperature dependent. There is a distinct splitting in the density of states below a particular temperature. The peak-to-peak separation at low temperature and the onset of the zero field splitting in the density of states are junction dependent. The peak-to-peak separation at 1.5 K is observed to range from 1.75 to 2.31 mV, and the onset temperature, T_s, of the zero field splitting varies from ~6 to ~8 K, respectively. The T_s is identified as the temperature where $G(0)$ deviates from either $\ln(T)$ or T^{-1} behavior, which is the expected functional temperature dependence for ZBCP's originating from spin-flip scattering or an Andreev bound state, respectively. The T_s is roughly the same regardless of the choice of the functional temperature dependence. Note that, due to thermal broadening effects, two peaks in the conductance are only resolved well below T_s, but the onset of splitting in the density of states manifests itself in the downward deviation of $G(0)$ and the broadening beyond $3.5k_BT$ of the region where G deviates from $\sim\ln(V)$ behavior.

As shown in Fig. 2(a), an externally applied magnetic field induces the ZBCP to split beyond its zero field value. The peak position, in energy, varies nonlinearly with increasing magnetic field, as shown in Fig. 2(b). For contrast, we also plot published experimental data representative of junctions with magnetic impurities in the insulating barrier [8,22–24]. The theoretical calculation (see below) of the magnetic field-induced ZBCP splitting is also shown in Fig. 2(b) for the case of an A_{1g}-symmetry (s wave) subdominant order parameter [14]. The theoretical

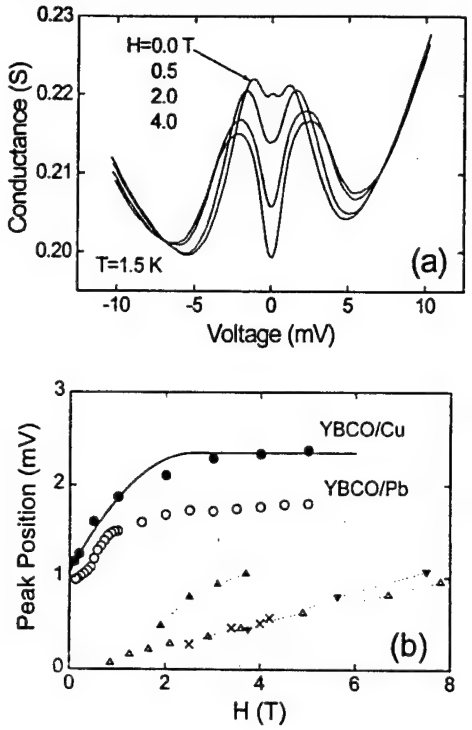

FIG. 2. (a) Magnetic field dependence of the ZBCP from a YBCO/Cu tunnel junction. A magnetic field induces further splitting of the ZBCP. (b) A compendium of data on the magnetic field-induced splitting of ZBCP's. Data from YBCO/Cu and YBCO/Pb [3] junctions are indicated by closed and open circles, respectively. The theoretical curve for the subdominant order parameter being A_{1g} (s wave) is shown as a full line [14]. As a comparison, data from other junctions with magnetic scattering centers are included. These are represented by (△) for $Ta/Ta_2O_5/Al$ [8], (▲) for $Sn/Sn_xO_y/Sn$ [23], (×) for Al/Ti-doped Al_2O_3/Al [24], and (▼) for a Au/Si:P Schottky barrier tunnel junction [25].

peak splitting is caused by currents induced by the magnetic field and the $\pi/2$ phase difference between the two order parameters. The saturation of the splitting around ~2 T is due to the screening current saturating at the bulk critical current.

It is important to emphasize just how strikingly different the behavior of the YBCO ZBCP is compared to ZBCP's originating from spin-flip scattering. First, a ZBCP arising from magnetic impurity scattering will split *only* in a finite magnetic field. Figure 2(b) implies that at least 4 T is required to split paramagnetic ZBCP's by the 1.16 mV zero field value observed in the YBCO/Cu junction. Second, the magnitude of the splitting from magnetic impurities is 5 to 10 times smaller at low fields. Third, the splitting for spin-flip scattering is roughly linear and extrapolates to zero at zero field. Fourth, the zero-bias conductance increases logarithmically as the temperature approaches absolute zero, in sharp contrast to the downturn we observe. Finally, we reproducibly observe a large magnetic hysteresis in the YBCO peak position that cannot be explained by spin-flip scattering [22].

A quantitative comparison of our measured results with the calculated phase diagram of Fogelström *et al.* [14] is now presented. Maximal pair breaking and a subdominant gap with s-wave symmetry are assumed. Using our data from Fig. 1, the onset of zero field splitting in the density of states occurs at 8 ± 1 K, which corresponds to the surface phase transition temperature of the subdominant order parameter, T_s. First, we note that the measured value of T_s corresponds to the relative strength of the subdominant to dominant pairing interactions of $T_{c2}/T_{c1} \sim 0.15$, obtained for the (110) orientation with surface roughness included. This coupling strength is below the threshold value for the formation of a spontaneously broken time-reversal symmetry state in the bulk. Second, our measured value of T_s gives a calculated shift in the bound-state energy of $\delta = 1.05$ meV. We directly measure a shift of $\delta = 1.16$ meV. Any additional pair breaking due to disorder and oxygen loss near the surface is only expected to modify the predicted value of δ and T_s, but the overall agreement with theory is good. The field dependence of the tunnel splitting is also in good agreement with the theoretical predictions. Note that the splitting saturates at fields higher than H_c, the pair breaking critical field. The theoretical curve shown in Fig. 2(b) corresponds to a critical field of $H_c = 2.5$ T [14].

The presence of a GLF and ZBCP of equal strength in the tunneling conductance of (100)- and (110)-oriented films implies comparable pair breaking for both orientations. This leaves s wave as the most plausible subdominant gap symmetry, as it is much less sensitive to surface-induced pair breaking than d_{xy} or A_{2g} (g wave). The comparison of theory and experiment in Fig. 2(b) also supports this conjecture. It is also worth noting that the value of $T_{c2} \approx 12$ K is a reasonable value for an electron-phonon mechanism as the subdominant interaction. The lack of anisotropy between (100)- and (110)-oriented films, although seemingly in contradiction with an anisotropic $d_{x^2-y^2}$ gap, can be explained by surface roughness, e.g., nm-scale faceting at the interface [14]. In this model, these facets penetrate into the copper oxide planes, locally forming multiple oriented reflecting surfaces. The global film orientation then becomes a less important variable than surface faceting and scattering.

In conclusion, planar tunneling spectroscopy of the ZBCP in ab-oriented YBCO thin films reveals spontaneous surface-induced broken time-reversal symmetry. Temperature, magnetic field, and crystallographic dependencies, respectively, show that the ZBCP splits at low temperature in zero applied magnetic field, the energy of the bound state varies nonlinearly with applied magnetic field, and the ZBCP is only observed in ab-plane tunneling. These behaviors are qualitatively and quantitatively different from those expected for ZBCP's originating from magnetic spin-flip scattering of tunneling electrons and in striking agreement with the introduction of a subdominant order parameter at the surface. Finally, the ZBCP provides further direct proof that the YBCO superconducting order parameter changes sign on the Fermi surface.

We are grateful to J. A. Sauls for many stimulating and inspiring discussions. We also acknowledge useful conversations with M. Fogelström and A. J. Leggett. This research is supported by the NSF through the STCS (NSF-DMR 91-20000). Support is also received from NSF (DMR 94-21957) and ONR (N00014-95-1-0831) for E.P. and L.H.G. and ONR (UR12126YIP) and AFOSR (F49620-96-1-0155) for F.X., J.Z., and C.A.M.

*Present address: NIST, Boulder, CO.

[1] W. L. McMillan and J. M. Rowell, in *Superconductivity*, edited by R. D. Parks (Marshall-Dekker, New York, 1969), p. 561.
[2] J. Geerk, X. X. Xi, and G. Linker, Z. Phys. B **73**, 329 (1988).
[3] J. Lesueur, L. H. Greene, W. L. Feldmann, and A. Inam, Physica (Amsterdam) **191C**, 325 (1992).
[4] M. Covington, R. Scheuerer, K. Bloom, and L. H. Greene, Appl. Phys. Lett. **68**, 1717 (1996).
[5] M. Covington, E. Paraoanu, and L. H. Greene (to be published).
[6] A. J. Sun *et al.*, Phys. Rev. B **54**, 6734 (1996).
[7] J. A. Appelbaum, Phys. Rev. **154**, 633 (1967).
[8] J. A. Appelbaum and L. Y. L. Shen, Phys. Rev. B **5**, 544 (1972).
[9] L. J. Buchholtz and G. Zwicknagl, Phys. Rev. B **23**, 5788 (1981).
[10] C.-R. Hu, Phys. Rev. Lett. **72**, 1526 (1994).
[11] Experiments supporting a $d_{x^2-y^2}$ symmetry order parameter in $YBa_2Cu_3O_7$ are reviewed in D. J. VanHarlingen, Rev. Mod. Phys. **67**, 515 (1995).
[12] Y. Tanaka and S. Kashiwaya, Phys. Rev. Lett. **74**, 3451 (1995).
[13] L. J. Buchholtz, M. Palumbo, D. Rainer, and J. A. Sauls, J. Low Temp. Phys. **101**, 1099 (1995).
[14] M. Fogelström, D. Rainer, and J. A. Sauls, Phys. Rev. Lett. **79**, XXX (1997).
[15] J. Yang and C.-R. Hu, Phys. Rev. B **50**, 16 766 (1994).
[16] M. Matsumoto and H. Shiba, J. Phys. Soc. Jpn. **65**, 2194 (1996).
[17] T. W. Lawerence, A. Szöker, and R. B. Laughlin, Phys. Rev. Lett. **69**, 1439 (1992).
[18] R. B. Laughlin, Physica (Amsterdam) **234C**, 280 (1994); M. Sigrist, D. B. Bailey, and R. B. Laughlin, Phys. Rev. Lett. **74**, 3249 (1995).
[19] L. H. Greene *et al.*, Appl. Phys. Lett. **59**, 1629 (1991).
[20] K. Chen *et al.*, J. Am. Chem. Soc. **117**, 6374 (1995).
[21] C. A. Mirkin, F. Xu, and J. Zhu, Adv. Mater. **9**, 167 (1997).
[22] M. Aprili, M. Covington, E. Paraoanu, and L. H. Greene (to be published).
[23] L. Y. L. Shen and J. M. Rowell, Phys. Rev. **165**, 566 (1968).
[24] D. J. Lythall and A. F. G. Wyatt, Phys. Rev. Lett. **20**, 1361 (1968).
[25] E. L. Wolf and D. L. Losee, Phys. Rev. B **2**, 3660 (1970).

Surface Cleaning and Adsorbate Layer Formation: Dual Role of Alkylamines in the Formation of Self-Assembled Monolayers on Cuprate Superconductors

Jason E. Ritchie,‡ William R. Murray, Katherine Kershan, Veronica Diaz, Long Tran, and John T. McDevitt*

Department of Chemistry and Biochemistry
The University of Texas at Austin
Austin, Texas 78712

Received April 13, 1999

The development of monolayer adsorption chemistry for superconductor surfaces is particularly important for a number of practical and fundamental reasons. As high-T_C superconductors begin to approach the marketplace in areas of communications, power industries, medical applications, and scientific instrumentation, the development of new "soft chemistry" approaches for the surface modification of these technologically relevant electronic materials becomes increasingly important. Monolayer adsorption chemistry has been developed extensively for electronic materials such as metals, semiconductors, and insulators.[1] These methodologies have been expanded recently to include a variety of high-temperature superconductors (HTSCs).[2−8] Furthermore, the McDevitt group has shown in a recent publication that certain amine compounds foster the formation of monolayers that exhibit a high degree of conformational order on (001)-oriented samples of $YBa_2Cu_3O_7$.[2] Arguably, these samples are, to date, the most complex substrate shown to support such organized self-assembled monolayer structures.

A recent study by Mirkin and co-workers makes an interesting hypothesis related to the surface interaction of amine monolayers with $YBa_2Cu_3O_7$.[9] According to this report, the alkylamine reagents become oxidized to alkylimines upon their exposure to HTSCs (Figure 1A,B). In addition, it is proposed that the surface region of the superconductor becomes reduced commensurate with the oxidation of alkylamines (Figure 1C). According to this model, the resulting oxygen-deficient exterior region supports the formation of an amine monolayer (Figure 1D).

Here, we describe a series of new X-ray photoelectron spectroscopy (XPS), four-point conductivity, critical current, atomic absorption spectroscopy (AAS), grazing angle infrared spectroscopy, and GC−MS experiments, which lead us to suggest that an entirely different mechanism is involved in the formation of HTSC-localized monolayers. According to our new model, the amine reagents serve two chemically distinct roles. In the initial phase, the degraded superconductor exterior is etched away with the help of the amine compounds, (Figure 1W). The etching process proceeds to the point where fresh $YBa_2Cu_3O_7$ is exposed, and only at this point do the amines adsorb and remain at the $YBa_2Cu_3O_7$ surface (Figure 1X,Y). As the adsorption process continues, there is an accumulation of an organized monolayer at the surface, which prevents further etching of the $YBa_2Cu_3O_7$ material (Figure 1Z).[10] The remainder of this paper describes the evidence we have acquired to support our alternative HTSC self-assembly mechanism.

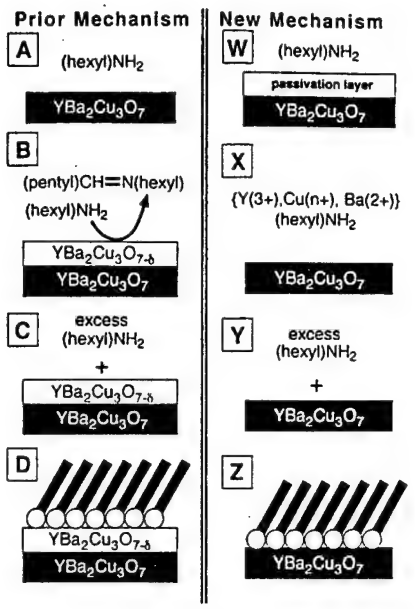

Figure 1. Schematic illustration showing the sequence of steps that are proposed to be involved in the formation of self-assembled monolayers atop the surface of the high-T_c superconductor, $YBa_2Cu_3O_{7-\delta}$. Steps A−D detail the adsorption scheme as proposed by in a recent paper Mirkin et al.[9] Steps W−Z summarize the new mechanism described herein.

Numerous studies of $YBa_2Cu_3O_7$ and related compounds have shown that even short atmospheric exposures cause chemical damage to the surface of the HTSC samples.[11−16] Since the anchoring of adsorbate layers occurs at the surface, the most accurate description of the mechanism of superconductor monolayer adsorption must include a description of the influence of surface-localized degradation layers. From our XPS studies, we find that even short exposures of HTSC samples to the atmosphere (i.e., exposure times consistent with the transfer of samples from our thin-film deposition chamber or furnace to the XPS chamber) lead to the formation of a contamination layer. This layer (20−50 Å in thickness) contains the reduced "green phase" (i.e., Y_2BaCuO_5), $BaCO_3$, and CuO.

To explore the mechanistic details of alkylamine adsorption on $YBa_2Cu_3O_7$ surfaces, we examined the XPS spectra of $YBa_2Cu_3O_7$ thin films taken directly from our deposition chamber to the XPS instrument (Figure 2, dashed curves). Even for samples that received atmospheric exposure for less than 2 min, the

‡ Current address: Kenan Laboratories of Chemistry, The University of North Carolina, Chapel Hill, NC 27599.

(1) Ulman, A. *An Introduction to Ultrathin Organic Films, From Langmuir−Blodgett to Self-Assembly*; Academic Press: Boston, 1991.
(2) Ritchie, J. E.; Wells, C. A.; Zhou, J.-P.; Zhao, J.; McDevitt, J. T.; Ankrum, C. R.; Jean, L.; Kanis, D. R. *J. Am. Chem. Soc.* **1998**, *120*, 2733−2745.
(3) McDevitt, J. T.; Haupt, S. G.; Jones, C. E. *Electrochemistry of High-T, Superconductors*; Marcel Dekker: New York, 1996; Vol. 19, pp 355−481.
(4) Clevenger, M. B.; Zhao, J.; McDevitt, J. T. *Chem. Mater.* **1996**, *8*, 2693−2696.
(5) Lo, R.-K.; Ritchie, J. E.; Zhou, J.-P.; Zhao, J.; McDevitt, J. T. *J. Am. Chem. Soc.* **1996**, *118*, 11295−11296.
(6) Chen, K.; Mirkin, C. A.; Lo, R.-K.; Zhao, J.; McDevitt, J. T. *J. Am. Chem. Soc.* **1995**, *117*, 1121−1122.
(7) Chen, S. C.; Yan, J.; Lee, J.; Chary, K. V. R.; Jones, E. B.; Zhang, Z.; Teweldemedhin, Z. S.; Greenblatt, M. *Synthesis of Superconducting Oxides*; John Wiley & Sons: New York, 1995; Vol. 30.
(8) Xu, F.; Chem, K.; Mirkin, C. A.; Ritchie, J. E.; McDevitt, J. T.; Cannon, M. O.; Kanis, D. R. *Langmuir* **1998**, *14*, 6505−6511.
(9) Zhu, J.; Mirkin, C. A.; Braun, R. M.; Winograd, N. *J. Am. Chem. Soc.* **1998**, *120*, 5126−5127.
(10) See Supporting Information
(11) Riley, D. R.; McDevitt, J. T. *J. Electroanal. Chem.* **1990**, *295*, 373−384.
(12) Riley, D. R.; Jurbergs, D. J.; Zhou, J.-P.; Zhao, J.; Markert, J. T.; McDevitt, J. T. *Solid State Commun.* **1993**, *88*, 431−434.
(13) Zhou, J.-P.; McDevitt, J. T. *Chem. Mater.* **1992**, *4*, 953−959.
(14) Zhou, J.-P.; Riley, D. R.; McDevitt, J. T. *Chem. Mater.* **1993**, *5*, 361−365.
(15) Zhou, J.-P.; Lo, R.-K.; Savoy, S. M.; Arendt, M.; Armstrong, J.; Yang, D.-Y.; Talvacchio, J.; McDevitt, J. T. *Physica C* **1997**, *273*, 223−232.
(16) Zhou, J.-P.; Savoy, S. M.; Zhao, J.; Lo, R.-K.; Borich, D.; McDevitt, J. T. *J. Am. Chem. Soc.* **1994**, *116*, 9389−9390.

10.1021/ja991165e CCC: $18.00
Published on Web 07/30/1999

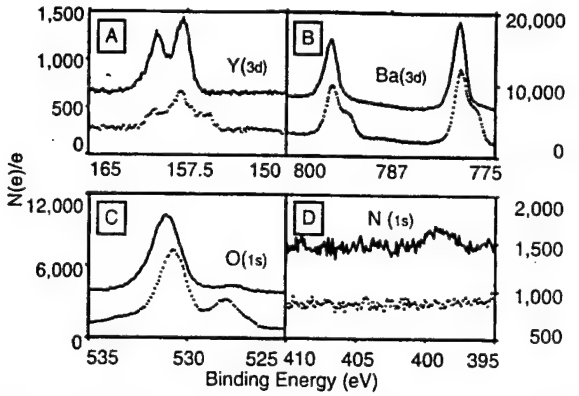

Figure 2. Data for the XPS spectra of $YBa_2Cu_3O_{7-\delta}$ thin film (1500 Å thick, *c*-axis oriented on MgO) before and after exposure for ~12 h to a 2 mM dodecylamine solutions. The following spectral regions are shown: (A) the Y(3d); (B) Ba(3d $^5/_2$); (C) O(1s); and (D) N(1s). In each panel, the lower/dashed curve shows data prior to any solution exposure. Similarly, the upper/solid curves show the spectral data obtained for the same set of films after their exposure to the amine solution.

acquired XPS signature is consistent with a degraded surface region. This degradation layer is characterized by a broad multiplet absorption in the Y(3d) region, the $BaCO_3$ signature in the Ba-(3d5/2) region (i.e., the lower energy humps on the main peaks), and a CO_3^{2-} signature in the O(1s) region (i.e., ~527 eV). These spectral signatures supports the presence of a degradation layer, in good agreement with the prior literature for similarly treated samples.[17-19] Quite interestingly, treatment of the "dirty" $YBa_2Cu_3O_7$ samples with a 2 mM solution of octadecylamine, butylamine, or hexylamine for 12 h leads to a dramatic improvement in the XPS signature for the cuprate powder, film, and pellet samples (Figure 2, solid curves). The presence of a clean exterior is noted by the doublet-like feature in the Y(3d) region, matching closely the pristine case that was prepared and evaluated in situ.[17-19] In addition, the amine exposure serves, for the most part, to eliminate the $BaCO_3$ surface layers, as evidenced by the clean Ba(3d5/2), Ba(3d3/2), and O(1s) transitions. Finally, the XPS signature of the adsorbed amine reagent is found in the N(1s) region of the spectra that was absent in the untreated samples. These results suggest that even carefully prepared $YBa_2Cu_3O_7$ samples are initially coated with corrosion products, and that after exposure to the amine reagent the majority of the surface corrosion layer is removed.

To further support the occurrence of an initial etching step, we completed a series of atomic absorption spectroscopy (AAS) experiments to search for copper dissolution products. These experiments indicate that a significant amount of copper is dissolved into the solution during the initial few minutes of exposure.[10] The initially rapid copper dissolution is followed by a leveling off, where little additional etching is observed. The latter behavior appears to be consistent with the occurrence of an adsorbate-induced surface passivation that limits subsequent etching. From measurements of the dissolved Cu ion concentration, it is estimated that 20−50 Å of $YBa_2Cu_3O_7$ is removed during this etching process. Similarly, from changes in resistivity of ~1000-Å-thick $YBa_2Cu_3O_7$ films, we obtain an independent estimate for the upper limit of the depth of etching of 50−100 Å for the $YBa_2Cu_3O_7$ thin-film specimen.[10] The resistivity measurements yield a slightly larger effective etching thickness due to a large sensitivity of the measurement to etching along the grain boundaries.

Although the above-described information strongly suggests the presence of a pre-etching step, these data do not exclude the possibility suggested by Mirkin and co-workers that the amine anchoring occurs with chemistry that results in the reduction of the exterior surface of the HTSC. While it is difficult to eliminate the possibility of ultrasmall amounts (<10 Å) of reduction to the HTSC surface, we note that previous publications have shown that ferrocenealkylamine adsorbed on $YBa_2Cu_3O_{6.94}$ displays facile electron transfer, consistent with a conductive metallic electrode, and behavior reminiscent of an ideal surface-confined redox species is obtained.[6,8,10,20] In addition, we have shown in a previous publication that a very dramatic oxygen content dependence is observed for the electrochemical data acquired at $YBa_2Cu_3O_{7-\delta}$ electrodes.[21] Although the above-mentioned studies do not exclude the possibility of an ultrasmall amount of surface reduction, they do question the presence of a systematically reduced exterior region with significant thickness.

While we do not challenge the formation of significant amounts of dialkylimine in the prior study, we do challenge its formation as being intrinsic to the monolayer formation process on superconductor surfaces. We completed a series of GC−MS experiments[10] analogous to those reported by Mirkin[9] for freshly prepared $YBa_2Cu_3O_7$ powders. In hexanes solutions that are kept under an inert argon atmosphere, no increase in the concentration of the dialkylimine is noted.[22] For our particle size distribution, we calculate that conversion of one monolayer of hexylamine to dialkylimine would yield a change in the concentration of the dialkylimine contaminant that could be detected by GC−MS. We note that samples having thick degradation layers require longer exposure time before the etching process becomes complete. Furthermore, our grazing angle reflectance infrared measurements and XPS studies have shown that it is possible to anchor amine adsorbate layers atop chemically damaged HTSC structures. The focus of our studies here has been placed on the evaluation of freshly prepared $YBa_2Cu_3O_7$ samples, where degradation layer thickness is minimized. With these types of samples, no detectable changes in the amounts of oxidized amine compounds are noted for the amine/$YBa_2Cu_3O_7$ exposure experiments.

In summary, a plausible new mechanism has been reported for the adsorption of alkylamine reagents on cuprate superconductor samples, in which the amine reagents serve two distinct roles. First, a variety of measurements provide convincing evidence that the alkylamines serve to remove the initially present degraded surface layer. Second, the amines are found to adsorb in a persistent manner on the high-T_c surface. Once the amines are anchored to the cuprate surface, the etching process ceases, and the adsorbate layer is found to be anchored atop a highly conductive exterior region. Unlike the vast majority of the prior processing methods for the cuprate phases, the amine monolayer procedure described herein serves to create and preserve pristine interfacial chemistry. The self-termination and surface passivation methods described in this paper may find utility in the future for the processing/packaging of high-T_c devices and conductors.

Acknowledgment. J.T.M. acknowledges the Air Force Office of Scientific Research, the National Science Foundation, the Texas Center for Superconductivity, and the Office of Naval Research for support of this work. J.E.R. thanks the Electrochemistry Society for a fellowship.

Supporting Information Available: Three figures, showing the time dependence of the copper dissolution; two resistivity vs temperature curves for a single $YBa_2Cu_3O_{7-\delta}$ thin film; and cyclic voltammetry for $YBa_2Cu_3O_{7-\delta}$ electrodes (PDF). This material is available free of charge via the Internet at http://pubs.acs.org.

JA991165E

(17) Behner, H.; Rührnschopf, K.; Rauch, W.; Wedler, G. *Appl. Surf. Sci.* **1993**, *68*, 179−188.
(18) Behner, H.; Rührnschopf, K.; Wedler, G.; Rauch, W. *Physica C* **1993**, *208*, 419−424.
(19) Behner, H.; Wecker, J.; Matthee, T.; Samwer, K. *Surf. Interface Anal.* **1992**, *18*, 685−690.
(20) Chen, K.; Xu, F.; Mirkin, C. A.; Lo, R.-K.; Nanjundaswamy, K. S.; Zhou, J.-P.; McDevitt, J. T. *Langmuir* **1996**, *12*, 2622−2624.
(21) Riley, D. R.; McDevitt, J. T. *J. Electrochem. Soc.* **1992**, *139*, 2340−2346.
(22) We noted the presence of the dialkylimine as a trace contaminant in two different lots of hexylamine obtained from Aldrich. The concentration of the dialkylimine was reduced by a factor of 10 by two successive vacuum transfers of the hexylamine.

Paper 8

Direct Oxidation of Alkylamines by $YBa_2Cu_3O_{7-\delta}$: A Key Step in the Formation of Self-Assembled Monolayers on Cuprate Superconductors

Jin Zhu and Chad A. Mirkin*

Department of Chemistry, Northwestern University
2145 Sheridan Rd., Evanston, Illinois 60201

Robert M. Braun and Nicholas Winograd*

Department of Chemistry, The Pennsylvania State University
University Park, Pennsylvania 16802

Received December 29, 1997
Revised Manuscript Received April 9, 1998

Molecular monolayer-based surface modification chemistry, often referred to in the literature as "self-assembly", has been extensively developed and proven to be a remarkably useful methodology for the construction of well-defined organic surfaces and interfaces for three of the four important classes of electronic materials: metals, semiconductors, and insulators.[1] Recently, comparable but chemically distinct methodology has been developed for the fourth important class of electronic materials, cuprate-based high-temperature superconductors (HTSCs).[2] Since then, a great deal has been learned about the utility of these new surface structures for tailoring HTSC surface and interfacial properties. Monolayers of HTSCs have been used as hydrophobic layers for corrosion passivation,[3a] prelayers for improving polymer adhesion[3a] and crystal growth,[3b] polymer nucleation layers,[4] and as the barrier layers in tunnel junction devices.[5] The latter is a very important discovery because tunnel junctions form the heart of the developing HTSC industry and are the core device structures used to interrogate many of the intrinsic properties of HTSCs.

Among the functionalities surveyed thus far,[2a] alkylamines have been found to form the most robust monolayer structures, and all of the above-mentioned applications have been based on monolayers formed from molecular reagents with this functional group. Therefore, a detailed understanding of the reaction between $YBa_2Cu_3O_{7-\delta}$ and alkylamines is especially important in order to obtain a better understanding of this important monolayer self-assembly process. Described herein are the results of experiments aimed at elucidating this coordination chemistry. On the basis of previous electrochemical experiments[2a] and Raman spectroscopy,[6] it is known that amines chemisorb onto $YBa_2Cu_3O_{7-\delta}$ to form strong surface adsorbate interactions. To date, however, little is known about this reaction, including the chemical fate of the amine and superconductor as well as the preferred adsorbate binding site. In general, the surface coordination chemistry of inorganic materials is a very difficult problem to solve; indeed, with over 15 years of effort devoted to determining the interaction between alkanethiols and Au, there is still debate over the nature of this reaction.[7] Herein, we show that an extraordinary, but very clean redox reaction takes place between alkylamines and the highly oxidized surface of $YBa_2Cu_3O_{7-\delta}$ prior to chemisorption of the monolayer. Moreover, we report secondary ion mass spectrometry (SIMS) data, which provide evidence for the final chemical state of the adsorbate and its preferred surface binding site. Taken together, these preliminary studies provide the basis for understanding this complex but useful reaction.

In a typical experiment, $YBa_2Cu_3O_{7-\delta}$ powder (Strem Chemical Co.; average size 0.2 μm) was stirred in a solution of a primary alkylamine (0.16 M $CH_3(CH_2)_5NH_2$ in CH_3CN) for 2 days under N_2 atmosphere. The powder was then filtered, and CH_3CN was removed under vacuum. GC-MS was used to characterize the organic product from the reaction. The retention time of $CH_3(CH_2)_5NH_2$ on the 5% phenylmethylsiloxane column was 3.92 min, and the mass spectrum of $CH_3(CH_2)_5NH_2$ exhibits the expected M^+ ion at *m/z* 101, Figure 1A. After the reaction, a new peak in the GC analysis of the solution emerged at 8.10 min in addition to the peak at 3.92 min for unreacted $CH_3(CH_2)_5NH_2$. This product is assigned as the dialkylimine, $CH_3(CH_2)_4CH{=}N(CH_2)_5CH_3$, based on (1) the $[M - H]^+$ ion as observed at *m/z* 182 and (2) a comparison of its mass spectrum with that for an authentic sample of the dialkylimine, which was independently synthesized in our laboratories.[8] These spectra are shown in parts B and C of Figure 1, respectively. In addition, GC analysis of $CH_3(CH_2)_4CH{=}N(CH_2)_5CH_3$ shows that it exhibits a retention time identical to that for the product generated from the reaction between $YBa_2Cu_3O_{7-\delta}$ and *n*-hexylamine.

X-ray photoelectron spectroscopy (XPS) was used to characterize the $YBa_2Cu_3O_{7-\delta}$ powder before and after the surface modification reaction (takeoff angle = 45°). Powder samples of $YBa_2Cu_3O_{7-\delta}$, unmodified and modified with *n*-hexylamine, were pressed into pellets in order to facilitate XPS studies. The XPS spectra of the powder before and after modification with *n*-hexylamine clearly show that a redox reaction is occurring between the amine and superconductor. The ratio of the O 1s peak to Ba $3d_{3/2}$ peak decreases from 1.15 to 0.78 upon surface modification. This ratio is a signature of surface reduction and loss of oxygen. Although there are no unambiguous XPS signatures which differentiate Cu(III) and Cu(II),[9] either Cu(III) or peroxide, the two cited potential oxidizing sites in the superconductor,[9] must be reduced in this process to form Cu(II) or oxide, respectively. Both of these processes would result in concomitant loss of oxygen from the superconductor. If Cu(III) is involved, the reaction stops at Cu(II) as evidenced by the signature $2p_{3/2}$ and $2p_{1/2}$ shake-up features in the XPS spectrum of the modified material (i.e., there is no evidence for formation of Cu(I) or Cu(0)).[10] Consistent with this hypothesis, cyclohexylamine reacts with Cu(II) to form a stable coordination complex, $[Cu(C_6H_{11}NH_2)_4]^{2+}$ (i.e., Cu(II) does not oxidize the alkylamine).[11]

The bulk structure of $YBa_2Cu_3O_{7-\delta}$, before and after treatment with *n*-hexylamine, was characterized by powder X-ray diffraction (XRD). There is no significant change in the phase structure of the $YBa_2Cu_3O_{7-\delta}$ as evidenced by virtually identical XRD patterns for the modified and unmodified samples, at least under the conditions used herein. Moreover, there is no change in the critical temperature (92 K), as determined by SQUID, for these materials even after they have been modified under these conditions (see Supporting Information). This indicates that in

* Address correspondence to: camirkin@chem.nwu.edu.

(1) Ulman, A. *Chem. Rev.* **1996**, *96*, 1533.

(2) Chen, K.; Mirkin, C. A.; Lo, R.-K.; Zhao, J.; McDevitt, J. T. *J. Am. Chem. Soc.* **1995**, *117*, 6374. (b) Mirkin, C. A.; Xu, F.; Zhu, J. *Adv. Mater.* **1997**, *9*, 167.

(3) McDevitt, J. T.; Mirkin, C. A.; Lo, R.-K.; Chen, K.; Zhou, J.-P.; Xu, F.; Haupt, S. G.; Zhao, J.; Jurbergs, D. C. *Chem. Mater.* **1996**, *8*, 811. (b) Clevenger, M. B.; Zhao, J.; McDevitt, J. T. *Chem. Mater.* **1996**, *8*, 2693.

(4) Lo, R.-K.; Ritchie, J. E.; Zhou, J.-P.; Zhao, J.; McDevitt, J. T.; Xu, F.; Mirkin, C. A. *J. Am. Chem. Soc.* **1996**, *118*, 11295.

(5) Covington, M.; Aprili, M.; Paraoanu, E.; Greene, L. H.; Xu, F.; Zhu, J.; Mirkin, C. A. *Phys. Rev. Lett.* **1997**, *79*, 277.

(6) Zhu, J.; Xu, F.; Schofer, S. J.; Mirkin, C. A. *J. Am. Chem. Soc.* **1997**, *119*, 235.

(7) Fenter, P.; Eberhardt, A.; Eisenberger, P. *Science* **1994**, *266*, 1216.

(8) The internal imine, $CH_3(CH_2)_4CH{=}N(CH_2)_5CH_3$, was prepared by reacting neat *n*-hexylamine with neat 1-hexanal.

(9) Bickley, R. I.; Fawcett, V.; Shields, C. *J. Mater. Sci. Lett.* **1989**, *8*, 745.

(10) Moulder, J. F.; Stickle, W. F.; Sobol, P. E.; Bomben, K. D. In *Handbook of X-ray Photoelectron Spectroscopy*; Chastain, J., Ed. Perkin-Elmer Corporation: Eden Prairie, 1992; pp 86−89.

(11) Cotton, F. A.; Wilkinson, G. *Advanced Inorganic Chemistry*; John Wiley & Sons: New York, 1988; pp 767−768.

S0002-7863(97)04348-5 CCC: $15.00
Published on Web 05/07/1998

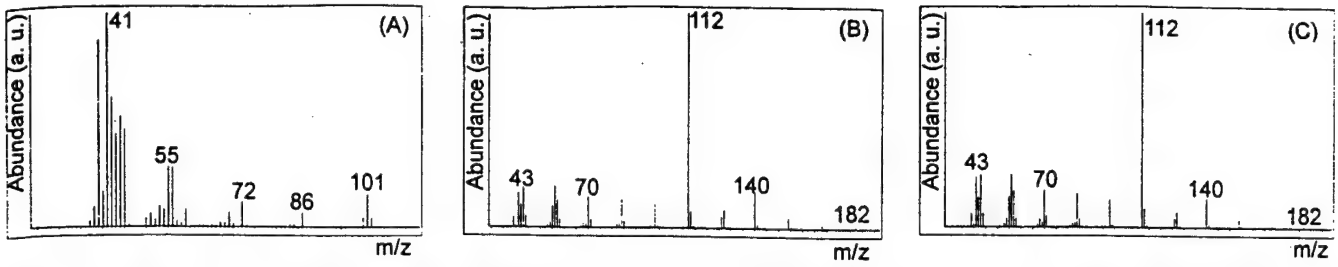

Figure 1. GC-MS of (A) the starting compound $CH_3(CH_2)_5NH_2$, (B) the only detectable organic product from the reaction between $YBa_2Cu_3O_{7-\delta}$ powder $CH_3(CH_2)_5NH_2$ in acetonitrile, and (C) an independently synthesized sample of $CH_3(CH_2)_4CH{=}N(CH_2)_5CH_3$.

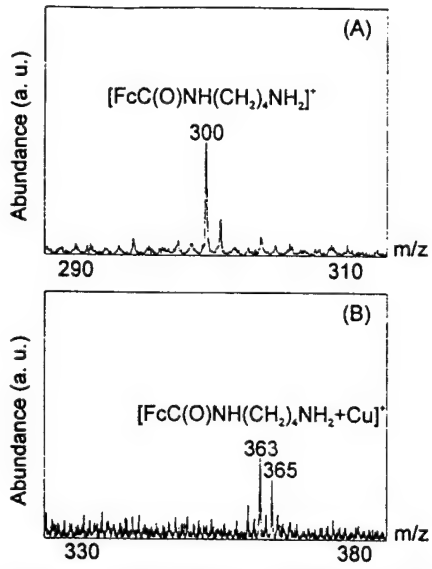

Figure 2. Two regions of the positive-ion secondary ion mass spectrum of a $YBa_2Cu_3O_{7-\delta}$ surface after modification with $FcC(O)NH(CH_2)_4NH_2$: (A) the region between *m/z* 288 and 312 showing the molecular ion (M^+) for the amine and (B) the region between *m/z* 328 and 382 showing the $[M + Cu]^+$ peak at 363 *m/z* with the expected isotopic pattern for Cu.

the monolayer "self-assembly" process the redox reaction primarily affects the chemical state of the superconductor surface, without causing significant reduction of the bulk material.

To further characterize the nature of the adsorption process, SIMS was used to study the superconductor surface after chemical modification. SIMS has been used extensively to characterize chemically modified surfaces and can provide information regarding the chemical fate of the adsorbate and, in some cases, the preferred surface binding site(s).[12] In these studies, we used an alkylamine with a Fc reporter group, $FcC(O)NH(CH_2)_4NH_2$ (Fc = Ferrocenyl), which allows us to confirm adsorption independently by electrochemical methods.[2] The positive-ion mode SIMS spectrum of a ceramic $YBa_2Cu_3O_{7-\delta}$ surface modified with $FcC(O)NH(CH_2)_4NH_2$ exhibits two very informative peaks in addition to a variety of background peaks associated with the inorganic substrate (not shown), Figure 2, parts A and B. An M^+ peak was observed at *m/z* 300 showing that the amine, and not imine oxidation product, adsorbs onto the reduced superconductor surface, Figure 2A. In addition, a $[M + Cu]^+$ peak is observed at *m/z* 363 with the expected Cu isotope distribution. No peaks were observed for $[M + Ba]^+$ and $[M + Y]^+$ fragments, which when combined with previous indirect evidence,[2b] strongly suggests that the preferred sites of amine binding for this superconducting oxide are Cu^{2+} atoms. Although it is possible for close, neighboring fragments to combine in the SIMS experiment,[13] the only atoms in this plane of the superconductor other than Cu are O atoms, and it is unlikely that the amine bonds to them.

(12) Winograd, N. *Anal. Chem.* **1993**, *65*, 622A.

Scheme 1

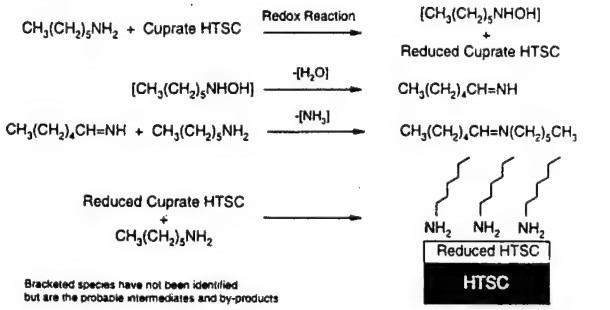

Taken together, our data support the following mechanism for the self-assembly of monolayers of alkylamines on $YBa_2Cu_3O_{7-\delta}$. The surface is initially reduced (Cu^{3+} to Cu^{2+} or peroxide to oxide) by the alkylamine, which results in formation of the dialkylimine, $CH_3(CH_2)_4CH{=}N(CH_2)_5CH_3$, and concomitant loss of oxygen from the superconductor. The oxidation of an alkylamine to alkylimine by inorganic oxidants in the presence of O_2 is a well-known process and often occurs through initial formation of a hydroxyamine, which is unstable and loses H_2O to form an imine. In the case of the $YBa_2Cu_3O_{7-\delta}$ oxidation of *n*-hexylamine, the initial product is $CH_3(CH_2)_4CH{=}NH$. Note that in some cases this product could be detected by GC-MS, but is clearly an intermediate that is consumed as it forms. This imine reacts with another equivalent of *n*-hexylamine to form the observed dialkylimine, $CH_3(CH_2)_4CH{=}N(CH_2)_5CH_3$, and presumably NH_3.[14] After initial reduction of the surface, another equivalent of alkylamine binds to the surface at Cu^{2+} sites to form a monolayer film. Although the precise thickness of the reduced surface layer is not known, it must be very thin (<20 Å) because these monolayers form adequate tunnel junction barrier layers.[5] In fact, these experiments suggest that in the fabrication of SIN (superconductor/insulator/normal metal) tunnel junctions from self-assembled monolayers of alkylamines, the junction layer is a combination of a thin reduced superconductor layer and the organic film.

Acknowledgment. C.A.M. acknowledges the AFOSR (F49620-96-1-0155) and NSF Science and Technology Center for Superconductivity for support for this work. C.A.M. also acknowledges the use of equipment purchased through the NU Materials Research Center (Award No. DMR-9120521). N.W. acknowledges the ONR and NSF for partial support of the mass spectrometry instrumentation. Feng Xu is acknowledged for helpful discussions.

Supporting Information Available: Figures showing the XPS of $YBa_2Cu_3O_{7-\delta}$ and the Cu 2p region and SQUID magnetization measurements for $YBa_2Cu_3O_{7-\delta}$ (3 pages, print/PDF). See any current masthead page for ordering information and web access instructions.

JA974348E

(13) Liu, K. S.; Vickerman, J. C.; Garrison, B. J. In *Secondary Ion Mass Spectrometry SIMS XI*; Gillen, G., Lareau, R., Bennett, J., Stevie, F., Eds.; John Wiley & Sons: New York, 1998; p 443.

(14) Millar, I. T.; Springall, H. D. *The Organic Chemistry of Nitrogen*; Oxford University Press: Glasgow, 1966; pp 112–113. (b) Brown, B. R. *The Organic Chemistry of Aliphatic Nitrogen Compounds*; Oxford University Press: Oxford, 1994; pp 130–133. (c) Miller, R. E. *J. Org. Chem.* **1960**, *25*, 2126.

Monolayer Growth and Exchange Kinetics for Alkylamines on the High-Temperature Superconductor $YBa_2Cu_3O_{7-\delta}$

Feng Xu, Jin Zhu, and Chad A. Mirkin*

Department of Chemistry, Northwestern University, 2145 Sheridan Road, Evanston, Illinois 60208-3113

Received July 12, 1999. In Final Form: November 4, 1999

Using redox-active alkylamine adsorbates, we have studied monolayer growth and adsorbate–adsorbate exchange kinetics on $YBa_2Cu_3O_{7-\delta}$. Herein we show that the formation kinetics for monolayers of $FcC(O)NH(CH_2)_4NH_2$ [$Fc = (\eta^5\text{-}C_5H_4)Fe(\eta^5\text{-}C_5H_5)$] do not follow typical Langmuir adsorption isotherm behavior. Specifically, a parabolic tailing in the isotherms has been attributed to the diffusion of adsorbates through the porous material. The displacement of surface-adsorbed $FcC(O)NH(CH_2)_4NH_2$ by another redox-active alkylamine, $Fc(CH_2)_6NH_2$, has been studied and determined to be a reversible and dynamic process. Concentration dependence studies suggest that the exchange takes place via an associative process involving surface Cu(II) sites. The lability of the surface-adsorbed alkylamine "ligands" and the proposed exchange mechanism are consistent with the solution coordination chemistry of Cu(II).

Introduction

Surface coordination chemistry and modification studies have led to the development of methods for tailoring the surface and interfacial properties of many important materials, some of which include Au,[1] Ag,[2] Pt,[3] CdS,[4] CdSe,[4] GaAs,[5] Si,[6] and TiO_2.[7] Chemically modified surfaces have provided important insight in the areas of interfacial electron transfer,[8] Raman spectroscopy,[9] tribology,[10] and, chemical force microscopy.[11] In addition, they have resulted in the development of many useful materials and technologies including sensors,[12,13] catalysts,[14] nonlinear optical materials,[15] lithographic resists,[16] nanolithography methods,[17] and optoelectronic materials.[13]

Recently, we developed a methodology for modifying cuprate high-temperature superconductors (HTSCs) with a variety of organic adsorbates.[18] Although these studies showed that alkanethiols, selenols, and amines all adsorb onto the surfaces of cuprate-based materials, the alkylamine reagent has emerged as the most efficient surface

* To whom correspondence should be addressed. E-mail: camirkin@chem.nwu.edu. Phone: (847) 491 2907. Fax: (847) 467 5123.

(1) (a) Ulman, A. *An Introduction to Ultrathin Organic Films: From Langmuir–Blodgett to Self*-assembly; Academic: Boston, 1991. (b) Bain, C. D.; Whitesides, G. M. *Angew. Chem., Int. Ed. Engl.* **1989**, *28*, 506. (c) Dubois, L. H.; Nuzzo, R. G. *Annu. Rev. Phys. Chem.* **1992**, *43*, 437. (d) Ulman, A. *Chem. Rev.* **1996**, *96*, 1533.

(2) (a) Laibinis, P. E.; Fox, M. A.; Folkers, J. P.; Whitesides, G. M. *Langmuir* **1991**, *7*, 3167. (b) Sellers, H.; Ulman, A.; Shnidman, Y.; Eilers, J. E. *J. Am. Chem. Soc.* **1993**, *115*, 9389. (c) Ye, Q.; Fang, J. X.; Sun, L *J. Phys. Chem. B.* **1997**, *101*, 8821. (d) Walczak, M. M.; Chung, C.; Stole, S. M.; Widrig, C. A.; Porter, M. D. *J. Am. Chem. Soc.* **1991**, *113*, 2370.

(3) (a) Lee, T. R.; Laibinis, P. E.; Folkers, J. P.; Whitesides, G. M. *Pure Appl. Chem.* **1991**, *63*, 821. (b) Lane, R. F.; Hubbard, A. T. *J. Phys. Chem.* **1973**, *77*, 1401. (c) Hickman, J. J.; Zou, C.; Ofer, D.; Harvey, P. D.; Wrighton, M. S.; Laibinis, P. E.; Bain, C. D.; Whitesides, G. M. *J. Am. Chem. Soc.* **1989**, *111*, 7271. (d) Stern, D. A.; Laguren-Davidson, L.; Frank, D. G.; Gui, J. Y.; Lin, C. H.; Lu, F.; Salaita, G. N.; Walton, N.; Zapien, D. C.; Hubbard, A. T. *J. Am. Chem. Soc.* **1989**, *111*, 877.

(4) Natan, M. J.; Thackeray, J. W.; Wrighton, M. S. *J. Phys. Chem.* **1986**, *90*, 4089.

(5) Sheen, C. W.; Shi, J.-X.; Martensson, J.; Parikh, A. N.; Allara, D. L. *J. Am. Chem. Soc.* **1992**, *114*, 1514.

(6) (a) Linford, M. R.; Chidsey, C. E. D. *J. Am. Chem. Soc.* **1993**, *115*, 5, 12631. (b) Keller, H.; Schrepp, W.; Fuchs, H. *Thin Solid Films* **1992**, *210/211*, 799.

(7) (a) Meyer, T. J.; Meyer, G. J.; Pfennig, B. W.; Schoonover, J. R.; Timpson, C. J.; Wall, J. F.; Obusch, C.; Chen, X. H.; Peek, B. M.; Wall, C. G.; Ou, W.; Erickson, B. W.; Bignozzi, C. A. *Inorg. Chem.* **1994**, *33*, 3952. (b) Allara, D. L.; Nuzzo, R. G. *Langmuir* **1985**, *1*, 45. (b) Allara, D. L.; Nuzzo, R. G. *Langmuir* **1985**, *1*, 52. (c) Ogawa, H.; Chihera, T.; Taya, K. *J. Am. Chem. Soc.* **1985**, *107*, 1365.

(8) (a) Finklea, H. O. In *Electroanalytical Chemistry*; Bard, A. J., Ed.; Marcel Dekker: New York, 1995; Vol. 19, Chapter II. (b) Campbell, D. J.; Herr, B. R.; Hulteen, J. C.; Van Duyne, R. P.; Mirkin, C. A. *J. Am. Chem. Soc.* **1996**, *118*, 10211. (c) Weber, K.; Hockett, L. A.; Creager, S. E. *J. Phys. Chem. B* **1997**, *101*, 8286. (d) Chidsey, C. E. D. *Science* **1991**, *251*, 919.

(9) (a) Freeman, R. G.; Grabar, K. C.; Allison, K. J.; Bright, R. M.; Davis, J. A.; Guthrie, A. P.; Hommer, M. B.; Jackson, M. A.; Smith, P. C.; Walter, D. G.; Natan, M. J. *Science* **1995**, *267*, 162. (b) Zhu, J.; Xu, F.; Schofer, S. J.; Mirkin, C. A. *J. Am. Chem. Soc.* **1997**, *119*, 235.

(10) Carpick, R. W.; Salmeron, M. *Chem. Rev.* **1997**, *97*, 1163.

(11) (a) Frisbie, C. D.; Rozsnyai, L. F.; Noy, A.; Wrighton, M. S.; Lieber, C. M. *Science* **1994**, *265*, 5181. (b) Noy, A.; Vezenov, D. V.; Lieber, C. M. *Annu. Rev. Mater. Sci.* **1997**, *27*, 381. (c) McKendry, R.; Theoclitou, M. E.; Rayment T.; Abell, C. *Nature* **1998**, *391*, 566.

(12) (a) Mirkin, C. A.; Ratner, M. A. *Annu. Rev. Phys. Chem.* **1992**, *43*, 719. (b) Mirkin, C. A.; Valentine, J. R.; Ofer, D.; Hickman, J. J.; Wrighton, M. S. In *Biosensors and Chemical Sensors*; Edelman, P. G., Wang J., Eds.; ACS Symposium Series 487; American Chemical Society: Washington, DC, **1992**; Chapter 17. (c) Hickman, J. J.; Ofer, D.; Laibinis, P. E.; Whitesides, G. M.; Wrighton, M. S. *Science* **1991**, *252*, 688. (d) Wells, M.; Crooks, R. M. *J. Am. Chem. Soc.* **1996**, *118*, 3988. (e) Crooks, R. M.; Ricco, A. J. *Acc. Chem. Res.* **1998**, *31*, 219.

(13) (a) Storhoff, J. J.; Mucic, R. C.; Mirkin, C. A.; Letsinger, R. L. *J. Am. Chem. Soc.* **1998**, *120*, 12674. (b) Mirkin, C. A.; Letsinger, R. L.; Mucic, R. C.; Storhoff, J. J. *Nature* **1996**, *382*, 607–609. (c) Elghanian, R.; Storhoff, J. J.; Mucic, R. C.; Letsinger, R. L.; Mirkin, C. A. *Science* **1997**, *277*, 1078–1080. (d) Storhoff, J. J.; Mucic, R. C.; Mirkin, C. A. *J. Clust. Sci.* **1997**, *8*, 179–216. (e) Hostetler, M. J.; Murray, R. W. *Curr. Opin. Colloid Interface Sci.* **1997**, *2*, 42.

(14) (a) Dalmia, A.; Liu, C. C.; Savinell, R. F. *J. Electroanal. Chem.* **1997**, *430*, 205. (b) Willner, I.; Lapidot, N.; Riklin, A.; Kasher, R.; Zanavy, E.; Katz, E. *J. Am. Chem. Soc.* **1994**, *116*, 1428. (c) Hutchison, J. E.; Postlethwaite, T. A.; Murray, R. W. *Langmuir* **1993**, *9*, 3277.

(15) Marks, T. J.; Ratner, M. A. *Angew. Chem., Int. Ed. Engl.* **1995**, *34*, 155.

(16) (a) Komeda, T.; Namba, K.; Nishioka, Y. *J. Vac. Sci. Technol. A* **1998**, *16*, 1680. (b) Tiberio, R. C.; Craighead, H. G.; Lercel, M.; Lau, T.; Sheen, C. W.; Allara, D. L. *Appl. Phys. Lett.* **1993**, *62*, 476. (c) Schoer, J. K.; Crooks, R. M. *Langmuir* **1997**, *13*, 2323. (d) Behm, J. M.; Lykke, K. R.; Pellin, M. J.; Hemminger, J. C. *Langmuir* **1996**, *12*, 2121. (e) Xu, S.; Liu, G. *Langmuir* **1997**, *13*, 127.

(17) (a) Piner, R. D.; Zhu, J.; Xu, F.; Hong, S.; Mirkin, C. A. *Science* **1999**, *283*, 661. (b) Xia, Y.; Whitesides, G. M. *Angew. Chem., Int. Ed. Engl.* **1998**, *37*, 550 and references therein.

(18) (a) Xu, F.; Chen, K.; Piner, R. D.; Mirkin, C. A.; Ritchie, J. E.; McDevitt, J. E.; Cannon, M. O.; Kanis, D. *Langmuir* **1998**, *14*, 6505. (b) Chen, K.; Mirkin, C. A.; Lo, R.; Zhao, J.; McDevitt, J. T. *J. Am. Chem. Soc.* **1995**, *117*, 6374. (c) For a review on the surface modification chemistry of cuprate HTSCs, see: Mirkin, C. A.; Xu, F.; Zhu, J. *Adv. Mater.* **1997**, *9 (2)*, 167.

10.1021/la990910y CCC: $19.00
Published on Web 01/04/2000

Scheme 1

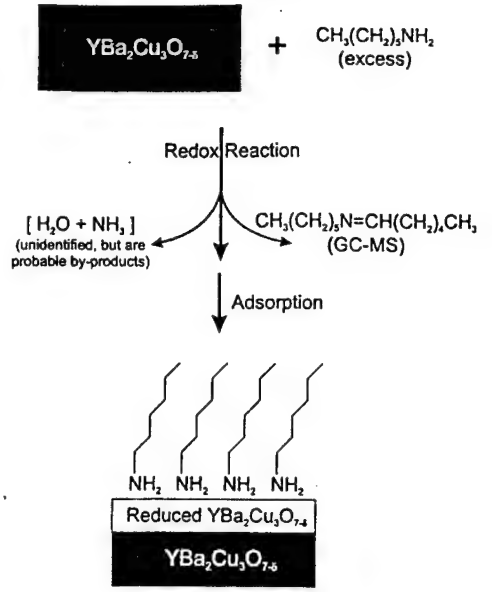

binder and is the adsorbate that leads to the most robust monolayer structures on $YBa_2Cu_3O_{7-\delta}$, the most extensively studied and commercially most promising HTSC material. The reaction between $YBa_2Cu_3O_{7-\delta}$ and an alkylamine is not just simple coordination chemistry. Indeed, other work has shown that the first step in the process involves a sacrificial redox reaction between the alkylamine and superconductor[19a] (Scheme 1). The second step involves another equivalent of amine binding to the resulting Cu^{2+} sites at the reduced superconductor surface.[18,19a] This has been confirmed by secondary ion mass spectrometery,[19a] X-ray photoelectron spectrometry,[19a] and surface-enhanced Raman spectroscopy.[19b] Nevertheless, the oxidative step in this proposed reaction pathway has recently been challenged by McDevitt et al.,[19c] but in that work the authors admittedly used corroded cuprate materials where the surface already was reduced, a fact that is clearly evident in a comparison of the XPS spectra of their starting materials with ours.[19a,c] A simple experiment involving the soaking of an amine in the presence of freshly prepared high surface area $YBa_2Cu_3O_{7-\delta}$ powder under anaerobic conditions unambiguously shows that the HTSC is capable of oxidizing the amine under the conditions used to modify its surface.[19a]

Other than the chemistry described above, very little is known about the dynamics associated with the monolayer formation process. The rates of the reaction under well-defined conditions, the mobility of the adsorbates on the surface of the superconductor surface, and the susceptibility of the surface bound adsorbates to exchange with solution adsorbates have not been evaluated. In contrast, much is known about the analogous processes involving alkanethiol adsorption,[20] migration,[21] and exchange on Au substrates,[22] and this information has been used to better understand the monolayer formation process and the environmental conditions that govern monolayer stability. In this paper, we explore the monolayer growth and exchange rates for alkylamines on $YBa_2Cu_3O_{7-\delta}$. In addition, we comment on the factors that influence monolayer formation, the mechanistic nature of the adsorbate exchange process, and the factors that contribute to the anomalously large surface coverages obtained from this type of surface modification chemistry.[18]

Experimental Section

General Methods. All manipulations were performed under air- and moisture-free conditions using standard Schlenk techniques or in an inert atmosphere glovebox, unless otherwise noted. Tetrabutylammonium hexafluorophosphate (n-Bu_4NPF_6), obtained from Aldrich Chemical Co., was recrystallized three times from ethanol and stored in a nitrogen atmosphere glovebox prior to use. Acetonitrile (CH_3CN) was dried by refluxing over calcium hydride, while diethyl ether (Et_2O) was dried and distilled over sodium–benzophenone. $YBa_2Cu_3O_{7-\delta}$ superconductor powder (99.999%, particle size 0.2 μm) was purchased from Strem Chemicals, Inc. NMR spectra were recorded on a Varian Gemini-300 FT NMR spectrometer. Electron impact (EI) mass spectra were obtained using a Fisions VG 70-250 SE mass spectrometer. Infrared absorption spectra were recorded on a Nicolet 520 Fourier transform infrared spectrometer with a liquid nitrogen cooled MCT (HgCdTe) detector. 6-Ferrocenylhexyl bromide was synthesized via modifications of a literature method.[23] The preparation of $FcC(O)NH(CH_2)_4NH_2$ (compound **1**) has been reported previously.[18a] ^1H NMR and mass spectra of these compounds match those reported in the literature.

Synthesis of 6-Aminohexylferrocene (Compound 2). 6-Ferrocenylhexyl bromide (1.25 g, 3.6 mmol) was dissolved in 50 mL of *N,N'*-dimethylformamide (DMF) in a 100 mL round-bottom flask. NaN_3 (0.26 g, 4.0 mmol) was added to the solution via a powder addition funnel, and the mixture was stirred at room temperature for 12 h. The reaction mixture was subsequently quenched with 100 mL of water. The solution was extracted with ethyl acetate (3 × 100 mL) and washed with brine (3 × 100 mL). After the organic extract was dried over magnesium sulfate, the solvent was removed by rotary evaporation, yielding 6-azidohexylferrocene (1.0 g, 3.2 mmol, yield = 89%). ^1H NMR (C_6D_6): δ 4.02 (s, 5H, η^5-C_5H_5), 3.97 (m, 4H, η^5-C_5H_4), 2.73 (t, 2H, CH_2N_3), 2.19 (t, 2H, η^5-$C_5H_4CH_2$), 1.36 (m, 2H, $CH_2CH_2N_3$), 1.20 (m, 2H, η^5-$C_5H_4CH_2CH_2$), 1.08 (m, 4H, $CH_2CH_2CH_2CH_2N_3$). HRMS (EI) (M^+) calcd for $C_{16}H_{21}N_3Fe$: 311.108 *m/z*. Found: 311.109 *m/z*. 6-Azidohexylferrocene (1.0 g, 3.2 mmol) was placed in a 100 mL Schlenk flask and dissolved in 50 mL of dry Et_2O. $LiAlH_4$ (0.18 g, 4.8 mmol) was added to a separate 100 mL Schlenk flask and suspended in 30 mL of Et_2O. The solution containing 6-azidohexylferrocene was transferred dropwise to the $LiAlH_4$ suspension via a cannula. The mixture was stirred under nitrogen for 2 h and then quenched with 20 mL of 1 mM aqueous NaOH. Fifty milliliters of Et_2O was added to extract the ferrocenyl-containing product from the aqueous suspension. The orange extract was dried over magnesium sulfate. Rotary evaporation of the solvent yielded the desired product as a yellow oil (0.82 g, 2.88 mmol, yield = 90%). ^1H NMR (C_6D_6): δ 4.01 (s, 5H, η^5-

(19) (a) Zhu, J.; Mirkin, C. A.; Braun, R. M.; Winograd, N. *J. Am. Chem. Soc.* **1998**, *120*, 5126. (b) Zhu, J.; Xu, F.; Schofer, S. J.; Mirkin, C. A. *J. Am. Chem. Soc.* **1997**, *119*, 235. (c) Ritchie, J. E.; Murray, W. R.; Kershan, K.; Diaz, V.; Tran, L.; McDevitt, J. T. *J. Am. Chem. Soc.* **1999**, *121*, 7447.

(20) (a) Bain, C. D.; Troughton, E. B.; Tao, Y. T.; Evall, J.; Whitesides, G. M.; Nuzzo, R. G. *J. Am. Chem. Soc.* **1989**, *111*, 321. (b) Biekuyck, H. A.; Bain, C. D.; Whitesides, G. M. *Langmuir* **1994**, *10*, 1825. (c) Schneider, T. W.; Buttry, D. A. *J. Am. Chem. Soc.* **1993**, *115*, 12391. (d) Forouzan, F.; Bard, A. J.; Mirkin, M. V. *Isr. J. Chem.* **1997**, *37*, 155. (e) Kim, Y.-T.; McCarley, R. L.; Bard, A. J. *Langmuir* **1993**, *9*, 1991. (f) Schessler, H. M.; Karpovich, D. S.; Blanchard, G. J. *J. Am. Chem. Soc.* **1996**, *118*, 9645. (g) Pan, W.; Durning, C. J.; Turro, N. J. *Langmuir* **1996**, *12*, 4469. (h) Schlenoff, J. B.; Li, M.; Ly, H. *J. Am. Chem. Soc.* **1995**, *117*, 12528. (i) Kajikawa, K.; Hara, M.; Sasabe, H.; Knoll, W. *Jpn. J. Appl. Phys. 2* **1997**, *36*, L1116. (j) Thomas, R. C.; Sun, L.; Crooks, R. M. *Langmuir* **1991**, *7*, 620. (k) Bensebaa, F.; Voicu, R.; Huron, L.; Ellis, T. H. *Langmuir* **1997**, *13*, 5335.

(21) (a) Kondoh, H.; Kodama, C.; Nozoye, H.; *J. Phys. Chem. B.* **1998**, *102*, 2310. (b) Cavalleri, O.; Hirstein, A.; Bucher, J. P.; Kern, K. *Thin Solid Films* **1996**, *285*, 392. (c) Sondaghuetorst, J. A. M.; Schonenberger, C.; Fokkink, L. G. J. *J. Phys. Chem.* **1994**, *98*, 6826.

(22) (a) Collard, D. M.; Fox, M. A. *Langmuir* **1991**, *7*, 1192. (b) Chidsey, C. E. D.; Carolyn, R. B.; Putvinski, T. M.; Mujsce, A. M. *J. Am. Chem. Soc.* **1990**, *112*, 4301. (c) Rowe, G. K.; Creager, S. E. *Langmuir* **1994**, *10*, 1186. (d) Hickman, J. J.; Ofer, D.; Zou, C. F.; Wrighton, M. S.; Laibinis, P. E.; Whitesides, G. M. *J. Am. Chem. Soc.* **1991**, *113*, 1128.

(23) Creager, S. E.; Rowe, G. K. *J. Electroanal. Chem.* **1994**, *370*, 203.

C_5H_5), 3.97 (m, 4H, η^5-C_5H_4), 2.52 (t, 2H, CH_2NH_2), 2.25 (t, 2H, η^5-$C_5H_4CH_2$), 1.48 (m, 2H, $CH_2CH_2NH_2$), 1.26 (m, 6H, η^5-C_5H_4-CH_2CH_2 CH_2CH_2), 0.65 (s, br, 2H, NH_2). HRMS (EI) (M^+) calcd for $C_{16}H_{23}NFe$: 285.118 *m/z*. Found: 285.117 *m/z*.

Preparation of $YBa_2Cu_3O_{7-\delta}$ Electrodes. $YBa_2Cu_3O_{7-\delta}$ powder was pressed into 13 mm diameter pellets (applied pressure ~4000 psi, ~1 mm thick), which were subsequently annealed at ~450 °C overnight under an oxygen flow (pressure = 1 atm), followed by slow cooling (18 °C/h), under oxygen flow, to room temperature. All of the resulting pellet samples displayed a superconducting transition temperature of ~92 K. XRD studies showed that the pellets prepared under these conditions are single-phase, orthorhombic $YBa_2Cu_3O_{7-\delta}$. Pellets were then fabricated into epoxy-encapsulated electrodes via literature methods.[24]

Procedure for Modifying $YBa_2Cu_3O_{7-\delta}$ Electrodes with Alkylamines. In a typical experiment, an epoxy-encapsulated $YBa_2Cu_3O_{7-\delta}$ ceramic electrode was cut with a razor blade to expose a fresh surface on the tip of the electrode. The exposed surface was then sanded and flattened with 600 grit sand paper, followed by sonication in dry CH_3CN for 1 min. The electrode was shaved with a new razor blade according to literature methods.[18b] The electrode was then immediately transferred into a glovebox filled with nitrogen. The freshly prepared $YBa_2Cu_3O_{7-\delta}$ ceramic electrode was immersed into a dry CH_3CN solution of alkylamine for a set period of time, which depended upon the particular experiment (vide infra). The modified electrode was removed from the soaking solution and rinsed throughly with copious amounts of dry CH_3CN prior to performing electrochemical measurements. After each electrochemical measurement, the electrode was rinsed with fresh CH_3CN to remove electrolyte before immersing it into a new CH_3CN solution of alkylamine adsorbate reagent for further studies.

Electrochemical Measurements. Cyclic voltammetry was performed with a Pine AFRDE4 bipotentiostat with a Linseis X-Y 1400 recorder. All electrochemical measurements were performed with a conventional three-electrode cell in a glovebox. Each cell consisted of a modified or unmodified $YBa_2Cu_3O_{7-\delta}$ ceramic working electrode, a Pt gauze counter electrode, and a nonaqueous $Ag/AgNO_3$ (0.01 M $AgNO_3/CH_3CN$) reference electrode. The electrolyte solution was 0.1 M n-Bu_4NPF_6/CH_3CN for all electrochemical experiments.

Scanning Electron Microscopy. Morphologies of ceramic $YBa_2Cu_3O_{7-\delta}$ electrodes were examined by a Hitachi S570 scanning electron microscope with an accelerating voltage of 25 keV. The working distance beteeen the electron gun and sample surface was in the 25−30 mm range, and samples were connected to a metal sample holder with a conducting graphite tape.

Results and Discussion

To probe monolayer growth and exchange kinetics, two ferrocenyl alkylamine adsorbates, $FcC(O)NH(CH_2)_4NH_2$ (**1**) and $Fc(CH_2)_6NH_2$ (**2**), were synthesized. Ferrocenyl-

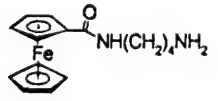

Compound 1

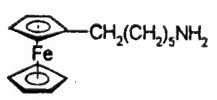

Compound 2

containing adsorbates have been extensively studied in the preparation and characterization of SAMs on various inorganic substrates.[2,25] Indeed, the surface coverage (Γ)

Scheme 2

Case 1: Growth

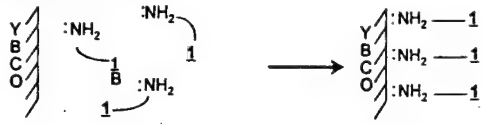

Case 2: "Quasi-Degenerate" Exchange

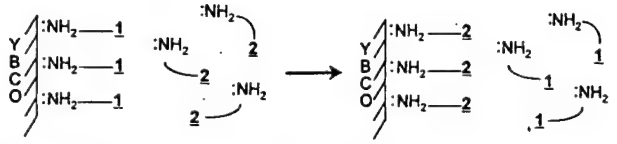

Case 3: "Non-Degenerate" Exchange

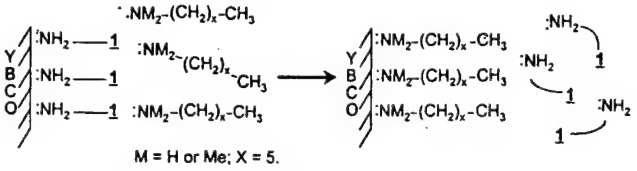

M = H or Me; X = 5.

of a ferrocenyl-containing adsorbate can be determined via eq 1,

$$\Gamma = Q/nFA \qquad (1)$$

where n is the number of electrons involved in the electron-transfer process ($n = 1$ for ferrocene/ferrocenium redox couple), F is the Faraday constant, Q is the charge passed across the electrode/monolayer interface, and A is the geometric surface area of the electrode (vide infra).

The charge Q can be determined by integrating the current associated with the ferrocenyl/ferrocenylium redox reaction when probed by cyclic voltammetry. One key assumption in this analysis is that all of the surface-adsorbed ferrocenyl alkylamines are electrochemically accessible. Although not safe for all adsorbates,[8b,26] this assumption has proven reasonable for monolayer studies on gold involving ferrocenyl alkyl adsorbates with less than 10 methylene units.[8a] The monolayer formation rate can be determined by measuring the change in surface coverage for ferrocenyl-containing adsorbate as a function of adsorption time (case 1 in Scheme 2). For compound **1**, a strongly electron-withdrawing amido functional group has been attached to one of the cyclopentadienyl rings of the ferrocenyl moiety, which makes the ferrocenyl group more electron deficient and thus more difficult to oxidize than ferrocene. For compound **2**, a slightly electron-donating methylene group is bound to one cyclopentadienyl ring, making it slightly easier to oxidize than ferrocene. Due to the different electronic influences of these two substituents, the redox potentials of **1** ($E_{1/2}$ − 300 mV vs $Ag/AgNO_3$) and **2** ($E_{1/2}$ − 80 mV vs $Ag/AgNO_3$) are separated by 220 mV in 0.1 M n-Bu_4NPF_6/CH_3CN (Figure 1). This difference in redox potential allows one to study adsorbate exchange reactions on $YBa_2Cu_3O_{7-\delta}$ via cyclic voltammetry (case 2 in Scheme 2). In general, one can examine the kinetics for adsorbate displacement of these molecules from an electrode surface as a function of incoming adsorbate concentration, structure, and size, all

(24) Riley, D. R.; McDevitt, J. T. *J. Electroanal. Chem.* **1990**, *295*, 373.

(25) (a) Hickman, J. J.; Laibinis, P. E.; Auerbach, D. I.; Zou, C.; Gardner, T. J.; Whitesides, G. M.; Wrighton, M. S. *Langmuir* **1992**, *8*, 357. (b) Shimazu, K.; Sato, Y.; Yagi, I.; Uosaki, K. *Bull. Chem. Soc. Jpn.* **1994**, *67*, 863. (c) Gardner, T. J.; Frisbie, C. D.; Wrighton, M. S. *J. Am. Chem. Soc.* **1995**, *117*, 6927. (d) Caldwell, W. B.; Campbell, D. J.; Chen, K.; Herr, B. R.; Mirkin, C. A.; Malik, A.; Durbin, M. K.; Huang, K. G.; Dutta. P. *J. Am. Chem. Soc.* **1995**, *117*, 6071.

(26) (a) Caldwell, W. B.; Campbell, D. J.; Chen, K.; Herr, B. R.; Mirkin, C. A.; Malik, A.; Durbin, M. K.; Huang, K. G. *J. Am. Chem. Soc.* **1995**, *117*, 6071. (b) Herr, B. R.; Mirkin, C. A. *J. Am. Chem. Soc.* **1994**, *116*, 1157. (c) Shi, X.; Caldwell, W. B.; Chen, K.; Mirkin, C. A. *J. Am. Chem. Soc.* **1994**, *116*, 11598. (d) Mirkin C. A.; Caldwell, W. B. *Tetrahedron* **1996**, *52*, 5113−5130. (e) Caldwell, W. B.; Chen, K.; Mirkin, C. A.; Babinec, S. J. *Langmuir* **1993**, *9*, 1945. (f) Chen, K.; Caldwell, W. B.; Mirkin, C. A. *J. Am. Chem. Soc.* **1993**, *115*, 1193.

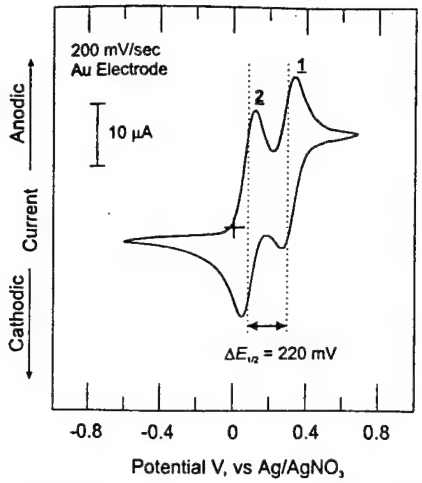

Figure 1. Cyclic voltammetry of compounds **1** and **2** in 0.1 M n-Bu_4NPF_6/CH_3CN. The scan rate is 200 mV/s.

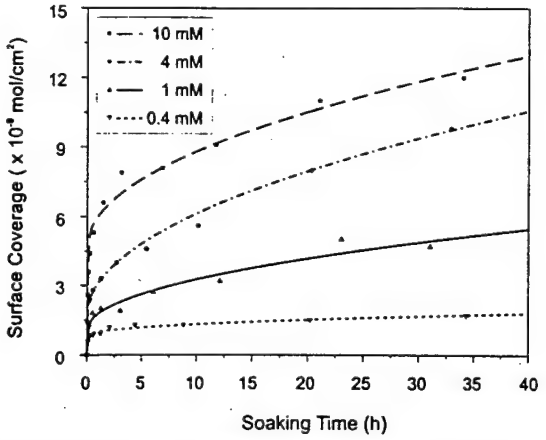

Figure 2. Surface coverages of redox-active adsorbate **1** on a ceramic $YBa_2Cu_3O_{7-\delta}$ electrode as a function of soaking time in solutions of **1**. Solution concentrations are given in the inset.

of which can provide valuable insight into the nature of the exchange process (case 3 in Scheme 2).

Growth of $FcC(O)NH(CH_2)_4NH_2$ (1) Monolayer on Ceramic $YBa_2Cu_3O_{7-\delta}$. Monolayer growth was followed by immersing a ceramic $YBa_2Cu_3O_{7-\delta}$ electrode (area = 0.03 cm^2) into a 1 mM CH_3CN solution of **1** and determining surface coverage by cyclic voltammetry at various stages throughout the process. The coverage of **1**, as determined by cyclic voltammetry, increased very steeply from 0 to 2 $\times 10^{-9}$ mol/cm^2 during the first 2 h of immersion (Figure 2, ▲). Then the growth process significantly slowed. After an additional 10 h of soaking, the coverage approached 2.8 $\times 10^{-9}$ mol/cm^2, and after 21 h, it reached a value of 4.5 $\times 10^{-9}$ mol/cm^2. After this experiment, the electrode was cut and sanded to generate a fresh surface (vide infra) for analogous kinetic studies in a 0.4 mM CH_3CN solution of **1** (▼). Kinetic studies in 4 mM (●) and 10 mM (■) CH_3CN solutions of compound **1** were conducted in a similar manner on the same electrode. All data from these studies are presented in Figure 2.

Generally speaking, the formation of a monolayer of **1** on a $YBa_2Cu_3O_{7-\delta}$ surface, regardless of conditions, consists of two distinct periods of growth. The first few hours of soaking leads to a very fast increase in adsorbate surface coverage. Then the adsorption rate slows down, but a limiting surface coverage is never reached, regardless of concentrations of adsorbate and soaking time (up to 30 days), and the tailing part is described by a parabolic curve (coverage $\propto t^{1/2}$) (Figure 2). Over the range of adsorbate concentrations studied, final surface coverage values are directly proportional with soaking time and adsorbate concentration in the soaking solutions and time. From these studies, it is clear that the monolayer growth kinetics for compound **1** do not fit a simple Langmuir adsorption isotherm. For a Langmuir adsorption isotherm, the surface coverage traces are expected to level off as adsorbates saturate surface adsorption sites. On the basis of our studies, we propose that the adsorption of alkylamines on ceramic $YBa_2Cu_3O_{7-\delta}$ is controlled by two major processes: (1) a relatively fast adsorption process, where the solution adsorbates adsorb onto external surface of the superconductor that is exposed to the solution, and (2) the diffusion of adsorbate molecules and solution through the electrode pores and channels, which are very characteristic of this type of ceramic material (Figure 3). Adsorbates then can adsorb onto the internal surface of the electrode with the effective electrode surface area increasing as electrolyte is wicked up into the material.

Surface coverage values for **1** and differential capacitance measurements for an electrode that was modified by immersing it in a 1 mM solution of **1** are plotted as a function of reaction time (Figure 4). The differential capacitance, which was measured at −0.35 V vs $Ag/AgNO_3$, decreased during the first ~15 h of monolayer adsorption with a concomitant increase in surface coverage of **1**. This is consistent with the expected passivation of the electrode surface as the monolayer of **1** forms. Importantly, the capacitance begins to increase thereafter, even though the surface coverage of **1** keeps increasing. This increase in differential capacitance with a simultaneous increase in surface coverage shows that the effective surface area is increasing as the electrode is exposed to solution-containing adsorbate.

In addition to capacitance measurements, three other observations support this hypothesis. First, assuming that the cross sectional area of the ferrocenyl group (36 $Å^2$) in **1** dictates its molecular footprint,[12a] a full monolayer of **1** on a perfectly flat substrate should be ~4.5 $\times 10^{-10}$ mol/cm^2. Surface coverages determined in our studies are on the order of 1 $\times 10^{-9}$ to 1 $\times 10^{-8}$ mol/cm^2, depending on the adsorbate concentrations and soaking time. These coverages are 1−2 orders of magnitude higher than the theoretical value mentioned above, and normal roughness factors cannot account for these high values.[27] However, ceramic superconductor $YBa_2Cu_3O_{7-\delta}$ electrodes are quite porous, as evidenced by SEM (Figure 3). Therefore, we conclude that these anomalously high surface coverages and non-Langmuir isotherms are primarily due to adsorbate solution being wicked into the porous structure via capillary action. Adsorbate molecules can access surface sites on the interior of the ceramic electrode as this happens. Thus, the effective surface area includes both external and internal contributions. A second important observation pertains to experiments that involved long electrode soaking times. If electrodes treated in this manner were subsequently cut or sanded approximately 1 mm to generate a fresh surface, small waves attributed to **1** often could be detected by cyclic voltammetry. This is strong evidence that adsorbates do diffuse into the ceramic material and adsorb onto the internal surface of the porous electrode. Finally, the growth traces at different concentrations are also consistent with this hypothesis. In 0.4 mM solutions of **1**, the first 2 h of soaking leads to an adsorbate surface coverage of 1.1 $\times 10^{-9}$ mol/cm^2, which

(27) (a) Trasatti, S.; Petrii, O. A. *Pure Appl. Chem.* **1991**, *63*, 711. (b) Alves, V. A.; da Silva, L. A.; de Castro, S. C.; Boodts, J. F. C. *J. Chem. Soc., Faraday Trans.* **1998**, *94*, 711.

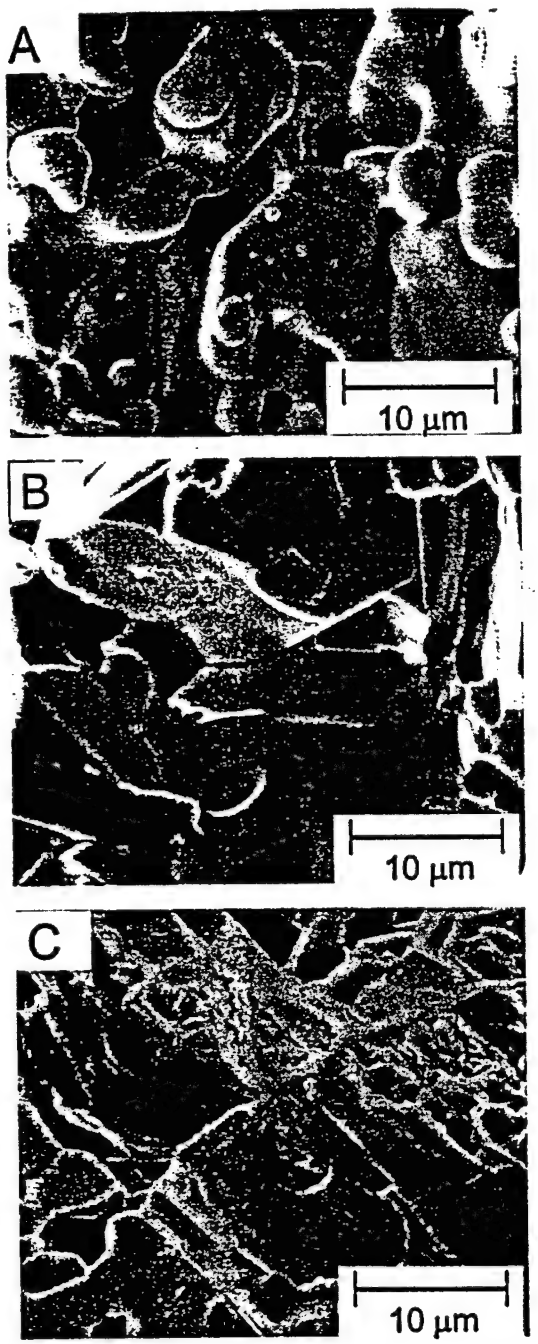

Figure 3. SEM images of a typical ceramic $YBa_2Cu_3O_{7-\delta}$ electrode: (A) as prepared; (B) after treatment with 600 grit sand paper, shaved with a razor blade, and sonicated in dry CH_3CN; and (C) a pellet treated as described in B after soaking in a 1 mM CH_3CN solution of **1** for 1 day.

is almost 80% of the coverage after 1 day of soaking (1.5×10^{-9} mol/cm^2). In the case of 4 mM solutions of **1**, 2 h of soaking generates only 45% of the surface coverage observed for 1 day of soaking (3.7×10^{-9} mol/cm^2 vs 8.5×10^{-9} mol/cm^2) (Figure 2). This concentration dependence is qualitatively consistent with the relationship between the adsorbate diffusion and concentration as predicted by Fick's first law of diffusion,[28]

$$J \propto -D\, \partial c/\partial x \qquad (2)$$

where D is the adsorbate diffusion constant, and $\partial c/\partial x$ is the concentration gradient. Note that because of this, at

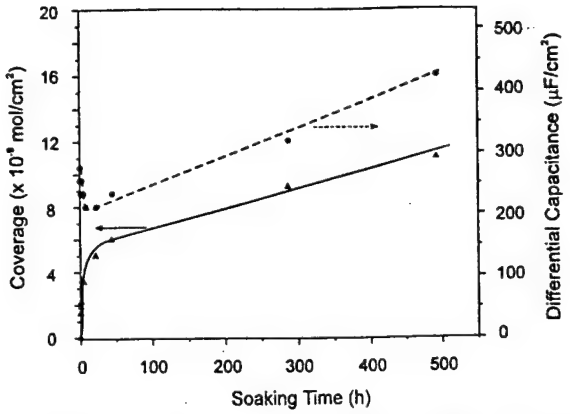

Figure 4. Surface coverage of **1** (solid line, left abscissa) vs time, and differential capacitance (dashed line, right abscissa) vs time for a ceramic $YBa_2Cu_3O_{7-\delta}$ electrode soaked in a 1 mM CH_3CN solution of **1**.

higher concentrations (>10 mM), adsorbate diffusion through the pores of $YBa_2Cu_3O_{7-\delta}$ and adsorption to internal sites likely contribute to a large portion of the electrochemically determined surface coverages, even for the first 2 h of soaking (Figure 2).

Ten electrodes were studied to test the reproducibility of these results. Similar adsorption trends were observed in all studies. Although the surface coverages obtained for different electrodes modified under identical conditions differed by as much as 50%, surface coverage determination experiments involving one electrode, used repeatedly via the sanding and shaving method, exhibited reproducibility within 10%. This observation is undoubtly due to the structural complexity and porosity of the ceramic materials used to make the electrodes.

Although surface Cu amine complexes with more than one amine ligand on each Cu atom might account for a surface coverage greater than the idealized case, it is unlikely to be responsible for the factor of 10 difference reported herein. If the system in question involved solution Cu amine complexes, this might be a plausible argument, but in the case of a surface, the exposed surface area, free volume, and the number of potential surface bonding sites dictate how much adsorbate can bond to the surface. Increasing the number of potential sites without increasing the available surface area and free volume could not account for a factor of 10 difference in adsorbate surface coverage. In fact, the number of copper sites is not the limiting factor in these systems. Molecular models show that the molecules are too large to occupy all available surface Cu sites.[18b] In other words, the Cu in this system is not coordinatively saturated with amine ligands and could accommodate other ligands, if there was room to do so.

"Quasi-Degenerate" Exchange of Surface Adsorbed $FcC(O)NH(CH_2)_4NH_2$ (1) with Solution $Fc(CH_2)_6NH_2$ (2). This type of exchange is termed "quasi-degenerate" since the chemistry of adsorption is degenerate in each case (primary alkylamine on $YBa_2Cu_3O_{7-\delta}$), and both alkylamine adsorbates (**1** and **2**) have ferrocenyl redox-active moieties of approximately the same size. With these molecules, the extent of exchange between **1** and **2** can be monitored easily through cyclic voltammetry.

In a typical experiment, a ceramic $YBa_2Cu_3O_{7-\delta}$ electrode (area = 0.04 cm^2) was soaked in a 1 mM CH_3CN solution of **1** for 2 days.[29] Cyclic voltammetry was

(28) Jost, W. *Diffusion in Solids, Liquids, Gases*; Academic: New York, 1960; Chapter 1, p 2.

(29) We chose 2 days of soaking to form the initial monolayer for experimental consistency.

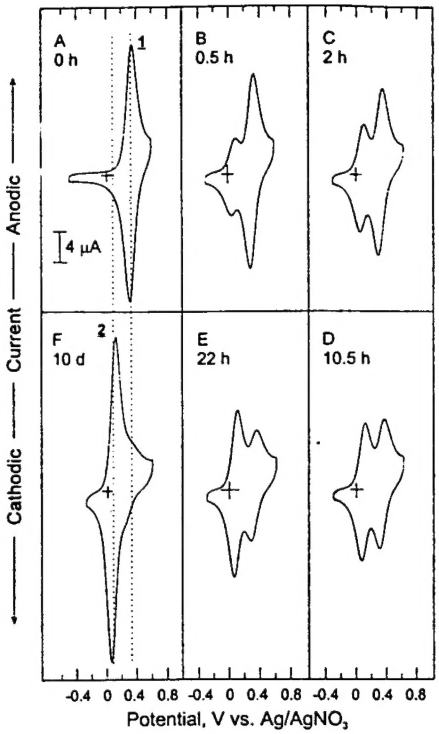

Figure 5. Cyclic voltammograms of a $YBa_2Cu_3O_{7-\delta}$ electrode modified with a monolayer of **1** after soaking in a 1mM CH_3CN solution of **2**. Scan rates are 200 mV/s and *Y* scales are 4 μm for all experiments.

performed on the modified electrode after it was removed from the soaking solution and rinsed with copious amounts of CH_3CN. As expected, cyclic voltammetry performed on this electrode showed a near-ideal wave associated with the oxidation/reduction of surface adsorbed **1** at +320 mV vs $Ag/AgNO_3$ (vide infra) (Figure 5A). This modified electrode was then immersed into a 1 mM CH_3CN solution of adsorbate **2**. The extent of exchange (**2** for **1**) was examined by cyclic voltammetry as a function of soaking time (Figure 5B–F). After 0.5 h the electrode was removed from the solution of **2**, rinsed with CH_3CN, and then placed into a clean electrolyte solution of 0.1 M *n*-Bu_4NPF_6/CH_3CN. Cyclic voltammetry shows two reversible waves with $E_{1/2}$ values at +80 and +320 mV vs $Ag/AgNO_3$, which correspond to surface-confined **2** and **1**, respectively. After each electrochemical measurement, the electrode was rinsed with CH_3CN before it was immersed in a 1 mM CH_3CN solution of **2**. Within the first 0.5 h, approximately 15% of **1** was displaced by **2**. After 10.5 h, there were nearly equal amounts of **1** and **2** on the electrode surface. This point is defined as the half-life of the exchange reaction. Significantly, near complete displacement (~95%) of **1** by **2** took 10 days. Another important observation during the exchange process is that the sum of the current associated with surface-confined **1** and **2** increased as the electrode was exposed to the soaking solution. For example, after 10 days of the exchanging reaction (Figure 5F), the total integrated current associated with surface-confined **1** and **2** is 1.5 times that of the starting monolayer (Figure 5A). This is further evidence that the alkylamine (**2**) in solution, in addition to exchange with adsorbed **1**, continues to diffuse through pores and channels to access new adsorption sites inside the ceramic material.

The reversibility of the exchange process has been demonstrated in the following way. The electrode, now covered with a monolayer of **2** (with less than 5% of **1**), was immersed into a 1 mM CH_3CN solution of **1**. After soaking for 1 day, it was removed from solution, rinsed, and studied by cyclic voltammetry. The wave at +320 mV vs $Ag/AgNO_3$ started growing at the expense of the one at +90 mV. Essentially this corresponds to the process involving the displacement of surface-confined **2** by **1**, which, after more than 30 days, leads to a monolayer consisting of greater than 95% of **1**.

Table 1. Wave Shape Analysis of the Quasi-Degenerate Exchange of 1 and 2

	1		2		
surface-confined **1** (%)	$E_{1/2}$ (mV)[a]	ΔE_{fwhm} (mV)	$E_{1/2}$ (mV)	ΔE_{fwhm} (mV)	$E_{1/2}$ (mV)
100 (Figure 5A)	320	160			
~85 (Figure 5B)	320	160	80	NA[b]	240
~70 (Figure 5C)	320	160	75	NA	245
~50 (Figure 5D)	340	NA	90	NA	250
~30 (Figure 5E)	320	NA	85	150	235
~5 (Figure 5F)	NA	NA	90	170	NA

[a] All potential data reported in this tablew have an error of ±10 mV. [b] No accurate data available due to the overlap of the cyclic voltammograms of **1** and **2**.

The cyclic voltammograms of the redox-active monolayers taken during the exchange reaction have been analyzed to probe the chemical environment of the adsorbates within the film. For an ideal surface-confined redox-active species, the peak current is linearly proportional to scan rate, the anodic wave is the mirror image of the cathodic wave reflected across the potential axis, and the full width at half-maximum of the peak (E_{fwhm}) is 90.6 mV for a one-electron-transfer process.[30] However, experimentally such ideal behavior is rarely observed due to a variety of factors, including local environment. Soaking a $YBa_2Cu_3O_{7-\delta}$ electrode in a 1 mM CH_3CN solution of **1** for 2 days results in a nonideal, but well-behaved, voltammetric wave for a surface-confined species ($\Delta E_p = 50$ mV, $E_{fwhm,a} = 160$ mV, $i_a/i_c = 0.98$ at a scan rate of 200 mV/s) (Figure 5A and Table 1). For a mixed monolayer consisting of two adsorbates with different redox potentials, the anodic and cathodic peak positions of the adsorbate with higher formal potential may be affected by the change in oxidation state of the adsorbate with lower formal potential, depending upon proximity and degree of phase segregation.[31] If **2** and **1** are in a densely packed monolayer, but mixed randomly at the molecular level on the surface, the oxidation of ferrocenyl to ferrocenylium [Fe(II) → Fe(III)] in **2** will influence nearby **1** due to electrostatic repulsions, which would make the oxidation of **1** more difficult (i.e. $E_{p,a}$ of **1** shifts to more positive potentials, and the wave broadens).[21,26,31] Peak shape analysis of the quasi-degenerate exchange reaction shows that, within experimental error, the formal potentials and relative peak positions ($E_{p,a}$ values and $\Delta E_{p,a}$) of the two adsorbates do not shift during the exchange process (Table 1). Furthermore, no significant peak broadening ($E_{fwhm,a}$ values) is observed during the 10 days of the exchange reaction. These data suggest that repulsive interactions between surface-confined oxidized **1** and **2** are not significant throughout the electrochemically assayed exchange process. Since these molecules are quite similar in structure, relatively poor adsorbate packing on these polycrystalline ceramic substrates, rather than phase segregation, is likely responsible for this response.

"Nondegenerate" Exchange of a $FcC(O)NH(CH_2)_4NH_2$ (1) Monolayer with Non-Redox-Active Alky-

(30) Murray, R. W. In *Eletroanalytical Chemistry*; Bard, A. J., Ed.; Marcel Dekker: New York, 1984; Vol. 13, pp 200–206.

(31) (a) Tirado, J. D.; Acevedo, D.; Bretz, R. L.; Abruna, H. D. *Langmuir* **1994**, *10*, 1971. (b) Tirado, J. D.; Abruna, H. D. *J. Phy. Chem.* **1996**, *100*, 4556. (c) Acevedo, D.; Bretz, R. L.; Tirado, J. D.; Abruna, H. D. *Langmuir* **1994**, *10*, 1300.

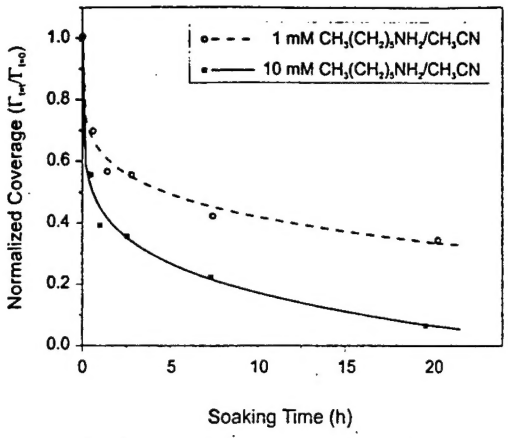

Figure 6. "Nondegenerate" exchange kinetics for surface-confined **1** and solution hexylamine. Surface coverages of redox-active **1** are normalized to the coverages prior to the exchange reactions. Experiments were conducted on the same piece of ceramic electrode for two different hexylamine concentrations (inset).

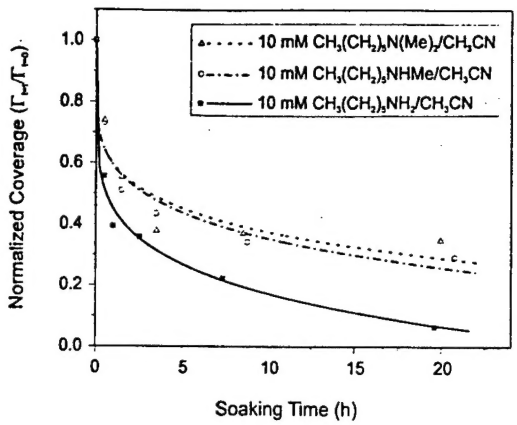

Figure 7. "Nondegenerate" exchange data for surface-confined **1** with amines possessing different headgroups. Data on this figure and Figure 4 were collected from the same electrode.

lamines. Additional experiments were designed to gain mechanistic information regarding the exchange process. Unlike the aforementioned "quasi-degenerate" exchange reaction, which involves exchange of solution and surface-bound redox-labeled primary amines, this series of experiments involves the displacement of a surface-confined redox-active primary alkylamine **1** by redox-inactive primary, secondary, and tertiary alkylamine reagents in solution (case 3 in Scheme 2). These processes are termed "nondegenerate" because of the dissimilarity of the exchanging adsorbates. In a typical experiment, a redox-active monolayer of **1** was prepared on $YBa_2Cu_3O_{7-\delta}$, and the displacement of surface-confined **1** by redox-inactive alkylamine reagents (i.e. hexylamine) was monitored via cyclic voltammetry by measuring the decrease in current associated with the oxidation/reduction of **1** as a function of exposure to the redox-inactive alkylamines. This method allows one to monitor the signal exclusively due to the exchange reaction, since the diffusion of redox-inactive solution species into the pores during the exchange process will not show up in the electrochemical experiment.

The mechanistic nature of this exchange reaction is likely quite complicated, but from such exchange studies, it may be possible to differentiate between associative and dissociative pathways. The latter has been reported to be the dominant mode of exchange for alkanethiol monolayers on Au[22] and Pt.[31] A diagnostic way of differentiating an associative process from a dissociative one is to monitor the reaction as a function of adsorbate concentration.[32] The rate of an associative process will be dependent upon incoming adsorbate concentration, while a dissociative process will be relatively unaffected.

A monolayer of **1** on a $YBa_2Cu_3O_{7-\delta}$ electrode ($\Gamma = 3.8 \times 10^{-9}$ mol/cm^2) was prepared as described earlier. The electrode was removed, rinsed vigorously with CH_3CN, and characterized by cyclic voltammetry before it was soaked in CH_3CN solutions of hexylamine. Data at two different concentrations of hexylamine (1 and 10 mM) were collected. For comparison purposes, surface coverages of **1** as a function of soaking time were normalized to those found prior to initiating the exchange reactions (Figure 6). Significant differences between exchange rates were observed. For the 1 mM hexylamine solution, about 30% of surface-confined **1** was displaced after 0.5 h, while for a 10 mM solution, 45% was displaced after 0.5 h. The exchange rates slowed with longer soaking times. For example, after soaking the modified electrode in a 1 mM hexylamine solution for 20 h, 35% of the original monolayer **1** remained, while only 5% of monolayer **1** remained on the surface after soaking for 20 h in a 10 mM solution of hexylamine. The dependence of the exchange rates on the concentration of attacking hexylamine strongly indicates that the exchange reaction occurs through an associative pathway.

To further test this hypothesis of an associative pathway, steric effects on the exchange dynamics were examined. We carried out nondegenerate exchange reactions of surface-confined **1** in 10 mM CH_3CN solutions of *N*-methyl hexylamine and *N,N'*-dimethylhexylamine. The interactions of primary, secondary, and tertiary amines with $YBa_2Cu_3O_{7-\delta}$ were previously shown to involve the same type of coordination chemistry.[18,19] Substituting protons on the amino group of the attacking ligand with one or two methyl groups increases its size and might be expected to affect the rate of exchange. The exchange behavior of surface-confined **1** with secondary and tertiary amines is presented in Figure 7. During the first 0.5 h, 25% of **1** was displaced by *N*-methylhexylamine, while 40% of **1** was displaced by hexylamine at the same concentration. Actually, the displacement reaction curve for 1 mM hexylamine is very comparable to that observed for *N*-methylhexylamine at 10 mM concentration (Figures 6 and 7). The exchange rate dependence upon size of incoming molecule also is consistent with an associative mechanism because the rate of a reaction which proceeds by a dissociative mechanism is typically independent of the size of the incoming molecule. No significant rate differences were observed for reactions in solutions of *N*-methylhexylamine and *N,N'*-dimethylhexylamine, which may be an implication of a saturation of the steric effects. Electronically these molecules are quite similar, although not identical.

When one compares the adsorbate exchange behavior reported herein for alkylamines and monolayer-modified $YBa_2Cu_3O_{7-\delta}$ with the analogous data for alkanethiols on monolayer-modified Au, it appears somewhat surprising. The former is dominated by an associative pathway while the latter proceeds via a dissociative pathway.[22] However, when one takes into account that the exchange chemistry on $YBa_2Cu_3O_{7-\delta}$ is occurring at Cu(II) sites, it is actually somewhat predictable, especially when one examines the literature base revolving around the amine coordination chemistry of Cu(II). It is well-known that Cu(II) can accommodate coordination numbers ranging from 4 to 7

(32) Steinfeld, J. J. *Chemical Kinetics and Dynamics*; Prentice Hall: Englewood Cliff, NJ, 1992; Chapter 1 and 2.

and that the transitions among such coordination environments are often dynamic at room temperature.[33,34] In fact, numerous solution studies have documented the susceptibility of Cu(II) to S_N2 type displacement reactions[35,36] like the type we are proposing to take place on the monolayer-modified reduced $YBa_2Cu_3O_{7-\delta}$ surface with alkylamines.

Conclusions

We have carried out studies on the growth and exchange processes for alkylamine monolayers on the cuprate HTSC, $YBa_2Cu_3O_{7-\delta}$, and although the porous structure of this type of ceramic substrate significantly complicates the growth kinetics of redox-active alkylamine monolayers, several important conclusions may be drawn from these studies. First, there are two main factors that control the adsorption process and contribute to the adsorption isotherms: (1) a rapid adsorption process that occurs on the external HTSC electrode surface and (2) a relatively slow pore diffusion process which results in the modification of the internal surface area of the substrate. Qualitatively, over millimolar concentration ranges, a major portion of alkylamine monolayer forms on the external surface of ceramic $YBa_2Cu_3O_{7-\delta}$ within a few hours after which the pore diffusion process dominates, contributing to the parabolic adsorption isotherm. Second, alkylamine adsorption on $YBa_2Cu_3O_{7-\delta}$ is based on Cu(II)−amine coordination chemistry and is chemically distinct from the previously studied systems involving thiol adsorption on Au and Pt. Accordingly, the exchange behavior of alkylamines on this novel substrate reflects much of the solution coordination chemistry of Cu(II).[33-36] It is very dynamic and occurs via an associative rather than a dissociative pathway.

Acknowledgment. C.A.M. acknowledges the AFOSR (F49620-96-1-0133) and the NSF (Grant DMR 91-20000) through the Science and Technology Center for Superconductivity for support of this work. C.A. M. also acknowledges use of instruments which were purchased by the MRSEC Program of the NSF at the MRC of NU, under Award No. DMR-9120521. Professor K. R. Poeppelmeier is thanked for use of instrumentation.

LA990910Y

(33) Gazo, J.; Bersuker, I. B.; Garaj, J.; Kabesova, M.; Kohout, J.; Langfelderova, J.; Melnik, M.; Serator, M.; Valach, F. *Coord. Chem. Rev.* **1976**, *19*, 253.

(34) Basolo, F. B.; Pearson, R. G. *Mechanisms of Inorganic Reactions*; John Wiley and Sons: New York, 1967; pp 145−158, pp 421−422.

(35) (a) Pearson, R. G.; Lanier, R. D. *J. Am. Chem. Soc.* **1964**, *86*, 765. (b) Pearson, R. G.; Anderson, M. M. *Angew. Chem., Intnl. Ed.* **1965**, *4*, 281.

(36) (a) Pasternack, R. F.; Huber, P. R.; Huber, U. M.; Sigel, H. *Inorg. Chem.* **1972**, *11*, 276. (b) Sharma, V. S.; Leussing, D. L. *Inorg. Chem.* **1972**, *11*, 138.

CHICAGO STATE UNIVERSITY

OFFICE OF RESEARCH &
SPONSORED PROGRAMS ADMINISTRATION

9501 S. King Drive / ADM 303
Chicago, Illinois 60628-1598
tel 773.995.3598 • fax 773.995.2490

February 13, 2001

Dr. Haddad
Department of the Air Force
Air Force Office of Scientific Research
810 North Randolph Street, Room 732
Arlington, VA 22203-1977

RE: F49620-96-1-0155 Final Technical Report

Dear Dr. Haddad:

Please find enclosed three copies of the referenced report and the Report Documentation Page.

Should you require any additional information please call 773-995-3598. I apologize for any inconvenience this may have caused.

Sincerely,

Angela M. Hopgood-Miller

Angela M. Hopgood-Miller
Grants and Contracts Administrator

Encls.

Cc: Dr. Kanis
Dr. Petty